

Chapter 2

Electronic Liquid Crystal Phases in Strongly Correlated Systems

Eduardo Fradkin

Abstract I discuss the electronic liquid crystal (ELC) phases in correlated electronic systems, what these phases are and in what context they arise. I will go over the strongest experimental evidence for these phases in a variety of systems: the two-dimensional electron gas (2DEG) in magnetic fields, the bilayer material $\text{Sr}_3\text{Ru}_2\text{O}_7$ (also in magnetic fields), and a set of phenomena in the cuprate superconductors (and more recently in the pnictide materials) that can be most simply understood in terms of ELC phases. Finally we will go over the theory of these phases, focusing on effective field theory descriptions and some of the known mechanisms that may give rise to these phases in specific models.

2.1 Electronic Liquid Crystal Phases

Electronic liquid crystal phases [1] are states of correlated quantum electronic systems that break spontaneously either rotational invariance or translation invariance. Since most correlated electronic systems arise in a solid state environment the underlying crystal symmetry plays a role as it is the unbroken symmetry of the system. Thus in practice these phases break the point group symmetry of the underlying lattice, in addition of the possible breaking of the lattice translation symmetry.

This point of view is commonplace in the classification of phases of *classical* liquid crystals [2]. Classical liquid crystal systems are assemblies of a macroscopically large number of molecules with various shapes. The shapes of the individual molecules (the “nematogens”) affect their mutual interactions, as well as enhancing entropically-driven interactions (“steric forces”) which, when combined, give rise to the dazzling phase diagrams of liquid crystals and the fascinating properties of their phases [2].

E. Fradkin (✉)

Department of Physics, University of Illinois at Urbana-Champaign,
1110 West Green Street, Urbana, IL 61801-3080 USA
e-mail: efradkin@illinois.edu

The physics of liquid crystals is normally regarded as part of “soft” condensed matter physics, while the physics of correlated electrons is usually classified as part of “hard” condensed matter physics. The necessity to use both points of view clearly brings to the fore the underlying unity of Physics as a science. Thus, one may think of this area as “soft quantum matter” or “quantum soft matter” depending on to which tribe you belong to.

These lectures are organized as follows. In [Sect. 2.1](#) ELC phases and their symmetries are described. In [Sect. 2.2](#) I cover the main experimental evidence for these phases in 2DEGs, in $\text{Sr}_3\text{Ru}_2\text{O}_7$ and in high temperature superconductors. In [Sect. 2.3](#) I present the theories of stripe phases, in [Sect. 2.4](#) the relation between electronic inhomogeneity and high temperature superconductivity is discussed, and [Sect. 2.5](#) is devoted to the theory of the pair density wave (the striped superconductor). [Section 2.6](#) is devoted to the theories of nematic phases and a theory of nematic electronic order in the strong coupling regime is discussed in [Sect. 2.7](#) The stripe-nematic quantum phase transition is discussed in [Sect. 2.8](#).

2.1.1 Symmetries of Electronic Liquid Crystal Phases

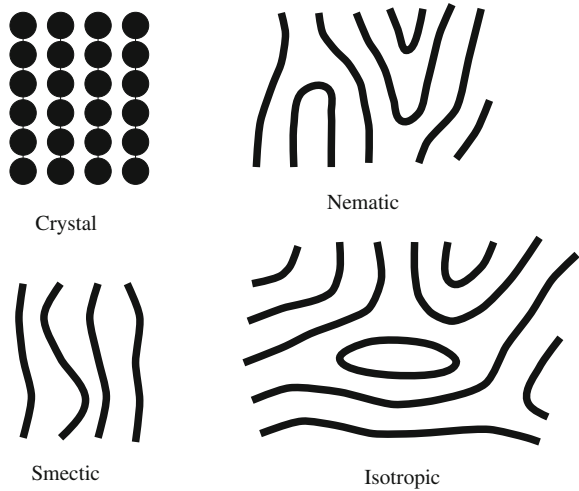
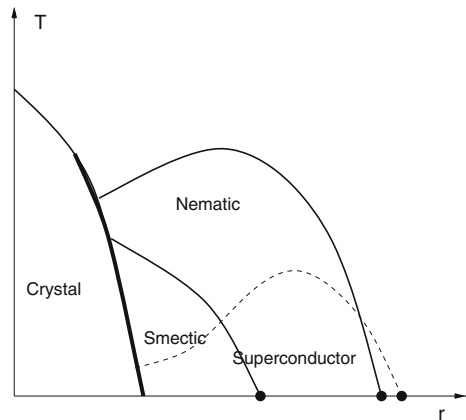
We will follow Ref.[1] and classify the ELC phases of strongly correlated electrons¹ following the symmetry-based scheme used in classical liquid crystals [2, 3]:

1. *Crystalline phases*: phases that break all continuous translation symmetries and rotational invariance.
2. *Smectic (“stripe”) phases*: phases break one translation symmetry and rotational invariance.
3. *Nematic and hexatic phases*: uniform (liquid) phases that break rotational invariance.
4. *Isotropic*: uniform and isotropic phases.

A cartoon of the real space structure of these ordered phases is shown in [Fig. 2.1](#).

Unlike classical liquid crystals, electronic systems carry charge and spin, and have strong quantum mechanical effects (particularly in the strong correlation regime). This leads to a host of interesting possibilities of ordered states in which the liquid crystalline character of the spatial structure of these states becomes intertwined with the “internal” degrees of freedom of electronic systems. These novel ordered phases will be the focus of these lectures. One of the aspects that we will explore is the structure of their phase diagrams. Thus in addition of considering the thermal melting of these phases, we will also be interested in the *quantum* melting of these states and the associated quantum phase transitions (see a sketch in [Fig. 2.2](#)).

¹ You may call the ELC phases the anisotropic states of point particles!

Fig. 2.1 Cartoon of liquid crystal phases**Fig. 2.2** Schematic phase diagram of electronic liquid crystal phases. Here T is temperature and r denotes a tuning parameter the controls the strength of the quantum fluctuations. In practice it can represent doping, magnetic field, pressure or even material. The full dots are quantum critical points

In this context, the *crystalline phases* are either insulating or “almost insulating”, e.g. multiple charge density waves (CDW) ordered states either commensurate or sliding (incommensurate). However, these phases may also be superconducting either by coexistence or, more interestingly, by modulating the superconducting states themselves. Similarly, electron nematics are anisotropic metallic or superconducting states, while the isotropic phases are also either metallic or superconducting. As we will see these phases display a set of rather striking and unusual behaviors, some of which have been observed in recent experiments.

2.1.2 Order Parameters and Their Symmetries

The order parameters of ELC phases are well known [1, 4]. In the crystalline phases, the order parameters are $\rho_{\mathbf{K}}$, the expectation values of the density operators at the set of ordering wave vectors $\{\mathbf{K}\}$ that defines the crystal [3].

$$\rho_{\mathbf{K}} = \int d\mathbf{r} \rho(\mathbf{r}) e^{i\mathbf{K}\cdot\mathbf{r}} \quad (2.1)$$

where $\rho(\mathbf{r})$ is the local charge density. Thus, under a uniform translation by \mathbf{R} , $\rho_{\mathbf{K}}$ transforms as

$$\rho_{\mathbf{K}} \rightarrow \rho_{\mathbf{K}} e^{i\mathbf{K}\cdot\mathbf{R}} \quad (2.2)$$

Smectic phases are unidirectional density waves and their order parameters are also expectation values $\rho_{\mathbf{K}}$ but for *only one* wave vector \mathbf{K} . For charged systems, $\rho(\mathbf{r})$ is the *charge density*, and the order parameter $\rho_{\mathbf{K}}$ is the *charge density wave* order parameter. Since $\rho(\mathbf{r})$ is *real*, $\rho_{\mathbf{K}} = \rho_{-\mathbf{K}}^*$, and the density can be expanded as

$$\rho(\mathbf{r}) = \rho_0(\mathbf{r}) + \rho_{\mathbf{K}}(\mathbf{r})e^{i\mathbf{K}\cdot\mathbf{r}} + \text{c.c.} \quad (2.3)$$

where $\rho_0(\mathbf{r})$ are the Fourier components *close* to zero wave vector, $\mathbf{k} = 0$, and $\rho_{\mathbf{K}}(\mathbf{r})$ are the Fourier components with wave vectors *close* to $\mathbf{k} = \mathbf{K}$. Hence, a density wave (a *smectic*) is represented by a *complex* order parameter field, in this case $\rho_{\mathbf{K}}(\mathbf{r})$. This is how we will describe a CDW and a charge stripe (which from the point of view of symmetry breaking have the same description).²

Smectic order is detected most easily in scattering experiments through the measurement of the *static structure factor*, usually denoted by $S(\mathbf{k})$,

$$S(\mathbf{k}) = \int \frac{d\omega}{2\pi} S(\mathbf{k}, \omega) \quad (2.5)$$

where $S(\mathbf{k}, \omega)$ is the *dynamical structure factor*, i.e. the Fourier transform of the (in this case) density-density correlation function. The signature of smectic order is the existence of a delta-function component of $S(\mathbf{k})$ at the ordering wave vector, $\mathbf{k} = \mathbf{K}$, with a prefactor that is equal to $|\langle \rho_{\mathbf{K}} \rangle|^2$ [3].

In the case of a *spin density wave* (a “spin stripe”) the picture is the same except that the order parameter field is multi-component, $\mathbf{S}_{\mathbf{K}}(\mathbf{r})$, corresponding to different spin polarizations. Thus, the local spin density $\mathbf{S}(\mathbf{r})$ has the expansion

$$\mathbf{S}(\mathbf{r}) = \mathbf{S}_0(\mathbf{r}) + \mathbf{S}_{\mathbf{K}}(\mathbf{r}) e^{i\mathbf{K}\cdot\mathbf{r}} + \text{c.c.} \quad (2.6)$$

² On the other hand, in the case of a crystal phase, the expansion is

$$\rho(\mathbf{r}) = \rho_0(\mathbf{r}) + \sum_{\mathbf{K} \in \Gamma} \rho_{\mathbf{K}}(\mathbf{r}) e^{i\mathbf{K}\cdot\mathbf{r}} + \text{c.c.} \quad (2.4)$$

where Γ denotes the set of primitive lattice vectors of the crystal phase [3].

where $\mathbf{S}_0(\mathbf{r})$ denotes the local (real) *ferromagnetic* order parameter and $\mathbf{S}_{\mathbf{K}}(\mathbf{r})$ is the (complex) SDW (or spin stripe) order parameter field, a complex vector in spin space.

One of the questions we will want to address is the connection between these orders and superconductivity. The superconducting order parameter, a pair condensate, is the *complex* field $\Delta(\mathbf{r})$. It is natural (and as we will see it is borne out by current experiments) to consider the case in which the superconducting order is also modulated, and admits an expansion of the form

$$\Delta(\mathbf{r}) = \Delta_0(\mathbf{r}) + \Delta_{\mathbf{K}}(\mathbf{r}) e^{i\mathbf{K}\cdot\mathbf{r}} + \Delta_{-\mathbf{K}}(\mathbf{r}) e^{-i\mathbf{K}\cdot\mathbf{r}} \quad (2.7)$$

where the uniform component Δ_0 is the familiar BCS order parameter, and $\Delta_{\mathbf{K}}(\mathbf{r})$ is the *pair-density-wave* (PDW) order parameter [5, 6], closely related to the Fulde-Ferrell-Larkin-Ovchinnikov (FFLO) order parameter [7, 8] (but without an external magnetic field). Since $\Delta(\mathbf{r})$ is complex, $\Delta_{\mathbf{K}}(\mathbf{r}) \neq \Delta_{-\mathbf{K}}(\mathbf{r})^*$, the PDW state has two complex order parameters.³

In contrast, nematic phases are translationally invariant but break rotational invariance. Their order parameters transform irreducibly under the rotation group for a continuous system, or under the point (or space) group of the lattice. Hence, the order parameters of a nematic phase (hexatic and their generalizations) are symmetric traceless tensors, that we will denote by Q_{ij} [2]. In 2D, as most of the problems we will be interested in are 2D systems (or quasi2D systems), the order parameter takes the form (with $i, j = x, y$)

$$Q_{ij} = \begin{pmatrix} Q_{xx} & Q_{xy} \\ Q_{xy} & -Q_{xx} \end{pmatrix} \quad (2.8)$$

which, alternatively, can be written in terms of a *director* N ,

$$N = Q_{xx} + i Q_{xy} = |N| e^{i\varphi}. \quad (2.9)$$

Under a rotation by a fixed angle θ , N transforms as⁴

$$N \rightarrow N e^{i2\theta}. \quad (2.10)$$

Hence, it changes sign under a rotation by $\pi/2$ and it is *invariant* under a rotation by π (hence the name *director*, a headless vector). On the other hand, it is invariant under uniform translations by \mathbf{R} .

In practice we will have great latitude when choosing a nematic order parameter since any symmetric traceless tensor in space coordinates will transform properly under rotations. In the case of a charged metallic system, a natural choice to describe

³ I will not discuss the case of spiral order here.

⁴ For a lattice system, rotational symmetries are those of the point (or space) group symmetry of the lattice. Thus, nematic order parameters typically become Ising-like (on a square lattice) or three-state Potts on a triangular lattice (and so forth).

a metallic nematic state is the traceless symmetric component of the *resistivity* (or conductivity) tensor [9–12]. In 2D we will use the traceless symmetric tensor

$$Q_{ij} = \begin{pmatrix} \rho_{xx} - \rho_{yy} & \rho_{xy} \\ \rho_{xy} & \rho_{yy} - \rho_{xx} \end{pmatrix} \quad (2.11)$$

where ρ_{xx} and ρ_{yy} are the *longitudinal* resistivities and $\rho_{xy} = \rho_{yx}$ is the transverse (*Hall*) resistivity. This tensor *changes sign* under a rotation by $\frac{\pi}{2}$ but is invariant under a rotation by π . A similar analysis can be done in terms of the dielectric tensor, which is useful in the context of light scattering experiments.

On the other hand, when looking at the spin polarization properties of a system other measures of nematic order are available. For instance, in a neutron scattering experiment, the anisotropy under a rotation \mathcal{R} (say, by $\pi/2$) of the structure factor $S(\mathbf{k})$

$$Q \sim S(\mathbf{k}) - S(\mathcal{R}\mathbf{k}) \quad (2.12)$$

is a measure of the nematic order parameter Q [4, 13].

Other, more complex, yet quite interesting phases are possible. One should keep in mind that the nematic order parameter (as defined above) corresponds to a field that transforms under the lowest (angular momentum $\ell = 2$) irreducible representation of the rotations group, compatible with inversion symmetry. The nematic phase thus defined has *d*-wave symmetry, the symmetry of a quadrupole. Higher symmetries are also possible, e.g. hexatic ($\ell = 6$). However it is also possible to have states that break both rotational invariance and 2D inversion (mirror reflection), as in the $\ell = 3$ channel. Such states break (although mildly) time-reversal invariance [14, 15]. Other complex phases arise by combining the nematic order in real space with those of some internal symmetry, e.g. spin or orbital degeneracies. Thus one can consider nematic order parameters in the *spin-triplet* channels, which give rise to a host of (as yet undetected) phases with fascinating behaviors in the spin channel or under time-reversal, such as the dynamical generation of spin orbit coupling or the spontaneous breaking of time-reversal invariance [14, 16, 17].

2.1.3 Electronic Liquid Crystal Phases and Strong Correlation Physics

One of the central problems in condensed matter physics is the understanding of doped Mott insulators. Most of the interesting systems in condensed matter, notably high temperature superconductors, are doped Mott insulators [18]. A Mott insulator is a phase of an electronic system in which there is a gap in the single particle spectrum due to the effects of electronic correlations and not to features of the band structure. Thus, Mott insulators have an odd number of electrons in the unit cell.

For a system like this, band theory would predict that such systems must be metallic, not insulating, and be described by the Landau theory of the Fermi liquid. Electronic systems that become insulating due to the effects of strong correlation are states of matter with non-trivial correlations.

Most known Mott insulating states are ordered phases, associated with the spontaneous breaking of some global symmetry of the electronic system, and have a clearly defined order parameter. Typically the Mott state is an antiferromagnetic state (or generalizations thereof). However there has been a sustained interest in possible non-magnetic Mott phases, e.g. dimerized, various sorts of conjectured spin liquids, etc., some of which do not admit an order parameter description (as in the case of the topological phases).

We will not concern ourselves on these questions here. What will matter to us is that doping this insulator by holes disrupts the correlations that define the insulating state. Consequently doped holes are more costly (energetically) if they are apart than if they are together. The net effect is that the disruption of the correlations of the Mott state results in an effective strong attractive interaction between the doped holes. This effect was early on mistaken for a sign of pairing in models of high temperature superconductors (such as the Hubbard and t - J models). Further analysis revealed that this effective attraction meant instead the existence of a *generic* instability of strongly correlated systems to *phase separation* [19]. This feature of strong correlation has been amply documented in numerical simulations (see, for instance, Ref. [20]).

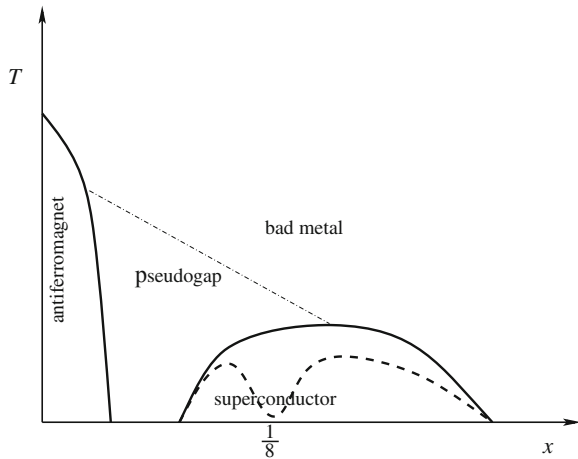
Due to the inherent tendency to phase separation of Hubbard-type models (and its descendants), the *insulating* nature of a Mott insulator cannot be ignored and, in particular, its inability to screen the longer range Coulomb interactions. Thus, quite generally, one can expect that the combined effects of the kinetic energy of the doped holes and the repulsive Coulomb interactions should in effect *frustrate* the tendency to phase separation of short-ranged models of strong correlation [21].

The existence of strong short range attractive forces and long range repulsion is a recipe for the formation of phases with complex spatial structure. As noted above, this is what happens in classical liquid crystals. It is also the general mechanism giving rise to generally inhomogeneous phases in classical complex fluids such as ferrofluids and heteropolymers [22], as well as in astrophysical problems such as the crusts of neutron stars [23].

The point of view that we take in these lectures is that the behavior observed in the underdoped regime of high temperature superconductors and in other strongly correlated systems is due to the strong tendency that these systems have to form generally inhomogeneous and anisotropic phases, “stripes”. In the following lectures we will go over the experimental evidence for these phases and for their theoretical underpinning.⁵

⁵ Ref. [24] is a recent, complementary, review of the phenomenology of nematic phases in strongly correlated systems.

Fig. 2.3 Schematic phase diagram of the cuprate superconductors. The full lines are the phase boundaries for the antiferromagnetic and superconducting phases. The broken line is the phase diagram for a system with static stripe order and a pronounced $1/8$ anomaly. The dotted line marks the crossover between the bad metal and pseudogap regimes



2.2 Experimental Evidence in Strongly Correlated Systems

During the past decade or so experimental evidence has been mounting of the existence of electronic liquid crystal phases in a variety of strongly correlated (as well as not as strongly correlated) electronic systems. We will be particularly interested in the experiments in the copper oxide high temperature superconductors, in the ruthenate materials (notably $\text{Sr}_3\text{Ru}_2\text{O}_7$), and in two-dimensional electron gases (2DEG) in large magnetic fields. However, as we will discuss below, these concepts are also relevant to more conventional CDW systems Fig. 2.3.

2.2.1 Nematic Phases in the 2DEG in High Magnetic Fields

To this date, the best documented electron nematic state is the anisotropic compressible state observed in 2DEGs in large magnetic fields near the middle of a Landau level, with Landau index $N \geq 2$ [25–28] (Figs. 2.4, 2.5). In ultra high mobility samples of a 2DEG in AlAs-GaAs heterostructures, transport experiments in the second Landau level (and above) near the center of the Landau level show a pronounced anisotropy of the longitudinal resistance rising sharply below $T \simeq 80$ mK, with an anisotropy that increases by orders of magnitude as the temperature is lowered. This effect is only seen in ultra-clean samples, with nominal mean free paths of about 0.5 mm (!) and nominal mobilities of $10 - 30 \times 10^6$.⁶

A nematic order parameter can be constructed phenomenologically from the measured resistivity tensor, by taking the symmetric traceless piece of it. This was done in Ref. [9] where a fit of the data of Lilly et al. [25, 26] was shown to be

⁶ The anisotropy is strongly suppressed by disorder.

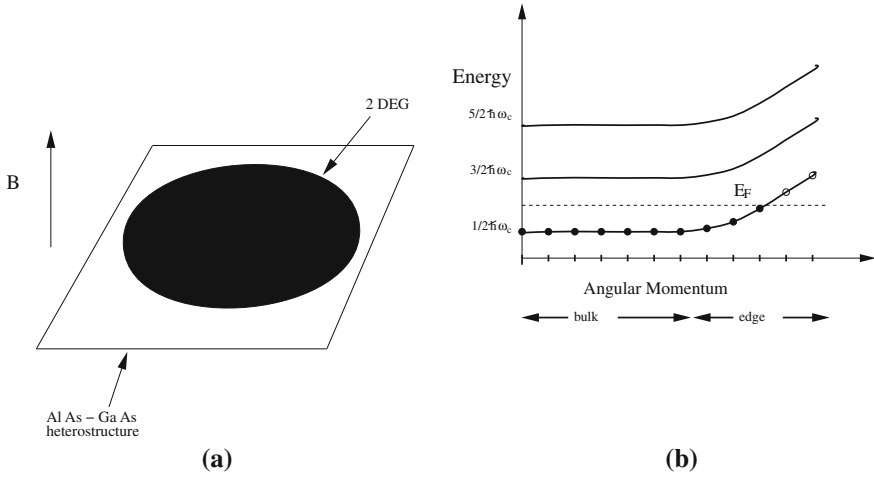


Fig. 2.4 **a** 2DEG in a magnetic field. **b** Landau levels

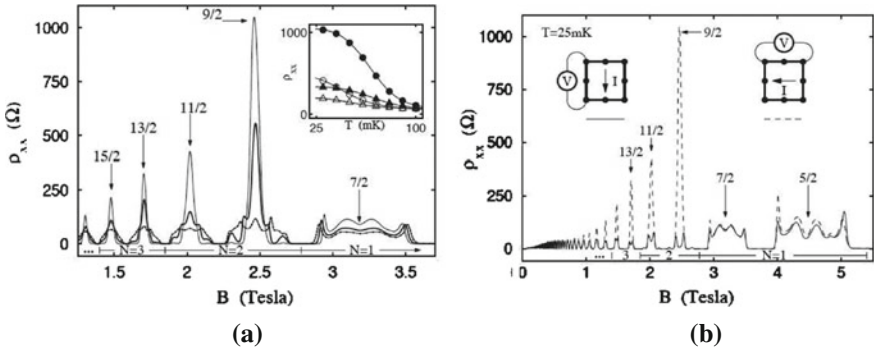


Fig. 2.5 Spontaneous magneto-transport anisotropy in the 2DEG: **a** peaks in ρ_{xx} developing at low T in high LLs (*dotted line*: $T=100$ mK; *thick line*: 65 mK; *thin line*: 25 mK). *Inset*: temperature dependence of peak height at $\nu = 9/2$ (*closed circles*), $11/2$ (*open circles*), $13/2$ (*closed triangles*) and $15/2$ (*open triangles*). **b** Anisotropy of ρ_{xx} at $T=25$ mK. From Lilly et al. [25], reprinted with permission from APS

consistent with a classical 2D XY model (in a weak symmetry breaking field). A 2D XY symmetry is expected for a planar nematic order provided the weak lattice symmetry breaking is ignored. Presumably lattice anisotropy is responsible for the saturation shown at low temperatures in Fig. 2.6 (left panel).

These experiments were originally interpreted as evidence for a quantum Hall smectic (stripe) phase [29–33]. However, further experiments ([10, 34, 35]) (Fig. 2.6, right panel) did not show any evidence of pinning of this putative unidirectional CDW as the I - V curves were found to be strictly linear at low bias. In addition, the observation of broadband noise in the current, which is a character-

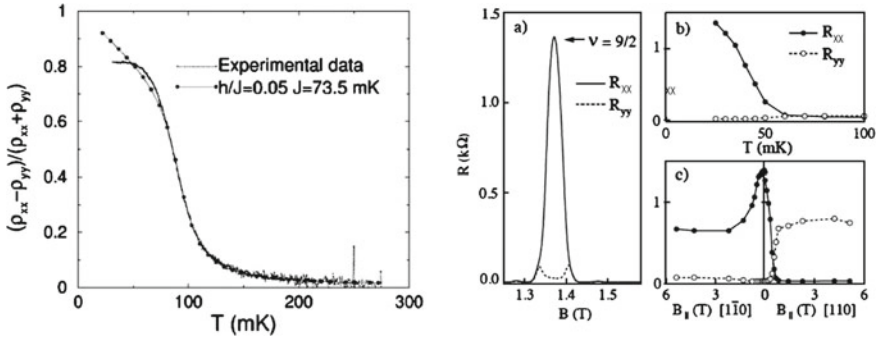


Fig. 2.6 *Left*: Nematic order in the 2DEG; fit of the resistance anisotropy to a 2D XY model Monte carlo simulation. From Fradkin et al [9], reprinted with permission from APS. *Right*: **a** Longitudinal resistance anisotropy around $\nu = 9/2$ at $T = 25$ mK. Solid trace: R_{xx} ; average current flow along $[110]$. **b** Temperature dependence of resistances at $\nu = 9/2$. **c** R_{xx} and R_{yy} at $\nu = 9/2$ at $T = 25$ mK vs in-plane magnetic field along $[110]$ and $[1\bar{1}0]$. From Cooper et al [10], reprinted with permission from APS

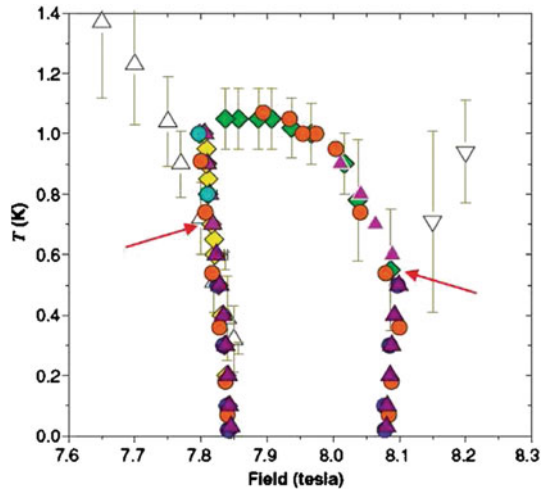
istic of CDW systems, has not been detected in the regime where this remarkable anisotropy is observed. In contrast, extremely sharp threshold electric fields and broadband noise in transport was observed in a nearby reentrant integer quantum Hall phase, suggesting a crystallized electronic state. These facts, together with a detailed analysis of the experimental data, suggested that the compressible state is in an electron nematic phase [9, 31, 36–38], which is better understood as a quantum melted stripe phase.⁷ An alternative picture, a nematic phase accessed by a Pomeranchuk instability from a “composite fermion” Fermi liquid is conceivable but hard to justify microscopically [38, 39].

2.2.2 The Nematic Phase of $\text{Sr}_3\text{Ru}_2\text{O}_7$

Recent magneto-transport experiments in the quasi-two-dimensional bilayer ruthenate $\text{Sr}_3\text{Ru}_2\text{O}_7$ by the St. Andrews group [12] have given strong evidence of a strong temperature-dependent in-plane transport anisotropy in strongly correlated materials at low temperatures $T \lesssim 800$ mK and for a window of perpendicular magnetic fields around 7.5 Tesla (see Fig. 2.7). $\text{Sr}_3\text{Ru}_2\text{O}_7$ is a quasi-2D bilayer material known to have a metamagnetic transition as a function of applied perpendicular magnetic field and temperature. Contrary to the case of the 2DEG in AlAs-GaAs heterostructures and quantum wells, the magnetic fields applied to $\text{Sr}_3\text{Ru}_2\text{O}_7$ are too weak to produce Landau quantization. However, as in the case of the 2DEG of the previous section, the transport anisotropy appears at very low temperatures and only in the cleanest samples. The observed transport anisotropy has a strong temperature

⁷ The 2DEG in a strong magnetic field is inherently a strongly correlated system as the interaction is always much bigger than the (vanishing) kinetic energy.

Fig. 2.7 Phase diagram of $\text{Sr}_3\text{Ru}_2\text{O}_7$ in the temperature-magnetic field plane. The nematic phase is the region comprised between $\sim 7.5T$ and $\sim 8.1T$. N transport anisotropy is detected outside this region where the system behaves as an isotropic (metamagnetic) metal. From Grigera et al. [40], reprinted with permission from AAAS



and field dependence (although not as pronounced as in the case of the 2DEG) is shown in Fig. 2.8. These experiments provide strong evidence that the system is in an electronic nematic phase in that range of magnetic fields [12, 41]. The electronic nematic phase appears to have preempted a metamagnetic QCP in the same range of magnetic fields [42–45]. This suggests that proximity to phase-separation may be a possible microscopic mechanism to trigger such quantum phase transitions, consistent with recent ideas on the role of Coulomb-frustrated phase separation in 2DEGs [46, 47].

2.2.3 Stripe Phases and Nematic Phases in the Cuprates

In addition to high temperature superconductivity, the copper oxide materials display a strong tendency to have charge-ordered states, such as stripes. The relation between charge ordered states [48], as well as other proposed ordered states [15, 49], and the mechanism(s) of high temperature superconductivity is a subject of intense current research. It is not, however, the main focus of these lectures. Stripe phases have been extensively investigated in high temperature superconductors and detailed and recent reviews are available on this subject [4, 52]. Stripe phases in high temperature superconductors have unidirectional order in both spin and charge (although not always) which are typically incommensurate. In general the detected stripe order (by low energy inelastic neutron scattering) in $\text{La}_{2-x}\text{Sr}_x\text{CuO}_4$, $\text{La}_{2-x}\text{Ba}_x\text{CuO}_4$ and $\text{YBa}_2\text{Cu}_3\text{O}_{6+x}$ (see Refs. [4, 52] and references therein) is not static but “fluctuating”. As emphasized in Ref. [4], “fluctuating order” means that there is no true long range unidirectional order. Instead, the system is in a (quantum) disordered phase, very close to a quantum phase transition to such an ordered phase, with very low energy fluctuations that reveal the character of the proximate ordered state. On the other hand,

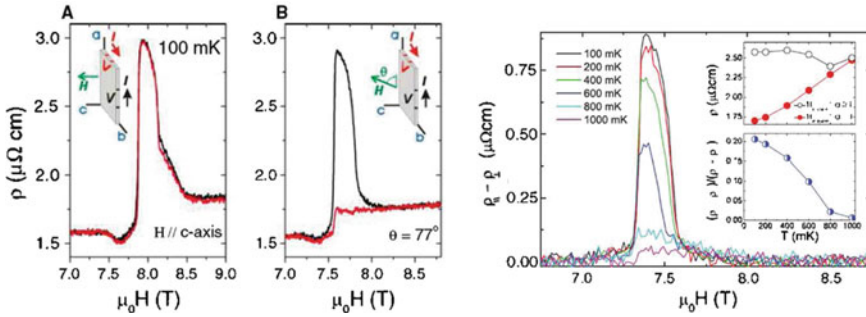


Fig. 2.8 Left: ρ_{aa} and ρ_{bb} of the in-plane magnetoresistivity tensor of a high-purity single crystal of $\text{Sr}_3\text{Ru}_2\text{O}_7$. (A) For an applied c-axis field, ρ_{aa} (upper curve) and ρ_{bb} (lower curve). (B) Tilted field (13° from c). Right: The temperature dependence difference of ρ_{aa} and ρ_{bb} for fields applied at $\theta = 72^\circ$ such that the in-plane field component lies along a (upper inset). Temperature dependence of ρ_{aa} (open symbols) and ρ_{bb} (filled symbols) for $\mu_0 H = 7.4$ T applied in the direction specified above. (Lower inset) The temperature dependence of the difference between the two magnetoresistivities shown in the upper inset, normalized by their sum. From Borzi et al. [12], reprinted with permission from AAAS

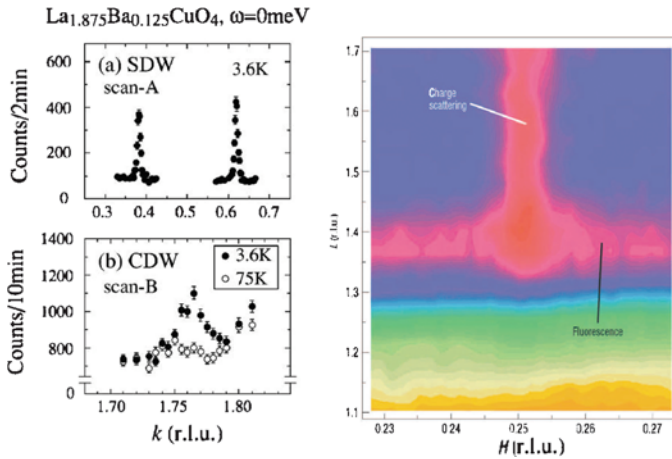


Fig. 2.9 Left: Static spin and charge stripe order in $\text{La}_{2-x}\text{Ba}_x\text{CuO}_4$ in neutron scattering. From Fujita et al. [50], reprinted with permission from APS. Right: resonant X-ray scattering. From Abbamonte et al. [51], reprinted with permission from Nature Physics

in $\text{La}_{2-x}\text{Ba}_x\text{CuO}_4$ near $x = 1/8$ (and in $\text{La}_{1.6-x}\text{Nd}_{0.4}\text{Sr}_x\text{CuO}_4$ also near $x = 1/8$ where they were discovered first [53]), the order detected by elastic neutron scattering [54], and resonant X-ray scattering in $\text{La}_{2-x}\text{Ba}_x\text{CuO}_4$ [51] also near $x = 1/8$, becomes true long range static order (see Fig. 2.9).

In the case of $\text{La}_{2-x}\text{Sr}_x\text{CuO}_4$, away from $x = 1/8$, and particularly on the more underdoped side, the in-plane resistivity has a considerable temperature-dependent anisotropy, which has been interpreted as an indication of electronic nematic

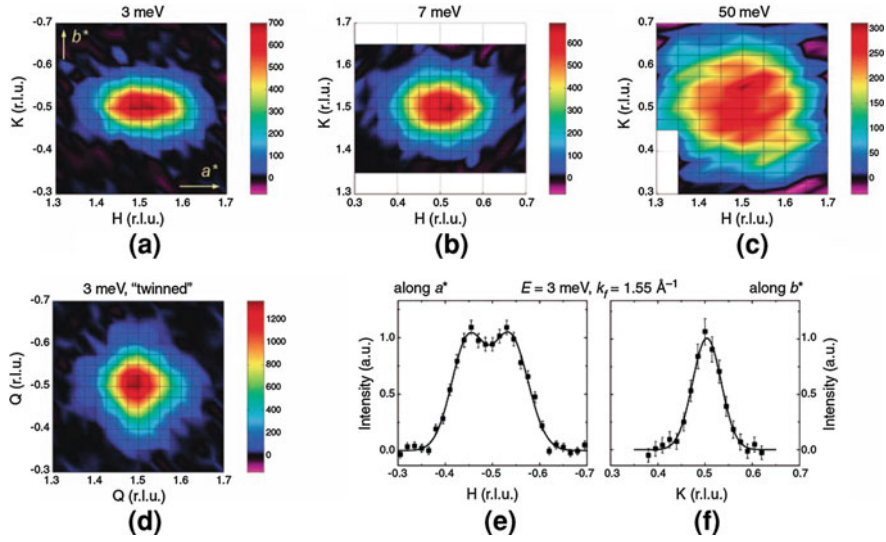


Fig. 2.10 Nematic order in underdoped $\text{YBa}_2\text{Cu}_3\text{O}_{6+x}$ ($y = 6.45$). (a) to (c) Intensity maps of the spin-excitation spectrum at 3, 7, and 50 meV, respectively. The a^* and b^* directions are indicated in (a). (d) Colormap of the intensity at 3 meV, as it would be observed in a crystal consisting of two perpendicular twin domains with equal population. (e) and (f) Scans along a^* and b^* through Q_{AF} . From Hinkov et al. [13], reprinted with permission from AAAS

order [11]. The same series of experiments also showed that very underdoped $\text{YBa}_2\text{Cu}_3\text{O}_{6+x}$ is an electron nematic as well.

The most striking evidence for electronic nematic order in high temperature superconductors are the recent neutron scattering experiments in $\text{YBa}_2\text{Cu}_3\text{O}_{6+x}$ at $y = 6.45$ [56] (see Figs. 2.10, 2.11). In particular, the temperature-dependent anisotropy of the inelastic neutron scattering in $\text{YBa}_2\text{Cu}_3\text{O}_{6+x}$ shows that there is a critical temperature for nematic order (with $T_c \sim 150$ K) where the inelastic neutron peaks also become incommensurate. Similar effects were reported by the same group [57] at higher doping levels ($y \sim 6.6$) who observed that the nematic signal was decreasing in strength suggesting the existence of a nematic-isotropic quantum phase transition closer to optimal doping. Fluctuating stripe order in underdoped $\text{YBa}_2\text{Cu}_3\text{O}_{6+x}$ has been detected earlier on in inelastic neutron scattering experiments [58, 59] which, in hindsight, can be reinterpreted as evidence for nematic order. However, as doping increases past a $y \sim 6.6$ a spin gap appears and magnetic scattering is strongly suppressed at low energies (in the absence of magnetic fields) making inelastic neutron scattering experiments less effective in this regime.

In a series of particularly interesting experiments, the Nernst coefficient was measured in $\text{YBa}_2\text{Cu}_3\text{O}_{6+x}$ ranging from the very underdoped regime, where inelastic neutron scattering detects nematic order, to a slightly overdoped regime [60]. The Nernst coefficient is defined as follows. Let j_e and j_Q be the charge and heat currents established in a 2D sample by an electric field \mathbf{E} and a temperature

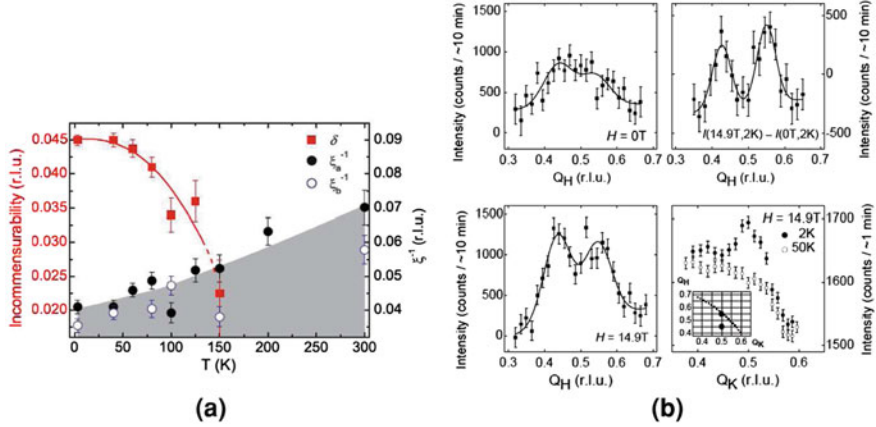


Fig. 2.11 **a** Incommensurability δ (squares), half-width-at-half-maximum of the incommensurate peaks along a^* (ξ_a^{-1} , dark circles) and along b^* (ξ_b^{-1} , white circles) in reciprocal lattice units. From Hinkov et al. [13], reprinted with permission from AAAS. **b** Static stripe order induced by an external magnetic field in $\text{YBa}_2\text{Cu}_3\text{O}_{6+x}$ at $y = 6.45$. From Haug et al. [55], reprinted with permission from APS

gradient ∇T :

$$\begin{pmatrix} j_e \\ j_Q \end{pmatrix} = \begin{pmatrix} \sigma & \alpha \\ T\alpha & \kappa \end{pmatrix} \begin{pmatrix} E \\ -\nabla T \end{pmatrix} \quad (2.13)$$

where σ , α and κ are 2×2 tensors for the conductivity, the thermoelectric conductivity and the thermal conductivity respectively. The Nernst coefficient, also a 2×2 tensor θ is measured (see Ref. [61]) say by applying a temperature gradient in the x direction and measuring the voltage along the y direction:

$$E = -\theta \nabla T \quad (2.14)$$

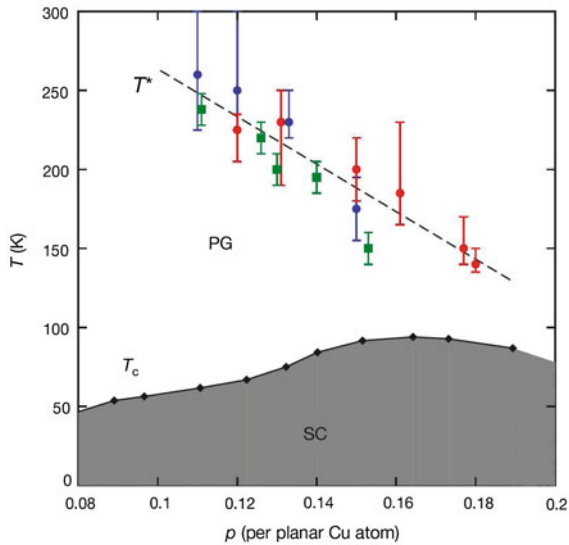
Since no current flows through the system, the Nernst tensor is

$$\theta = -\sigma^{-1} \alpha \quad (2.15)$$

These experiments revealed that the Nernst (tensor) coefficient has an anisotropic component whose onset coincides (within the error bars) with the conventionally defined value of the pseudogap temperature T^* , and essentially tracks its evolution as a function of doping. Thus, it appears that, at least in $\text{YBa}_2\text{Cu}_3\text{O}_{6+x}$, the pseudogap is a regime with nematic order (see Fig. 2.12). The same group had shown earlier than the Nernst coefficient is a sensitive indicator of the onset of stripe charge order in $\text{La}_{1.6-x}\text{Nd}_{0.4}\text{Sr}_x\text{CuO}_4$ [62].

Inelastic neutron scattering experiments have found nematic order also in $\text{La}_{2-x}\text{Sr}_x\text{CuO}_4$ materials where fluctuating stripes were in fact first discovered

Fig. 2.12 The pseudogap as a regime with of charge nematic order in $\text{YBa}_2\text{Cu}_3\text{O}_{6+x}$: measured from the Nernst effect, the onset (data) coincides with the T^* of the pseudogap PG (broken line). Here T_c is the superconducting (SC) critical temperature of $\text{YBa}_2\text{Cu}_3\text{O}_{6+x}$ plotted as a function of p (the hole concentration). From Ref. [60], reprinted with permission from Nature



[53]. Matsuda et al. [63] have found in underdoped $\text{La}_{2-x}\text{Sr}_x\text{CuO}_4$ ($x = 0.05$), a material that was known to have “fluctuating diagonal stripes”, evidence for nematic order similar to what Hinkov et al. [56] found in underdoped $\text{YBa}_2\text{Cu}_3\text{O}_{6+x}$. Earlier experiments in $\text{La}_{2-x}\text{Sr}_x\text{CuO}_4$ in moderate magnetic fields had also shown that a spin stripe state became static over some critical value of the field [64]. These experiments strongly suggest that the experiments that had previously identified the high temperature superconductors as having “fluctuating stripe order” (both inside and outside the superconducting phase) were most likely detecting an electronic nematic phase, quite close to a state with long range stripe (smectic) order. In all cases the background anisotropy (due to the orthorhombic distortion of the crystal structure) acts as a symmetry breaking field that couples linearly to the nematic order, thus rounding the putative thermodynamic transition to a state with spontaneously broken point group symmetry. These effects are much more apparent at low doping where the crystal orthorhombicity is significantly weaker.

In $\text{La}_{2-x}\text{Ba}_x\text{CuO}_4$ at $x=1/8$ there is strong evidence for a complex stripe ordered state that intertwines charge, spin and superconducting order [5, 65] (shown in Fig. 2.13). In fact $\text{La}_{2-x}\text{Ba}_x\text{CuO}_4$ at $x=1/8$ appears to have some rather fascinating properties. As summarized in Fig. 2.14, $\text{La}_{2-x}\text{Ba}_x\text{CuO}_4$ at $x=1/8$ has a very low critical superconducting $T_c \sim 4$ K (where the Meissner state sets in). However it is known from angle-resolved photoemission (ARPES) experiments that the anti-nodal gap (which roughly gives the pairing scale) is actually largest at $x=1/8$ [66] (or unsuppressed by the $1/8$ anomaly according to Ref. [67].) Static charge stripe order sets in at 54 K (where there is a structural transition from the LTO to the LTT lattice structure), but static spin stripe order only exists below 42 K. As soon as static spin order sets in, the in-plane resistivity begins to decrease very rapidly with decreasing

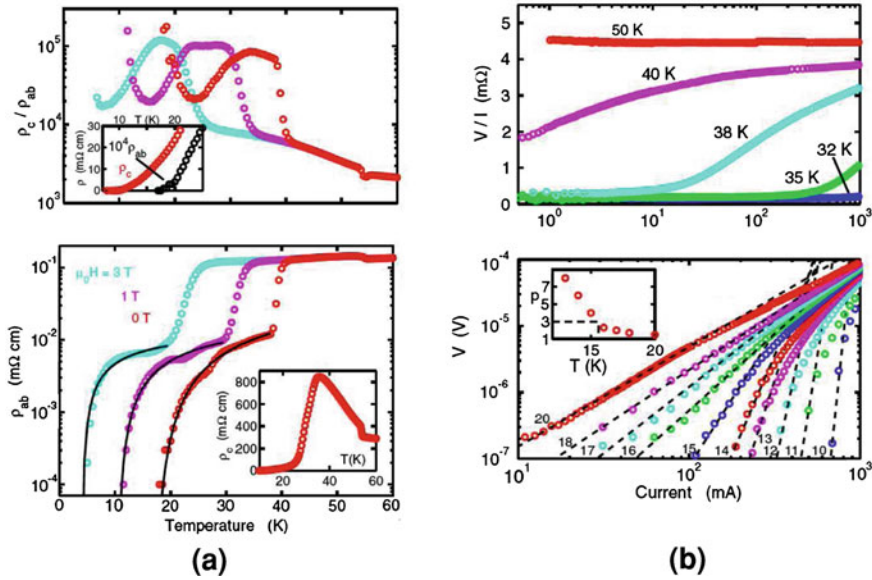
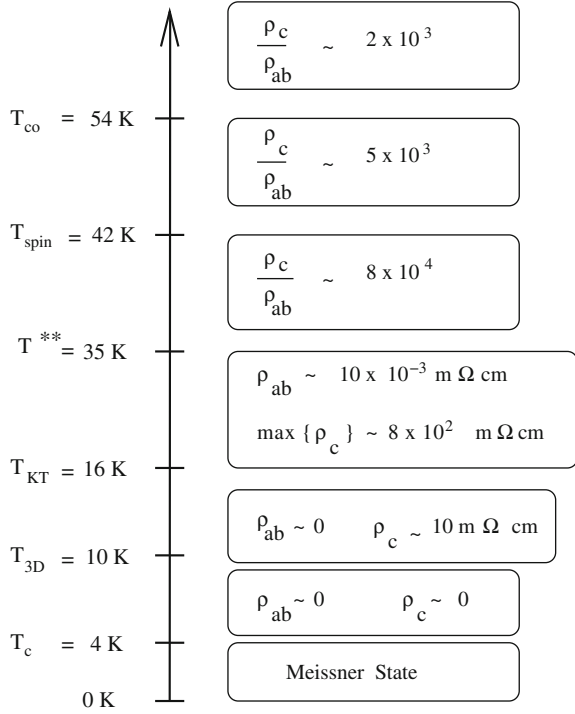


Fig. 2.13 **a** Dynamical layer decoupling in $\text{La}_{2-x}\text{Ba}_x\text{CuO}_4$ at $x=1/8$ from transport data. **b** Kosterlitz-Thouless transition in $\text{La}_{2-x}\text{Ba}_x\text{CuO}_4$ at $x=1/8$. From Q. Li et al. [65], reprinted with permission from APS

temperature, while the c -axis resistivity increases (see Fig. 2.13, left panel). Below 35 K strong 2D superconducting fluctuations are observed and at 16 K the in-plane resistivity vanishes at what appears to be a Kosterlitz–Thouless transition (shown in Fig. 2.13, right panel). However, the full 3D resistive transition is only reached at 10 K (where $\rho_c \rightarrow 0$) although the Meissner state is only established below 4 K! This dazzling set of phenomena shows clearly that spin, charge and superconducting order are forming a novel sort of *intertwined* state, rather than *compete*. We have conjectured that a pair density wave is stabilized in this intermediate temperature regime [5, 6, 68]. Similar phenomenology, i.e. a dynamical layer decoupling, has been seen in $\text{La}_{2-x}\text{Sr}_x\text{CuO}_4$ at moderate fields where the stripe order is static [69]. We will return below on how a novel state, the pair-density wave, explains these phenomena.

An important caveat to the analysis we presented here is that in doped systems there is always quenched disorder, which has different degrees of short range “organization” in different high temperature superconductors. Since disorder also couples linearly to the charge order parameters it ultimately also rounds the transitions and renders the system to a glassy state (as noted already in Refs. [1, 4]). Such effects are evident in scanning tunneling microscopy (STM) experiments in $\text{Bi}_2\text{Sr}_2\text{CaCu}_2\text{O}_{8+\delta}$ which revealed that the high energy (local) behavior of the high temperature superconductors has charge order and it is glassy [4, 70–73]. This is most remarkable as the STM data on $\text{Bi}_2\text{Sr}_2\text{CaCu}_2\text{O}_{8+\delta}$ at low bias shows quasiparticle propagation in

Fig.2.14 Summary of the behavior of the stripe-ordered superconductor $\text{La}_{2-x}\text{Ba}_x\text{CuO}_4$ near $x = 1/8$: T_{co} is the charge ordering temperature, T_{spin} the spin ordering temperature, T^{**} marks the beginning of layer decoupling behavior, T_{KT} is the 2D superconducting temperature (“KT”), T_{3D} is the 3D resistive transition, and T_c is the 3D Meissner transition



the superconducting state (but not above T_c). Yet, at high bias (i.e. high energies) there are no propagating “quasiparticles” but, instead, provides a vivid image of electronic inhomogeneity with short range charge order. This behavior is contrary to what is commonly the case in conventional superconductors where STM at high energies shows Fermi-liquid like electronic quasiparticles. Similarly, the high energy spectrum of ARPES has never resembled that of a conventional metal. We note that a recent analysis of this data by Lawler and coworkers has revealed the existence of nematic order over much longer length scales than the broken positional order [74] (Fig. 2.15).

Finally, we note that in the recently discovered iron pnictides based family of high temperature superconductors, such as $\text{La}(\text{O}_{1-x}\text{F}_x)\text{FeAs}$ and $\text{Ca}(\text{Fe}_{1-x}\text{Co}_x)_2\text{As}_2$ [75, 76], a unidirectional spin-density-wave has been found. It has been suggested [77] that the undoped system LaOFeAs and CaFe_2As_2 may have a high-temperature nematic phase and that quantum phase transitions also occur as a function of fluorine doping [78, 79]. This suggests that many of the ideas and results that we present here may be relevant to these still poorly understood materials.

The existence of stripe-ordered phases is well established in other complex oxide materials, particularly the manganites and the nickelates. In general, these materials tend to be “less quantum mechanical” than the cuprates in that they are typically insulating (although with interesting magnetic properties) and the observed

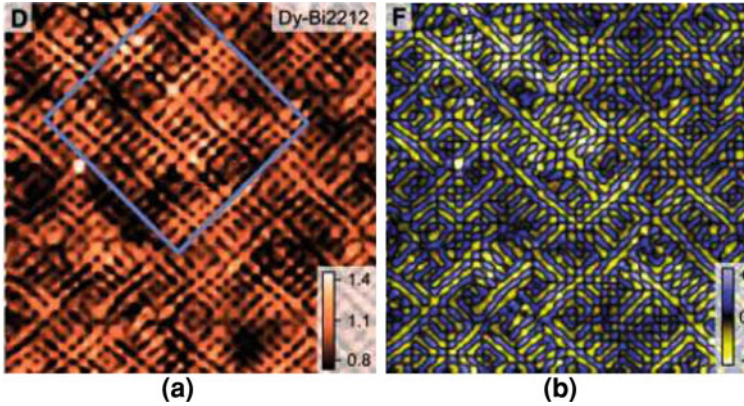


Fig. 2.15 Short range stripe order in $\text{Bi}_2\text{Sr}_2\text{CaCu}_2\text{O}_{8+\delta}$ (Dy-Bi2212) as seen in STM experiments. **a** R maps taken at 150 mV; **b** $\nabla^2 R$ shows the local nematic order. From Kohsaka et al. [70], reprinted with permission from AAAS

charge-ordered phases are very robust. These materials typically have larger electron-phonon interactions and electronic correlation are comparatively less dominant in their physics. For this reason they tend to be “more classical” and less prone to quantum phase transitions. However, at least at the classical level, many of the issues we discussed above, such as the role of phase separation and Coulomb interactions, also play a key role [80]. The thermal melting of a stripe state to a nematic has been seen in the manganite material $\text{Bi}_x\text{Ca}_x\text{MnO}_3$ [81].

2.2.4 Conventional CDW Materials

CDWs have been extensively studied since the mid-seventies and there are extensive reviews on their properties [82, 83]. From the symmetry point of view there is no difference between a CDW and a stripe (or electron smectic). CDW states are usually observed in systems which are not particularly strongly correlated, such as the quasi-one-dimensional and quasi-two-dimensional dichalcogenides, and the more recently studied tritellurides. These CDW states are reasonably well described as Fermi liquids (FL) which undergo a CDW transition, commensurate or incommensurate, triggered by a nesting condition of the FS [84, 85]. As a result, a part or all of the FS is gapped in which case the CDW may or may not retain metallic properties. Instead, in a strongly correlated stripe state, which has the same symmetry breaking pattern, at high energy has Luttinger liquid behavior [1, 86, 87].

What will interest us here is that conventional quasi-2D dichalcogenides, the also quasi-2D tritellurides and other similar CDW systems can quantum melt as a function of pressure in TiSe_2 [88], or by chemical intercalation as in Cu_xTiSe_2 [89, 90] and Nb_xTaS_2 [91]. Thus, CDW phases in chalcogenides can serve as a weak-coupling version of the problem of quantum melting of a quantum smectic. Interestingly, there

is strong experimental evidence that both TiSe_2 [88] and Nb_xTaS_2 [91] do not melt directly to an isotropic Fermi fluid but go instead through an intermediate, possibly hexatic, phase.⁸ Whether or not the intermediate phases are anisotropic is not known as no transport data is yet available in the relevant regime.

The case of the CDWs in tritellurides is more directly relevant to the theory we will present here. Tritellurides are quasi-2D materials which for a broad range of temperatures exhibit a unidirectional CDW (i.e. an electronic smectic phase) and whose anisotropic behavior appears to be primarily of electronic origin [93–96]. However, the quantum melting of this phase has not been observed yet. Theoretical studies have also suggested that it may be possible to have a quantum phase transition to a state with more than one CDW in these materials [97].

2.3 Theories of Stripe Phases

2.3.1 Stripe Phases in Microscopic Models

Of all the electronic liquid crystal phases, stripe states have been studied most. There are in fact a number of excellent reviews on this topic [4, 87, 98] covering both the phenomenology and microscopic mechanisms. I will only give a brief summary of important results and refer to the literature for details.

As we noted in Sect. 2.1.2, stripe and CDW (and SDW) phases have the same order parameter as they correspond to the same broken symmetry state, and therefore the same order parameter ρ_K (and S_Q).⁹ There is however a conceptual difference. CDW and SDW are normally regarded as weak coupling instabilities of a Fermi liquid (or free fermion state) typically triggered by a nesting condition satisfied by the ordering wave vector [82, 84]. In this context, the quasiparticle spectrum is modified by the partial opening of gaps and a change in the topology of the original Fermi surface (or, equivalently, by the formation of “pockets”). Because of this inherently weak coupling physics, the ordering wave vector is rigidly tied to the Fermi wave vector k_F .

In one-dimensional systems, non-linearities lead to a more complex form of density wave order, a lattice of solitons, known in this context as discommensurations [85, 99] whose ordering wavevector is no longer necessarily tied to k_F . A stripe state is essentially a two-dimensional generally incommensurate ordered state which is an analog of this strong coupling one-dimensional lattice of discommensurations [100]. Thus, in this picture, the spin stripe seen in neutron scattering [53] is pictured as regions of antiferromagnetic (commensurate) order separated by anti-phase domain walls (the discommensurations) where the majority of the doped

⁸ Cu_xTiSe_2 is known to become superconducting [89]. The temperature-pressure phase diagram of TiSe_2 exhibits a superconducting dome enclosing the quantum critical point at which the CDW state melts [92].

⁹ In principle the order parameter of the stripe state may not be pure sinusoidal and will have higher harmonics of the fundamental order parameter.

holes reside. This picture is quite hard to achieve by any weak coupling approximation such as Hartree–Fock.

Stripe phases were first found in Hartree–Fock studies of Hubbard and t - J models in two dimensions [101–105]. In this picture stripe phases are unidirectional charge density waves with or without an associated spin-density-wave (SDW) order. As such they are characterized by a CDW and/or SDW order parameters, $\rho_{\mathbf{K}}$ and $\mathbf{S}_{\mathbf{Q}}$ respectively.¹⁰ A Hartree–Fock theory of stripe phases was also developed in the context of the 2DEG in large magnetic fields [29, 30, 32] to describe the observed and very large transport anisotropy we discussed above.

As it is usually the case, a serious limitation of the Hartree–Fock approach is that it is inherently reliable only at weak coupling, and hence away from the regime of strong correlation of main interest. In particular, all Hartree–Fock treatments of the stripe ground state typically produce an “empty stripe state”, an insulating crystal and therefore not a metallic phase. Thus, in this approach a conducting (metallic) stripe phase can only arise from some sort of quantum melting of the insulating crystal and hence not describable in mean-field theory. The phenomenological significance of stripe phases was emphasized by several authors, particularly by Emery and Kivelson [21, 106, 107].

Mean field theory predicts that, at a fixed value of the electron (or hole) density (doping), the generally incommensurate ordering wave vectors satisfy the relation $\mathbf{K} = 2\mathbf{Q}$. That this result should generally hold follows from a simple Landau–Ginzburg (LG) analysis of stripe phases (see, e.g. [108, 109] where it is easy to see that a trilinear term of the form $\rho_{\mathbf{K}}^* \mathbf{S}_{\mathbf{Q}} \cdot \mathbf{S}_{\mathbf{Q}}$ (and its complex conjugate) is generally allowed in the LG free energy. In an ordered state of this type the antiferromagnetic spin order is “deformed” by anti-phase domain walls whose periodic pattern coincides with that of the charge order, as suggested by the observed magnetic structure factor of the stripe state first discovered in the cuprate $\text{La}_{1.6-x}\text{Nd}_{0.4}\text{Sr}_x\text{CuO}_4$ [53].

This pattern of CDW and SDW orders has suggested the popular cartoon of stripe phases as antiferromagnetic regions separated by narrow “rivers of charge” at antiphase domain walls. The picture of the stripe phase as an array of rivers suggests a description of stripe phases as a quasi-one-dimensional system. As we will see in the next subsection, this picture turned out to be quite useful for the construction of a strong coupling theory of the physics of the stripe phase. On the other hand, it should not be taken literally in the sense that these rivers always have a finite width which does not have to be small compared with the stripe period and in many cases they may well be of similar magnitude. Thus, one may regard this phase as being described by narrow 1D regions with significant transversal quantum fluctuations in shape (as it was presented in Ref.[1]) or, equivalently, as quasi-1D regions with a significant transversal width.

An alternative picture of the stripe phases can be gleaned from the t - J model, the strong coupling limit of the Hubbard model. Since in the resulting effective model there is no small parameter, the only (known) way to treat it is to extend the $SU(2)$ symmetry of the Hubbard (and Heisenberg) model to either $SU(N)$ or $Sp(N)$ and to

¹⁰ I will ignore here physically correct but more complex orders such as helical phases.

use the large N expansion to study its properties [98, 110–112]. In this (large N) limit the undoped antiferromagnet typically has a dimerized ground state, a periodic (crystalline) pattern of valence bond spin singlets. Since all degrees of freedom are bound into essentially local singlets this state is a quantum paramagnet. However, it is also “striped” in the sense that the valence bond crystalline state breaks at least the point group symmetry C_4 of the square lattice as well as translation invariance: it is usually a period 2 columnar state.¹¹ In the doped system the valence bond crystal typically becomes a non-magnetic incommensurate insulating system. Mean-field analyses of these models [112] also suggest the existence of superconducting states, some of which are “striped”. Similar results are suggested by variational wave functions based on the RVB state [114–116]. We should note, however, that mean-field states are no longer controlled by a small parameter, such as $1/N$, and hence it is unclear how reliable they may be at the physically relevant case $N=2$. For a detailed (and up-to-date) review of this approach see Ref. [98].

There are also extensive numerical studies of stripe phases in Hubbard type models. The best numerical data to date is the density matrix renormalization group (DMRG) work of White and Scalapino (and their collaborators) on Hubbard and t - J ladders of various widths (up to 5) and varying particle densities [117–120] and by Jackelmann et al. in fairly wide ladders (up to 7) [121]. An excellent summary and discussion on the results from various numerical results (as well as other insights) can be found in Ref. [87]. The upshot of all the DMRG work is that there are strong stripe correlations in Hubbard and t - J models which may well be the ground state.¹²

Much of the work on microscopic mechanisms of stripe formation has been done in models with short range interactions such as the Hubbard and t - J models. As it is known [19, 20, 122], models of this type have a strong tendency to *electronic phase separation*. As we noted in the introduction, the physics of phase separation is essentially the disruption of the correlations of the Mott (antiferromagnetic) state by the doped holes which leads to an effective *attractive* interaction among the charge carriers. When these effects overwhelm the stabilizing effects of the Fermi pressure (i.e. the fermion kinetic energy), phase separation follows. In more realistic models, however, longer range (and even Coulomb) interactions must be taken into account which tend to frustrate this tendency to phase separation [21], as well as a more complex electronic structure [123]. The structure of actual stripe phases in high T_c materials results from a combination of these effects. One of the (largely) unsolved questions is the relation between the stripe period and the filling fraction of each stripe at a given density. Most simple minded calculation yield simple commensurate filling fractions for each stripe leading to insulating states. At present time, except for results from DMRG studies on wide ladders [121], there are no controlled calculations that reproduce these effects, although suggestive variational estimates have been published [124].

¹¹ This state is a close relative of the resonating valence bond (RVB) state originally proposed as a model system for a high T_c superconducting state [18, 113], i.e. a (non-resonating) valence bond (VB) state.

¹² A difficulty in interpreting the DMRG results lies in the boundary conditions that are used that tend to enhance inhomogeneous, stripe-like, phases.

2.3.2 Phases of Stripe States

We will now discuss the strong coupling picture of the stripe phases [48, 86, 87, 112, 125, 126]. We will assume that a stripe phase exists with a fixed (generally incommensurate) wave vector \mathbf{K} and a fixed filling fraction (or density) on each stripe. In this picture a stripe phase is equivalent to an array of ladders of certain width. In what follows we will assume that each stripe has a finite *spin gap*: a *Luther–Emery liquid* [127, 128].

2.3.2.1 Physics of the 2-Leg Ladder

The assumption of the existence of a finite spin gap in ladders can be justified in several ways. In DMRG studies of Hubbard and t - J ladders in a rather broad density range, $0 < x < 0.3$, it is found that the ground state has a finite spin gap [129]. Similar results were found analytically in the weak coupling regime [130–133].

Why there is a spin gap? There is actually a very simple argument for it [134]. In the non-interacting limit, $U = V = 0$, the two-leg ladder has two bands with two different Fermi wave vectors, $p_{F1} \neq p_{F2}$. Let us consider the effects of interactions in this weak coupling regime. The only allowed processes involve an *even* number of electrons. In this limit it is easy to see that the coupling of CDW fluctuations with $Q_1 = 2p_{F1} \neq Q_2 = 2p_{F2}$ is suppressed due to the mismatch of their ordering wave vectors. In this case, scattering of electron pairs with zero center of mass momentum from one system to the other is a perturbatively (marginally) relevant interaction. The spin gap arises since the electrons can gain zero-point energy by delocalizing between the two bands. To do that, the electrons need to pair, which may cost some energy. When the energy gained by delocalizing between the two bands exceeds the energy cost of pairing, the system is driven to a spin-gap phase.

This physics is borne out by detailed numerical (DMRG) calculations, even in systems with only repulsive interactions. Indeed, at $x=0$ (the undoped ladder) the system is in a Mott insulating state, with a unique fully gapped ground state (“C0S0” in the language of Ref. [130]). In the strong coupling limit (in which the rungs of the ladder are spin singlet valence bonds), $U \gg t$, the spin gap is large: $\Delta_s \sim J/2$ [135].

At low doping, $0 < x < x_c \sim 0.3$, the doped ladder is in a Luther–Emery liquid: there is no charge gap and large spin gap (“C1S0”). In fact, in this regime the spin gap is found to decrease monotonically as doping increases, $\Delta_s \downarrow$ as $x \uparrow$, and vanishes at a critical value x_c : $\Delta_s \rightarrow 0$ as $x \rightarrow x_c$.

The most straightforward way to describe this system is to use bosonization. Although the ladder system has several bands of electrons that have charge and spin degrees of freedom, in the low energy regime the effective description is considerably simplified. Indeed, in this regime it is sufficient to consider only one effective bosonized charge field and one bosonized spin field. Since there is a spin gap, $\Delta_s \neq 0$,

the spin sector is massive. In contrast, the charge sector is only massive at $x=0$, where there is a finite Mott gap Δ_M .

The effective Hamiltonian for the charge degrees of freedom in this (Luther–Emery) phase is

$$H = \int dy \frac{v_c}{2} \left[\frac{1}{K} (\partial_y \theta)^2 + K (\partial_x \phi)^2 \right] + \dots \quad (2.16)$$

where ϕ is the CDW phase field, and θ is the SC phase field. They satisfy canonical commutation relations

$$[\phi(y'), \partial_y \theta(y)] = i\delta(y - y'). \quad (2.17)$$

The parameters of this effective theory, the spin gap Δ_s , the charge Luttinger parameter K , the charge velocity v_c , and the chemical potential μ , have non-universal but smooth dependences on the doping x and on the parameters of the microscopic Hamiltonian, the hopping matrix elements t'/t and the Hubbard interaction U/t . The ellipsis \dots in the effective Hamiltonian represent cosine potentials responsible for the Mott gap Δ_M in the undoped system ($x=0$). It can be shown that the spectrum in the low doping regime, $x \rightarrow 0$, consists of gapless and spinless charge $2e$ fermionic solitons.

The charge Luttinger parameter is found to approach $K \rightarrow 1/2$ as $x \rightarrow 0$. As x increases, so does K reaching the value $K \sim 1$ for $x \sim 0.1$. On the other hand $K \sim 2$ for $x \sim x_c$ where the spin gap vanishes. The temperature dependence of the superconducting and CDW susceptibilities have the scaling behavior

$$\chi_{SC} \sim \frac{\Delta_s}{T^{2-K}} \quad (2.18)$$

$$\chi_{CDW} \sim \frac{\Delta_s}{T^{2-K^{-1}}}. \quad (2.19)$$

Thus, both susceptibilities diverge $\chi_{CDW}(T) \rightarrow \infty$ and $\chi_{SC}(T) \rightarrow \infty$ for $0 < x < x_c$ as $T \rightarrow 0$. However, for $x \lesssim 0.1$, the SC susceptibility is more divergent: $\chi_{SC} \gg \chi_{CDW}$. Hence, the doped ladder in the Luther–Emery regime is effectively a 1D superconductor even for a system with nominally repulsive interactions (i.e. without “pairing”).

2.3.2.2 The spin-Gap Stripe State

Now consider a system with N stripes, each labeled by an integer $a = 1, \dots, N$. We will consider first the phase in which there is a spin gap. Here, the spin fluctuations are effectively frozen out at low energies. Nevertheless each stripe a has two degrees of freedom [1]: a transverse displacement field which describes the local dynamics of the configuration of each stripe, and the phase field ϕ_a for the charge fluctuations on each stripe. The action of the generalized Luttinger liquid which describes the

smectic charged fluid of the stripe state is obtained by integrating out the local shape fluctuations associated with the displacement fields. These fluctuations give rise to a finite renormalization of the Luttinger parameter and velocity of each stripe. More importantly, the shape fluctuations, combined with the long-wavelength inter-stripe Coulomb interactions, induce inter-stripe density-density and current-current interactions, leading to an imaginary time Lagrangian density of the form

$$\mathcal{L}_{\text{smectic}} = \frac{1}{2} \sum_{a,a',\mu} j_{\mu}^a(x) \tilde{W}_{\mu}(a-a') j_{\mu}^{a'}(x). \quad (2.20)$$

where the current operators on stripe a are $j_{\mu}^a(x) = \frac{1}{\sqrt{\pi}} \epsilon_{\mu\nu} \partial_{\nu} \phi^a(x)$; here $\mu = t, x$. These operators are *marginal*, i.e., have scaling dimension 2, and preserve the *smectic symmetry* $\phi_a \rightarrow \phi_a + \alpha_a$ (where α_a is constant on each stripe) of the decoupled Luttinger fluids. Notice that the current (and density) operators of *each stripe* are invariant under these transformations. Whenever this symmetry is exact, the charge-density-wave order parameters of the individual stripes do not lock with each other, and the charge density profiles on each stripe can slide relative to each other without an energy cost. In other words, there is no rigidity to shear deformations of the charge configuration on nearby stripes. This is the *smectic metal* phase [1], a *sliding Luttinger liquid* [136].

The fixed point action for a generic smectic metal phase thus has the form (in Fourier space)

$$\begin{aligned} S &= \sum_Q \frac{K(Q)}{2} \left\{ \frac{\omega^2}{v(Q)} + v(Q)k^2 \right\} |\phi(Q)|^2 \\ &= \sum_Q \frac{1}{2K(Q)} \left\{ \frac{\omega^2}{v(Q)} + v(Q)k^2 \right\} |\theta(Q)|^2 \end{aligned} \quad (2.21)$$

where $Q = (\omega, k, k_{\perp})$. Here θ_a is the field *dual* to ϕ_a and obey the canonical (equal-time) commutation relations

$$[\phi_a(x'), \partial_x \theta_b(x)] = i \delta(x' - x) \delta_{ab} \quad (2.22)$$

In Eq. 2.21 k is the momentum *along* the stripe and k_{\perp} perpendicular to the stripes. The kernels $K(Q)$ and $v(Q)$ are analytic functions of Q whose form depends on microscopic details, e.g. at weak coupling they are functions of the inter-stripe Fourier transforms of the forward and backward scattering amplitudes $g_2(k_{\perp})$ and $g_4(k_{\perp})$, respectively. In practice, up to irrelevant operators, it is sufficient to keep the dependence of the kernels only on the transverse momentum k_{\perp} . Thus, the smectic fixed point is characterized by the effective Luttinger parameter and velocity (functions), $K(k_{\perp})$ and $v(k_{\perp})$. Much like the ordinary 1D Luttinger liquid, this “fixed point” is characterized by power-law decay of correlations functions. This effective field theory also yields the correct low energy description of the quantum Hall stripe phase of the 2DEG in large magnetic fields [31–33, 137, 138].

In the presence of a spin gap, single electron tunneling is irrelevant [134], and the only potentially relevant interactions involving pairs of stripes a, a' are singlet pair (Josephson) tunneling, and the coupling between the CDW order parameters. These interactions have the form $\mathcal{H}_{\text{int}} = \sum_n (\mathcal{H}_{\text{SC}}^n + \mathcal{H}_{\text{CDW}}^n)$ for $a' - a = n$, where

$$\begin{aligned}\mathcal{H}_{\text{SC}}^n &= \left(\frac{\Lambda}{2\pi}\right)^2 \sum_a \mathcal{J}_n \cos[\sqrt{2\pi}(\theta_a - \theta_{a+n})] \\ \mathcal{H}_{\text{CDW}}^n &= \left(\frac{\Lambda}{2\pi}\right)^2 \sum_a \mathcal{V}_n \cos[\sqrt{2\pi}(\phi_a - \phi_{a+n})].\end{aligned}\quad (2.23)$$

Here \mathcal{J}_n are the inter-stripe Josephson couplings (SC), \mathcal{V}_n are the $2k_F$ component of the inter-stripe density-density (CDW) interactions, and Λ is an ultra-violet cutoff, $\Lambda \sim 1/a$ where a is a lattice constant. A straightforward calculation, yields the scaling dimensions $\Delta_{1,n} \equiv \Delta_{\text{SC},n}$ and $\Delta_{-1,n} \equiv \Delta_{\text{CDW},n}$ of $\mathcal{H}_{\text{SC}}^n$ and $\mathcal{H}_{\text{CDW}}^n$:

$$\Delta_{\pm 1,n} = \int_{-\pi}^{\pi} \frac{dk_{\perp}}{2\pi} [\kappa(k_{\perp})]^{\pm 1} (1 - \cos nk_{\perp}), \quad (2.24)$$

where $\kappa(k_{\perp}) \equiv K(0, 0, k_{\perp})$. Since $\kappa(k_{\perp})$ is a periodic function of k_{\perp} with period 2π , $\kappa(k_{\perp})$ has a convergent Fourier expansion of the form $\kappa(k_{\perp}) = \sum_n \kappa_n \cos nk_{\perp}$. We will parametrize the fixed point theory by the coefficients κ_n , which are smooth non-universal functions. In what follows we shall discuss the behavior of the simplified model with $\kappa(k_{\perp}) = \kappa_0 + \kappa_1 \cos k_{\perp}$. Here, κ_0 can be thought of as the intra-stripe inverse Luttinger parameter, and κ_1 is a measure of the nearest neighbor inter-stripe coupling. For stability we require $\kappa_0 > \kappa_1$.

Since it is unphysical to consider longer range interactions in H_{int} than are present in the fixed point Hamiltonian, we treat only perturbations with $n=1$, whose dimensions are

$$\Delta_{\text{SC},1} \equiv \Delta_{\text{SC}} = \kappa_0 - \frac{\kappa_1}{2} \quad (2.25)$$

and

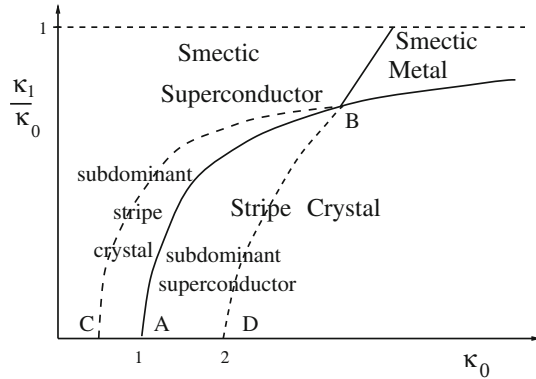
$$\Delta_{\text{CDW},1} \equiv \Delta_{\text{CDW}} = \frac{2}{\left(\kappa_0 - \kappa_1 + \sqrt{\kappa_0^2 - \kappa_1^2}\right)} \quad (2.26)$$

For a more general function $\kappa(k_{\perp})$, operators with larger n must also be considered, but the results are qualitatively unchanged [136, 139].¹³

In Fig. 2.16 we present the phase diagram of this model. The dark AB curve is the set of points where $\Delta_{\text{CDW}} = \Delta_{\text{SC}}$, and it is a line of first order transitions.

¹³ $\Delta_{\text{SC},2}$ is the most relevant operator. For a model with $\kappa(k_{\perp}) = [\kappa_0 + \kappa_1 \cos(k_{\perp})]^2$, all perturbations are irrelevant for large κ_0 and small $|\kappa_0 - \kappa_1|$.

Fig. 2.16 Phase diagram for a stripe state with a spin gap



To the right of this line the inter-stripe CDW coupling is the most relevant perturbation, indicating an instability of the system to the formation of a 2D stripe crystal [1]. To the left, Josephson tunneling (which still preserves the smectic symmetry) is the most relevant, so this phase is a 2D smectic superconductor. (Here we have neglected the possibility of coexistence since a first order transition seems more likely). Note that there is a region of $\kappa_0 \geq 1$, and large enough κ_1 , where the global order is superconducting although, in the absence of inter-stripe interactions (which roughly corresponds to $\kappa_1 = 0$), the superconducting fluctuations are subdominant. There is also a (strong coupling) regime above the curve CB where *both* Josephson tunneling *and* the CDW coupling *are irrelevant* at low energies. Thus, in this regime *the smectic metal state is stable*. This phase is a 2D smectic non-Fermi liquid in which there is coherent transport *only* along the stripes.

To go beyond this description we need to construct an effective theory of the *two-dimensional* ordered phase. For instance, the superconducting state is a 2D striped superconductor, whereas the crystal is a bidirectional charge density wave. A theory of these 2D ordered phases can be developed by combining the quasi-one-dimensional renormalization group with an effective inter-stripe mean field theory, as in Ref. [140], which in turn can be fed into a 2D renormalization group theory [141]. One advantage of this approach is that the inter-stripe mean field theory has the same analytic structure as the dimensional crossover RG (see Ref. [126]).

Let us consider the superconducting state, a *striped* superconductor. In the way we constructed this state all ladders are *equivalent*. Hence this is a period 2 stripe (columnar) SC phase, similar to the one discussed by Vojta [98]. Let us use inter-stripe mean field theory to estimate the critical temperature of the 2D state. For the isolated ladder, $T_c = 0$ as required by the Mermin-Wagner theorem. If the inter-stripe Josephson and CDW couplings are non-zero, $\mathcal{J} \neq 0$ and $\mathcal{V} \neq 0$, the system will now have a finite SC critical temperature, $T_c > 0$. Now, for $x \lesssim 0.1$, CDW couplings are irrelevant as in this range $1/2 < K < 1$. Hence, in the same range, the inter-ladder Josephson coupling are relevant and lead to a SC state in a small x with a somewhat low T_c which, in inter-stripe (or ‘chain’) mean field theory can be estimated by

$$2\mathcal{J}\chi_{SC}(T_c) = 1. \quad (2.27)$$

In this regime, however, $T_c \propto \delta t x$ and it is low due to the low carrier density. Conversely, for larger x , $K > 1$ and χ_{CDW} is more strongly divergent than χ_{SC} . Thus, for $x \gtrsim 0.1$ the CDW couplings become more relevant. This leads to an insulating incommensurate CDW state with ordering wave number $P = 2\pi x$.

In the scenario we just outlined [48, 126] in the 2D regime the system has a *first order* transition from a superconducting state to a non-superconducting phase with charge order. However at large enough inter-stripe forward scattering interactions both couplings become irrelevant and there is a quantum *bicritical* point separating both phases from a smectic metal (as depicted in Fig. 2.16). However, an alternative possibility is that instead of a bicritical point, we may have a quantum *tetracritical* point and a phase in which SC and CDW orders coexist.

2.4 Is Inhomogeneity Good or Bad for Superconductivity?

The analysis we just did raises the question of whether stripe order (that is, some form of spatial charge inhomogeneity) is good or bad for superconductivity. This question was addressed in some detail in Refs. [48, 126] where it was concluded that (a) there is an *optimal degree of inhomogeneity at which T_c reaches a maximum*, and (b) that charge order in a system with a spin gap can provide a mechanism of “high temperature superconductivity” (the meaning of which we will specify below).

The argument goes as follows. Consider a system with a *period 4* stripe phase, consisting of an alternating array of inequivalent *A* and *B* type ladders in the Luther–Emery regime.¹⁴ The inter-stripe mean field theory estimate for the superconducting and CDW critical temperatures now takes the somewhat more complex form:

$$(2\mathcal{J})^2 \chi_{SC}^A(T_c) \chi_{SC}^B(T_c) = 1 \quad (2.28)$$

for the superconducting T_c , and

$$(2\mathcal{V})^2 \chi_{CDW}^A(P, T_c) \chi_{CDW}^B(P, T_c) = 1 \quad (2.29)$$

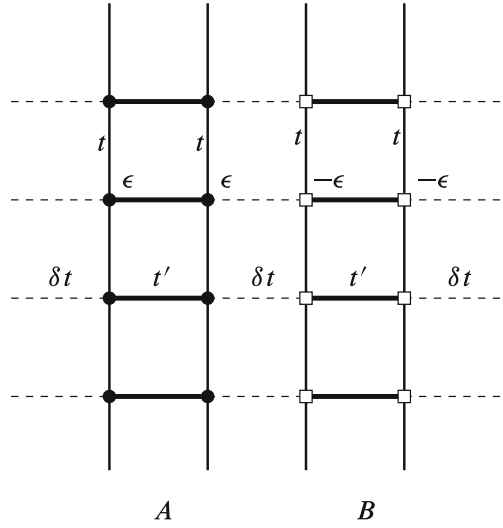
for the CDW T_c . In particular, the 2D CDW order is greatly suppressed due to the mismatch between ordering vectors, P_A and P_B , on neighboring ladders.

For inequivalent *A* and *B* ladders SC beats CDW if the corresponding Luttinger parameters satisfy the inequalities

$$2 > K_A^{-1} + K_B^{-1} - K_A; \quad 2 > K_A^{-1} + K_B^{-1} - K_B. \quad (2.30)$$

¹⁴ In Ref. [125] a similar pattern was also considered except that the (say) ‘*B*’ stripes do not have a spin gap. This pattern was used to show how a crude model with nodal quasiparticles can arise in an inhomogeneous state.

Fig. 2.17 Model of a period 4 stripe phase



The SC critical temperature is then found to obey a *power law* scaling form (instead of the essential singularity of the BCS theory of superconductivity):

$$T_c \sim \Delta_s \left(\frac{\mathcal{J}}{\tilde{W}} \right)^\alpha ; \alpha = \frac{2K_A K_B}{[4K_A K_B - K_A - K_B]}. \quad (2.31)$$

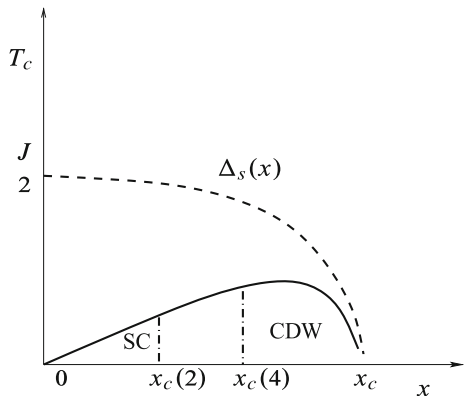
A simple estimate of the effective inter-stripe Josephson coupling,¹⁵ $\mathcal{J} \sim \delta t^2/J$ and of the high energy scale $\tilde{W} \sim J$, implies that the superconducting critical temperature T_c is (power law) small for small \mathcal{J} !, with an exponent that typically is $\alpha \sim 1$ (Fig. 2.17).

These arguments can be used to sketch a phase diagram of the type presented in Fig. 2.18 which shows the qualitative dependence of the SC T_c with doping x . The broken line shown is the spin gap $\Delta_s(x)$ as a function of doping x and, within this analysis, it must be an upper bound on T_c . Our arguments then showed that a period 4 structure can have a substantially larger T_c than a period 2 stripe. Consequently, the critical dopings, $x_c(2)$ and $x_c(4)$, for the SC-CDW quantum phase transition must move to higher values of x for period 4 compared with period 2. On the other hand, for $x \gtrsim x_c$ the isolated ladders do not have a spin gap, and this strong coupling mechanism is no longer operative.

How reliable are these estimates? What we have are mean-field estimates for T_c and it is an upper bound to the actual T_c . As it is usually the case, T_c should be suppressed by phase fluctuations by up to a factor of 2. On the other hand, perturbative RG studies for small \mathcal{J} yield the *same power law dependence*. This result

¹⁵ Josephson coupling is due to pair tunneling from one stripe to a neighboring one. Josephson processes arise in second order in perturbation theory and involve intermediate states with excitations energies of order J and have an amplitude controlled by δt .

Fig. 2.18 Evolution of the superconducting critical temperature with doping



is asymptotically exact for $\mathcal{J} \ll \tilde{W}$. Since T_c is a smooth function of $\delta t/\mathcal{J}$, it is reasonable to extrapolate for $\delta t \sim \mathcal{J}$. Hence, $T_c^{\max} \propto \Delta_s$ and we have a “high T_c ”. This is in contrast to the exponentially small T_c obtained in a BCS-like mechanism.

Now, having convinced ourselves that a period 4 stripe will have a larger SC T_c than a period 2 stripe one may wonder if an even longer period stripe state would do better. It is easy to see that there will be a problem with this proposal. Clearly, although the argument we just presented would suggest that the exponents will also be of order 1 for longer periods, the problem now is that the effective couplings become very small very quickly as the Josephson coupling has an *exponential* dependence on distance (tunneling!). Thus, there must be an optimal period for this mechanism and it is likely to be a number larger than 2 but smaller than (say) 6.

In summary, we have shown that in systems with strong repulsive interactions (and without attractive interactions), an (inhomogeneous) stripe-ordered state can support a 2D superconducting state with a high critical temperature, in the sense that it is not exponentially suppressed, with a high pairing scale (the spin gap). This state is an inhomogeneous version of the RVB mechanism [18, 113, 142]. The arguments suggest that there is an optimal degree of inhomogeneity. There is suggestive evidence in ARPES data in $\text{La}_{2-x}\text{Ba}_x\text{CuO}_4$ that show a large pairing scale in the stripe-ordered state which support this picture [66, 67].

2.5 The Striped Superconductor: A Pair Density Wave State

We now turn to a novel type of striped superconductor, the pair density wave state. Berg et al. [5, 109, 143] have recently proposed this state as a symmetry-based explanation of the spectacular dynamical layer decoupling seen in stripe-ordered $\text{La}_{2-x}\text{Ba}_x\text{CuO}_4$ (and $\text{La}_{1.6-x}\text{Nd}_{0.4}\text{Sr}_x\text{CuO}_4$) [65, 144, 145], and in $\text{La}_{2-x}\text{Sr}_x\text{CuO}_4$ in magnetic fields [69].

Summary of experimental facts for $\text{La}_{2-x}\text{Ba}_x\text{CuO}_4$ near $x=1/8$:

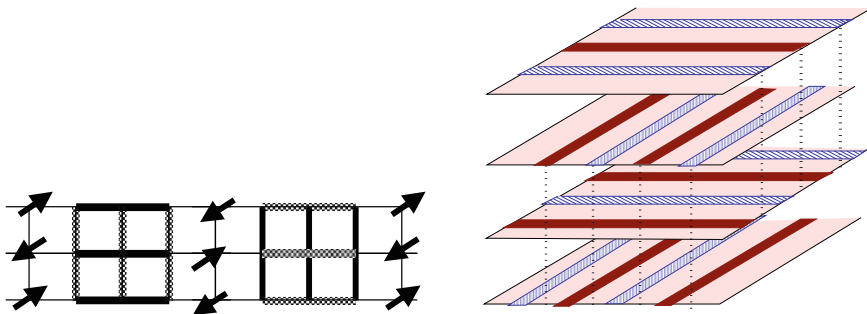


Fig. 2.19 Period 4 striped superconducting state

- ARPES finds an anti-nodal d-wave SC gap that is large and unsuppressed at $x = 1/8$. Hence, there is a large pairing scale in the stripe-ordered state.
- Resonant X-Ray scattering finds static charge stripe order for $T < T_{charge} = 54$ K.
- Neutron Scattering finds static Stripe Spin order $T < T_{spin} = 42$ K.
- The in-plane resistivity ρ_{ab} drops rapidly to zero from T_{spin} to T_{KT} (the Kosterlitz–Thouless (KT) transition).
- ρ_{ab} shows KT behavior for $T_{spin} > T > T_{KT}$.
- ρ_c increases as T decreases for $T > T^{**} \approx 35$ K.
- $\rho_c \rightarrow 0$ as $T \rightarrow T_{3D} = 10$ K (the bulk 3D resistive transition).
- $\rho_c / \rho_{ab} \rightarrow \infty$ for $T_{KT} > T > T_{3D}$.
- There is a Meissner state only below $T_c = 4$ K.

How do we understand these remarkable effects that can be summarized as follows: There is a broad temperature range, $T_{3D} < T < T_{2D}$ with 2D superconductivity but not in 3D, as if there is no interlayer Josephson coupling. In this regime there is both striped charge and spin order. This can only happen if there is a special symmetry of the superconductor in the striped state that leads to an almost complete cancellation of the c-axis Josephson coupling.

What else do we know? The stripe state in the LTT (“low temperature tetragonal”) crystal structure of $\text{La}_{2-x}\text{Ba}_x\text{CuO}_4$ has two planes in the unit cell. Stripes in the 2nd neighbor planes are shifted by half a period to minimize the Coulomb interaction: 4 planes per unit cell. The anti-ferromagnetic spin order suffers a π phase shift across the charge stripe which has period 4. Berg et al. [5] proposed that the superconducting order is also striped and also suffers a π phase shift. The superconductivity resides in the spin gap regions and there is a π phase shift in the SC order across the anti-ferromagnetic regions (Fig. 2.19).

The PDW SC state has *intertwined* striped charge, spin and superconducting orders.¹⁶

¹⁶ While there is some numerical evidence for a state of this type in variational Monte Carlo calculations [115] and in slave particle mean field theory [114, 146] (see, however, Ref.[147, 148]), a consistent and controlled microscopic theory is yet to be developed. Since the difference between

How does this state solve the puzzle? If this order is perfect, the Josephson coupling between neighboring planes cancels exactly due to the symmetry of the periodic array of π textures, i.e. the spatial average of the SC order parameter is exactly zero. The Josephson couplings J_1 and J_2 between planes two and three layers apart also cancel by symmetry. The first non-vanishing coupling J_3 occurs at four spacings. It is quite small and it is responsible for the non-zero but very low T_c . Defects and/or discommensurations give rise to small Josephson coupling J_0 between neighboring planes.

Are there other interactions? It is possible to have an inter-plane biquadratic coupling involving the product of the SC order parameters between neighboring planes $\Delta_1 \Delta_2$ and the product of spin stripe order parameters also on neighboring planes $\mathbf{M}_1 \cdot \mathbf{M}_2$. However in the LTT structure $\mathbf{M}_1 \cdot \mathbf{M}_2 = 0$ and there is no such coupling. In a large enough perpendicular magnetic field it is possible (spin flop transition) to induce such a term and hence an effective Josephson coupling. Thus in this state there should be a strong suppression of the 3D SC T_c , but not of the 2D SC T_c .

On the other hand, away from $x = 1/8$ there is no perfect commensuration. Discommensurations are defects that induce a finite Josephson coupling between neighboring planes $J_1 |x - 1/8|^2$, leading to an increase of the 3D SC T_c , away from $x = 1/8$. Similar effects arise from disorder which also lead to a rise in the 3D SC T_c .

2.5.1 Landau–Ginzburg Theory of the Pair Density Wave

In what follows we will rely heavily on the results of Refs. [68, 109, 143]. We begin with a description of the order parameters:

1. PDW (Striped) SC:

$$\Delta(\mathbf{r}) = \Delta_{\mathbf{Q}}(\mathbf{r})e^{i\mathbf{Q} \cdot \mathbf{r}} + \Delta_{-\mathbf{Q}}(\mathbf{r})e^{-i\mathbf{Q} \cdot \mathbf{r}} \quad (2.32)$$

complex charge $2e$ singlet pair condensate with wave vector \mathbf{Q} , (i.e. an FFLO type state at zero magnetic field)¹⁷

2. Nematic: detects breaking of rotational symmetry: N , a real neutral pseudo-scalar order parameter
3. Charge stripe: ρ_K , unidirectional charge stripe with wave vector \mathbf{K}
4. Spin stripe order parameter: $S_{\mathbf{Q}}$, a neutral complex spin vector order parameter.

These order parameters have the following transformation properties under rotations by $\pi/2$, $\mathcal{R}_{\pi/2}$:

(Footnote 16 continued)

the energies of the competing states seen numerically is quite small one must conclude that they are all reasonably likely.

¹⁷ A state that is usually described as a pair crystal is commonly known as a pair density wave [149, 150]. However that state cannot be distinguished by symmetry from a (two) CDWs coexisting with a uniform SC.

1. The nematic order parameter changes sign: $N \rightarrow -N$
2. The CDW ordering wave vector rotates: $\rho_{\mathbf{K}} \rightarrow \rho_{\mathcal{R}_{\pi/2}\mathbf{K}}$
3. The SDW ordering wave vector also rotates: $\mathbf{S}_{\mathbf{Q}} \rightarrow \mathbf{S}_{\mathcal{R}_{\pi/2}\mathbf{Q}}$
4. The striped SC (s or d wave) order parameter: $\Delta_{\pm\mathbf{Q}} \rightarrow \pm\Delta_{\pm\mathcal{R}_{\pi/2}\mathbf{Q}}$ (+ for s -wave, - for d - wave)

and by translations by \mathbf{R}

$$N \rightarrow N, \quad \rho_{\mathbf{K}} \rightarrow e^{i\mathbf{K}\cdot\mathbf{R}}\rho_{\mathbf{K}}, \quad \mathbf{S}_{\mathbf{Q}} \rightarrow e^{i\mathbf{Q}\cdot\mathbf{R}}\mathbf{S}_{\mathbf{Q}} \quad (2.33)$$

The Landau–Ginzburg free energy functional is, as usual, a sum of terms of the form

$$\mathcal{F} = \mathcal{F}_2 + \mathcal{F}_3 + \mathcal{F}_4 + \dots \quad (2.34)$$

where \mathcal{F}_2 , the quadratic term, is simply a sum of decoupled terms for each order parameter. There exist a number of trilinear terms mixing several of the order parameters described above. They are

$$\begin{aligned} \mathcal{F}_3 = & \gamma_s[\rho_{-\mathbf{K}}\mathbf{S}_{\mathbf{Q}} \cdot \mathbf{S}_{\mathbf{Q}} + \rho_{-\bar{\mathbf{K}}}\mathbf{S}_{\bar{\mathbf{Q}}} \cdot \mathbf{S}_{\bar{\mathbf{Q}}} + \text{c.c.}] \\ & + \gamma_{\Delta}[\rho_{-\mathbf{K}}\Delta_{-\mathbf{Q}}^*\Delta_{\mathbf{Q}} + \rho_{-\bar{\mathbf{K}}}\Delta_{-\bar{\mathbf{Q}}}^*\Delta_{\bar{\mathbf{Q}}} + \text{c.c.}] \\ & + g_{\Delta}N[\Delta_{\mathbf{Q}}^*\Delta_{\mathbf{Q}} + \Delta_{-\mathbf{Q}}^*\Delta_{-\mathbf{Q}} - \Delta_{\bar{\mathbf{Q}}}^*\Delta_{\bar{\mathbf{Q}}} - \Delta_{-\bar{\mathbf{Q}}}^*\Delta_{-\bar{\mathbf{Q}}}] \\ & + g_s N[\mathbf{S}_{-\mathbf{Q}} \cdot \mathbf{S}_{\mathbf{Q}} - \mathbf{S}_{-\bar{\mathbf{Q}}} \cdot \mathbf{S}_{\bar{\mathbf{Q}}}] \\ & + g_c N[\rho_{-\mathbf{K}}\rho_{\mathbf{K}} - \rho_{-\bar{\mathbf{K}}}\rho_{\bar{\mathbf{K}}}], \end{aligned} \quad (2.35)$$

where $\bar{\mathbf{Q}} = \mathcal{R}_{\pi/2}\mathbf{Q}$, and $\bar{\mathbf{K}} = \mathcal{R}_{\pi/2}\mathbf{K}$. The fourth order term, which is more or less standard, is shown explicitly below.

Several consequences follow directly from the form of the trilinear terms, Eq. 2.35. One is that, at least in a fully translationally invariant system, the first two terms of Eq. 2.35 imply a relation between the ordering wave vectors: $\mathbf{K} = 2\mathbf{Q}$. Also, as we will see below, these terms imply the existence of vortices of the SC order with *half* the flux quantum.

Another important feature of the PDW SC is that it implies the existence of a non-zero charge $4e$ uniform SC state. Indeed, if we denote by Δ_4 the (uniform) charge $4e$ SC order parameter, then the following term in the LG expansion is allowed

$$\mathcal{F}'_3 = g_4 \left[\Delta_4^* \left(\Delta_{\mathbf{Q}}\Delta_{-\mathbf{Q}} + \text{rotation by } \frac{\pi}{2} \right) + \text{c.c.} \right] \quad (2.36)$$

Hence, the existence of striped SC order (PDW) implies the existence of uniform charge $4e$ SC order!¹⁸

¹⁸ A charge $4e$ SC order parameter is an expectation value of a four fermion operator.

We should also consider a different phase in which there are coexisting uniform and striped SC orders, as it presumably happens at low temperatures in $\text{La}_{2-x}\text{Ba}_x\text{CuO}_4$. If this is so, there is a non-zero PDW SC order parameter $\Delta_{\mathbf{Q}}$ as well as an uniform (d-wave) SC order parameter Δ_0 which are coupled by new (also trilinear) terms in the LG free energy of the form

$$\mathcal{F}_{3,u} = \gamma_{\Delta} \Delta_0^* (\rho_{\mathbf{Q}} \Delta_{-\mathbf{Q}} + \rho_{-\mathbf{Q}} \Delta_{\mathbf{Q}}) + g_{\rho} \rho_{-2\mathbf{Q}} \rho_{\mathbf{Q}}^2 + \frac{\pi}{2} \text{rotation} + \text{c.c.} \quad (2.37)$$

If $\Delta_0 \neq 0$ and $\Delta_{\mathbf{Q}} \neq 0$, there is a new $\rho_{\mathbf{Q}}$ component of the charge order!. Also, the small uniform component Δ_0 removes the sensitivity to quenched disorder of the PDW SC state.

2.5.2 Charge $4e$ SC Order and the Topological Excitations of the PDW SC State

If there is a uniform charge $4e$ SC order, its vortices must be quantized in units of $hc/4e$ instead of the conventional $hc/2e$ flux quantum. Hence, half- vortices are natural in this state. To see how they arise let us consider a system deep in the PDW SC state so that the magnitude of all the order parameters is essentially constant, but their phases may vary. Thus we can write the PDW SC order parameter as

$$\Delta(\mathbf{r}) = |\Delta_{\mathbf{Q}}| e^{i\mathbf{Q} \cdot \mathbf{r} + i\theta_{+}(\mathbf{r})} + |\Delta_{-\mathbf{Q}}| e^{-i\mathbf{Q} \cdot \mathbf{r} + i\theta_{-}(\mathbf{r})} \quad (2.38)$$

where (by inversion symmetry) $|\Delta_{\mathbf{Q}}| = |\Delta_{-\mathbf{Q}}| = \text{const.}$ It will be convenient to define the new phase fields $\theta_{\pm}(\mathbf{r})$ by

$$\theta_{\pm}(\mathbf{r}) = \frac{1}{2} (\theta_{+}(\mathbf{r}) \pm \theta_{-}(\mathbf{r})) . \quad (2.39)$$

Likewise, in the same regime the CDW order parameter can be written as

$$\rho(\mathbf{r}) = |\rho_{\mathbf{K}}| \cos(\mathbf{K} \cdot \mathbf{r} + \phi(\mathbf{r})) \quad (2.40)$$

(and a similar expression for the SDW order parameter.) In this notation, the second trilinear term shown in Eq. 2.35 takes the form

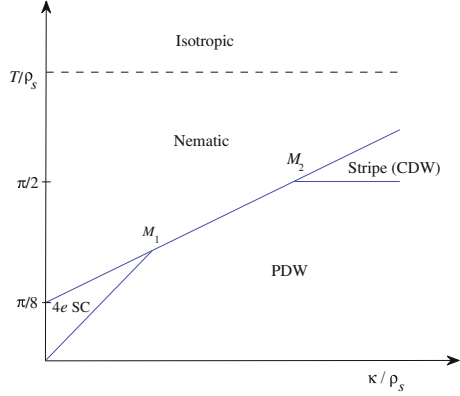
$$\mathcal{F}_{3,\gamma} = 2\gamma_{\Delta} |\rho_{\mathbf{K}} \Delta_{\mathbf{Q}} \Delta_{-\mathbf{Q}}| \cos(2\theta_{-}(\mathbf{r}) - \phi(\mathbf{r})) \quad (2.41)$$

Hence, the *relative phase* θ_{-} is locked to ϕ , the Goldstone boson of the CDW (the phason), and they are not independently fluctuating fields. Furthermore, the phase fields $\theta_{\pm\mathbf{Q}}$ are defined modulo 2π while θ_{+} is defined only modulo π .

This analysis implies that the allowed topological excitations of the PDW SC are

1. A conventional SC vortex with $\Delta\theta_{+} = 2\pi$ and $\Delta\phi = 0$, with topological charges (1,0).

Fig. 2.20 Schematic phase diagram of the thermal melting of the PDW state



2. A bound state of a $1/2$ vortex and a CDW dislocation, $\Delta\theta_+ = \pi$ and $\Delta\phi = 2\pi$, with topological charges $(\pm 1/2, \pm 1/2)$ (any such combination is allowed).
3. A double dislocation, $\Delta\theta_+ = 0$ and $\Delta\phi = 4\pi$, with topological charge $(0, 1)$.

All three topological defects have logarithmic interactions.

There are now three different pathways to melt the PDW SC [68], depending which one of these topological excitations becomes relevant (in the Kosterlitz–Thouless RG sense [151]) first. To determine the relevance or irrelevance of an operator \mathcal{O} one must first compute its scaling dimension $\Delta_{\mathcal{O}}$ given by the exponent of its correlation function

$$\langle \mathcal{O}(\mathbf{x}) \mathcal{O}(\mathbf{y}) \rangle = \frac{1}{|\mathbf{X} - \mathbf{y}|^{2\Delta_{\mathcal{O}}}} \quad (2.42)$$

For the case of a topological excitation (vortices, dislocations, etc) this amounts to the computation of the ratio of the partition function of a system without topological excitations with two operators that create these excitations inserted at \mathbf{X} and \mathbf{y} (respectively) with the free partition function without these insertions. It is straightforward to show [3, 152, 153] that at temperature T , the scaling dimension of a topological excitation of topological charge (p, q) is

$$\Delta_{p,q} = \frac{\pi}{T} \left(\rho_{sc} p^2 + \kappa_{CDW} q^2 \right) \quad (2.43)$$

where ρ_{sc} is the superfluid density (the stiffness of the θ_+ phase field) and κ_{CDW} is the CDW stiffness (that is, of the ϕ phase field).

As usual the criterion of relevance is that an operator that creates an excitation is relevant if its scaling dimension is equal to the space dimension (for details see, for instance, Ref.[153]) which in this case is 2. This condition, $\Delta_{p,q} = 2$ for each one

of the topological excitations listed above, leads to the phase thermal phase diagram shown in Fig. 2.20.¹⁹

Thus, the PDW state may thermally melt in three possible ways:

1. First into a CDW phase by proliferating conventional SC vortices, a $(1, 0)$ topological excitation, followed by a subsequent melting of the CDW into the normal (Ising nematic) high temperature phase. This scenario corresponds to the right side of the phase diagram and, presumably, is what happens in $\text{La}_{2-x}\text{Ba}_x\text{CuO}_4$.
2. A direct melting into the normal (Ising nematic) phase by proliferation of fractional vortices, with topological charge $(\pm 1/2, \pm 1/2)$.
3. Melting into a charge $4e$ uniform SC phase by proliferation of double dislocations, with topological charge $(0, 1)$.

The prediction that the PDW state should effectively have a uniform charge $4e$ SC order with an anomalous $hc/4e$ flux quantization leads to a direct test of this state. this can be done by searching for fractional vortices, and similarly of fractional periodicity in the Josephson effect (and Shapiro steps). Similarly, the prediction that in the phase in which an uniform (d-wave) SC is present there should be a charge-ordered state with period equal to that of the SC (and of the SDW) is another direct test of this theory.

2.6 Nematic Phases in Fermi Systems

We now turn to the theory of the nematic phases. The nematic phase is the simplest of the liquid crystal states. In this state the system is electronically uniform but anisotropic. There are two ways to access this phase. One is by a direct transition from the isotropic electronic fluid. The other is by melting (thermal or quantum mechanical) the stripe phase. We will consider both cases. We will begin with the first scenario in its simplest description as a *Pomeranchuk instability* of a Fermi liquid.

2.6.1 The Pomeranchuk Instability

The central concept of the Landau theory of the Fermi liquid [157] is the quasiparticle. A Landau quasiparticle is the elementary excitation of a Fermi liquid with the same quantum numbers as a non-interacting electron. A necessary condition for the Landau theory to work is the condition that the quasiparticle becomes sharp (or well defined) at asymptotically low energies, i.e. as the Fermi surface is

¹⁹ A more elaborate version of this phase diagram, based on a one-loop Kosterlitz RG calculation for physically very different systems with the same RG structure system, was given in Refs. [154–156].

approached. For the Landau quasiparticle to be well defined it is necessary that the quasiparticle width, i.e. the quasiparticle scattering rate, to be small on the scale of the quasiparticle energy. The quasiparticle scattering rate, the imaginary part of the electron self energy, $\Sigma''(\omega, \mathbf{p})$, is determined by the quasiparticle interactions, which in the Landau theory of the Fermi liquid are parametrized by the *Landau parameters*. Except for the BCS channel, the forward scattering interactions (with or without spin flip) are the only residual interactions among the quasiparticles that survive at low energies [158, 159].

The Landau “parameters” are actually functions $F^{S,A}(\mathbf{p}, \mathbf{p}')$ that quantifying the strength of the forward scattering interactions among quasiparticles at low energies with momenta \mathbf{p} and \mathbf{p}' close to the Fermi surface in the singlet (charge) channel (S) or the triplet (spin) channel (A). For a translationally invariant system it depends only on the difference of the two momenta, $F(\mathbf{p}, \mathbf{p}') = F(\mathbf{p} - \mathbf{p}')$. Furthermore, if the system is also rotationally invariant, the Landau parameters can be expressed in an angular momentum basis. In 3D they take the form $F_{\ell,m}^{S,A}$ (with $\ell = 0, 1, 2, \dots$ and $|m| \leq \ell$), while in 2D they are simply $F_m^{S,A}$ (where $m \in \mathbb{Z}$). We will see below that in some cases of interest we will also need to keep the dependence on a small momentum transfer in the Landau parameters (i.e. \mathbf{p} and \mathbf{p}' will not be precisely at the FS) even though it amounts to keeping a technically irrelevant interaction. On the other hand, for a lattice model rotational invariance is always broken down to the point (or space) group symmetry of the lattice. In that case the Landau parameters are classified according to the irreducible representations of the point (or space) group of the lattice, e.g. the \mathcal{C}_4 group of the square lattice.

It is well known in the Landau theory of the Fermi liquid that the thermodynamic stability of the Fermi liquid state requires that the Landau parameters cannot be too negative. This argument, due to Pomeranchuk [160], implies that if in one channel the forward scattering interaction becomes sufficiently negative (attractive) to overcome the stabilizing effects of the Pauli pressure, the Fermi liquid becomes unstable to a distortion of the FS with the symmetry of the unstable channel.²⁰

Oganesyan et al. [39] showed that in a 2D system of interacting fermions, the Pomeranchuk instability in fact marks a quantum phase transition to a *nematic Fermi fluid*. We will discuss this theory below in some detail. While the theory of Oganesyan and coworkers applied to a system in the continuum, Kee and coworkers [161, 162] considered a lattice model. Hints of nematic order in specific models had in fact been discovered independently (but not recognized as such originally), notably by the work of Metzner and coworkers [163–167].²¹

There is by now a growing literature on the nematic instability. Typically the models, both in the continuum [39] or on different lattices [161, 171, 172], are

²⁰ Although the Pomeranchuk argument is standard and reproduced in all the textbooks on Fermi liquid theory (see, e.g. Ref.[157]) the consequences of this instability were not pursued until quite recently.

²¹ In fact, perturbative renormalization group calculations [168, 169] have found a runaway flow in the $d_{x^2-y^2}$ particle-hole channel, which is a nematic instability, but it was not recognized as such. See, however, Ref.[170].

solved within a Hartree–Fock type approximation (with all the limitations that such an approach has), or in special situations such as vicinity to Van Hove singularities [162, 163] and certain degenerate band crossings [173] (where the theory is better controlled), or using uncontrolled approximations to strong coupling systems such as slave fermion/boson methods [174, 175]. A strong coupling limit of the Emery model of the cuprates was shown to have a nematic state in Ref. [176] (we will review this work below). Finally some non-perturbative work on the nematic quantum phase transition has been done using higher dimensional bosonization in Refs. [177, 178] and by RG methods [179].

Extensions of these ideas have been applied to the problem of the nematic phase seen in the metamagnetic bilayer ruthenate $\text{Sr}_3\text{Ru}_2\text{O}_7$ relying either on the van Hove mechanism [180–183] or on an orbital ordering mechanism [184, 185], and in the new iron-based superconducting compounds [77, 78]. More recently nematic phases of different types have been argued to occur in dipolar Fermi gases of ultra-cold atoms [186, 187].²²

2.6.2 The Nematic Fermi Fluid

Here I will follow the work of Oganesyan, Kivelson and Fradkin [39] and consider first the instability in the charge (symmetric) channel. Oganesyan et al. defined a charge nematic order parameter for a two-dimensional Fermi fluid as the 2×2 symmetric traceless tensor of the form

$$\hat{Q}(x) \equiv -\frac{1}{k_F^2} \Psi^\dagger(\mathbf{r}) \begin{pmatrix} \partial_x^2 - \partial_y^2 & 2\partial_x\partial_y \\ 2\partial_x\partial_y & \partial_x^2 - \partial_y^2 \end{pmatrix} \Psi(\mathbf{r}), \quad (2.44)$$

It can also be represented by a complex valued field $Q_2(x)$ whose expectation value in the nematic phase is

$$\langle Q_2 \rangle \equiv \langle \Psi^\dagger (\partial_x + i\partial_y)^2 \Psi \rangle = |Q_2| e^{2i\theta_2} = Q_{11} + iQ_{12} \neq 0 \quad (2.45)$$

Q_2 transforms under rotations in the representation of angular momentum $\ell = 2$. Oganesyan et al. showed that if $\langle Q_2 \rangle \neq 0$ then the Fermi surface *spontaneously* distorts and becomes an ellipse with eccentricity $\propto Q$. This state breaks rotational invariance mod π .

More complex forms of order can be considered by looking at particle-hole condensates with angular momenta $\ell > 2$ (see Ref. [14])

$$\langle Q_\ell \rangle = \langle \Psi^\dagger (\partial_x + i\partial_y)^\ell \Psi \rangle \quad (2.46)$$

²² Another class of nematic state can occur inside a $d_{x^2-y^2}$ superconductor. This quantum phase transition involves primarily the nodal quasiparticles of the superconductor and it is tractable within large N type approximations [188, 189].

For ℓ odd, this condensate breaks rotational invariance (mod $2\pi/\ell$). It also breaks parity \mathcal{P} and time reversal \mathcal{T} but \mathcal{PT} is invariant. For example the condensate with $\ell = 3$ is effectively equivalent to the “Varma loop state” [15, 190]. The states with ℓ even are also interesting, e.g. a hexatic state is described by a particle-hole condensate with $\ell = 6$ [191].

In a 3D system, the anisotropic state is described by an order parameter Q_{ij} which is a traceless symmetric tensor (as in conventional liquid crystals [2, 3]). More generally, we can define an order parameter that transforms under the (ℓ, m) representation of the group of $SO(3)$ spatial rotations.

Oganesyan et al. considered in detail a Fermi liquid type model of the nematic transition and developed a (Landau) theory of the transition (“Landau on Landau”). The Hamiltonian of this model describes (spinless) fermions in the continuum with a two-body interaction corresponding to the $\ell = 2$ particle-hole angular momentum channel. The Hamiltonian is

$$H = \int d\mathbf{r} \Psi^\dagger(\mathbf{r}) \epsilon(\nabla) \Psi(\mathbf{r}) + \frac{1}{4} \int d\mathbf{r} \int d\mathbf{r}' F_2(\mathbf{r} - \mathbf{r}') \text{Tr}[\hat{Q}(\mathbf{r}) \hat{Q}(\mathbf{r}')] \quad (2.47)$$

where the free-fermion dispersion (near the FS) is $\epsilon(\mathbf{k}) = v_F q [1 + a(\frac{q}{k_F})^2]$ (here $q \equiv |\mathbf{k}| - k_F$), and the interaction is given in terms of the coupling

$$F_2(\mathbf{r}) = (2\pi)^{-2} \int d\mathbf{q} e^{i\mathbf{q} \cdot \mathbf{r}} \frac{F_2}{1 + \kappa F_2 q^2} \quad (2.48)$$

where F_2 is the $\ell = 2$ Landau parameter, and κ measures the range of these interactions. Notice that we have kept a cubic momentum dependence in the dispersion, which is strongly irrelevant in the Landau Fermi liquid phase (but it is needed to insure stability in the broken symmetry state).

The Landau energy density functional for this model has the form (which can be derived by Hartree–Fock methods or, equivalently, using a Hubbard–Stratonovich decoupling)

$$\mathcal{U}[Q] = \mathcal{E}(Q) - \frac{\tilde{\kappa}}{4} \text{Tr}[Q D Q] - \frac{\tilde{\kappa}'}{4} \text{Tr}[Q^2 D Q] + \dots \quad (2.49)$$

Here we have used the 2×2 symmetric tensor $D_{ij} \equiv \partial_i \partial_j$, and $\tilde{\kappa}$ and $\tilde{\kappa}'$ are the two effective Franck constants (see Ref. [3, 39]). The uniform part of the energy functional, $\mathcal{E}(Q)$, is given by

$$\mathcal{E}(Q) = \mathcal{E}(\mathbf{0}) + \frac{A}{4} \text{Tr}[Q^2] + \frac{B}{8} \text{Tr}[Q^4] + \dots \quad (2.50)$$

where

$$A = \frac{1}{2N_F} + F_2 \quad (2.51)$$

N_F is the density of states at the Fermi surface, and the coefficient of the quartic term is

$$B = \frac{3aN_F|F_2|^3}{8E_F^2} \quad (2.52)$$

$E_F \equiv v_F k_F$ is the Fermi energy [39]. The (normal) Landau Fermi liquid phase is stable provided $A > 0$, or, what is the same, if $2N_F F_2 > -1$ which is the Pomeranchuk condition (in this notation). On the other hand, thermodynamic stability also requires that $B > 0$, which implies that the coefficient of the cubic correction in the dispersion be positive, $a > 0$. If this condition is not satisfied, as it is the case in simple lattice models [161], higher order terms must be kept to insure stability.

However, in this case the transition is typically first order.

This model has two phases:

- an isotropic Fermi liquid phase, $A > 0$
- a nematic (non-Fermi liquid) phase, $A < 0$

separated by a quantum critical point at the Pomeranchuk value, $2N_F F_2 = -1$.

Let us discuss the quantum critical behavior. We will parametrize the distance to the Pomeranchuk QCP by

$$\delta = \frac{1}{2N_F} + F_2 \quad (2.53)$$

and define $s = \omega/qv_F$. The transverse collective nematic modes have Landau damping at the QCP [39]. Their effective action has the form

$$S_{\perp} = \int d\omega d\mathbf{q} \left(\kappa q^2 + \delta - i \frac{|\omega|}{qv_F} \right) |\mathcal{Q}_{\perp}(\omega, \mathbf{q})|^2 \quad (2.54)$$

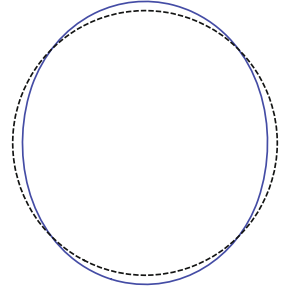
which implies that the dynamic critical exponent is $z=3$.²³

According to the standard perturbative criterion of Hertz [193] and Millis [194], the quantum critical behavior is that of an equivalent ϕ^4 type field theory in dimensions $D = d + z$ which in this case is $D=5$. Since the upper critical (total) dimension is 4, the Hertz-Millis analysis would predict that mean field theory is asymptotically exact and that the quartic (and higher) powers of the order parameter field are *irrelevant* at the quantum critical point (for an extensive discussion see Ref. [195]). However we will see below that while this analysis is correct for the bosonic sector of the theory, i.e. the behavior of the bosonic collective modes such as the order parameter itself, the situation is far less clear in the fermionic sector. We will come back to this question below.

Let us discuss now the physics of the nematic phase. In the nematic phase the FS is spontaneously distorted along the direction of the (director) order parameter

²³ There are other collective modes at higher energies. In particular there is an underdamped longitudinal collective mode with $z=2$ [39]. These higher energy modes contribute to various crossover effects [192], but decouple in the asymptotic quantum critical regime.

Fig. 2.21 Spontaneous distortion of the Fermi surface in the nematic phase of a 2D Fermi fluid



(see Fig. 2.21) and exhibits a quadrupolar (*d*-wave) pattern, i.e. the Fermi wave vector has an angular dependence $k_F(\theta) \propto \cos 2\theta$ (in 2D). Indeed, in the nematic phase the Hartree–Fock wave function is a Slater determinant whose variational parameters determine the shape of the FS.

In principle, a wave function with a similar structure can be used to suggest (as it was done in Ref. [39]) that it should also apply to the theory of the electronic nematic state observed in the 2DEG in large magnetic fields. In that framework one thinks of the 2DEG in a half-filled Landau level as an equivalent system of “composite fermions” [196], fermions coupled to a Chern-Simons gauge field [197, 198]. It has been argued [199] that this state can be well described by a Slater determinant wave function, projected onto the Landau level. The same procedure can be applied to the nematic wave function, and some work has been done along this direction [200]. A problem that needs to be solved first is the determination of the Landau parameters of the composite fermions of which very little (that makes sense) is known.

A simple (Drude) calculation then shows that the transport is anisotropic. The resistivity in the nematic phase, due to scattering from structureless isotropic impurities, yields the result that the resistivity tensor is anisotropic with an anisotropy controlled by the strength of the nematic order parameter:

$$\frac{\rho_{xx} - \rho_{yy}}{\rho_{xx} + \rho_{yy}} = \frac{1}{2} \frac{m_y - m_x}{m_y + m_x} = \frac{\text{Re } Q}{E_F} + O(Q^3) \quad (2.55)$$

where m_x and m_y are the (anisotropic) effective masses of the quasiparticles in the nematic state. In general it is a more complex odd function of the order parameter.

In the nematic phase the transverse Goldstone boson is generically *overdamped* (Landau damping) except for a finite set of symmetry directions, $\phi = 0, \pm\pi/4, \pm\pi/2$, where it is *underdamped*. Thus, $z=3$ scaling also applies to the nematic phase for general directions. Naturally, in a lattice system the rotational symmetry is not continuous and the transverse Goldstone modes are gapped. However, the continuum prediction still applies if the lattice symmetry breaking is weak and if either the energy or the temperature is larger than the lattice anisotropy scale.

On the other hand, the behavior of the fermionic correlators is much more strongly affected. To one loop order, the quasiparticle scattering rate, $\Sigma''(\omega, \mathbf{p})$ is found to have the behavior

$$\Sigma''(\omega, \mathbf{k}) = \frac{\pi}{\sqrt{3}} \frac{(\kappa k_F^2)^{1/3}}{\kappa N_F} \left| \frac{k_x k_y}{k_F^2} \right|^{4/3} \left| \frac{\omega}{2v_F k_F} \right|^{2/3} + \dots \quad (2.56)$$

for \mathbf{k} along a general direction. On the other hand, along a symmetry direction

$$\Sigma''(\omega) = \frac{\pi}{3N_F \kappa} \frac{1}{(\kappa k_F^2)^{1/4}} \left| \frac{\omega}{v_F k_F} \right|^{3/2} + \dots \quad (2.57)$$

Hence, the entire nematic phase is a non-Fermi liquid (again, with the caveat on lattice symmetry breaking effects).

At the Pomeranchuk quantum critical point the quasiparticle scattering rate obeys the same (one loop) scaling shown in Eq. 2.56, $\Sigma''(\omega) \propto |\omega|^{2/3}$, both in continuum [39] and lattice models [167], but it is isotropic. In the quantum critical regime the electrical resistivity obeys a $T^{4/3}$ law [201]. Also, both in the nematic phase (without lattice anisotropy) and in the quantum critical regime, the strong nematic fluctuations yield an electronic contribution to the specific heat that scales as $T^{2/3}$ (consistent with the general scaling form $T^{d/z}$ [195]) which dominates over the standard Fermi liquid linear T dependence at low temperatures [157].

Since $\Sigma''(\omega) \gg \Sigma'(\omega)$ (as $\omega \rightarrow 0$), we need to assess the validity of these results as they signal a *failure of perturbation theory*. To this end we have used higher dimensional bosonization as a non-perturbative tool [202–206]. Higher dimensional bosonization reproduces the collective modes found in Hartree–Fock+ RPA and is consistent with the Hertz-Millis analysis of quantum criticality:

$d_{\text{eff}} = d + z = 5$ [177, 178]. Within the higher bosonization approach, the fermion propagator takes the form

$$G_F(x, t) = G_0(x, t) Z(x, t) \quad (2.58)$$

where $G_0(x, t)$ is the free fermion propagator. In the Fermi liquid phase the quantity $Z(x, t)$ approaches a finite constant at long distances and at long times leading to a reduction of the quasiparticle residue Z (see, e.g. [178] and references therein). However, at the Nematic-FL QCP, $Z(x, t)$ becomes singular, and the full quasiparticle propagator now has the form

$$G_F(x, 0) = G_0(x, 0) e^{-\text{const.} |x|^{1/3}} \quad (2.59)$$

at equal times, and

$$G_F(0, t) = G_0(0, t) e^{-\text{const.} |t|^{-2/3} \ln t} \quad (2.60)$$

at equal positions. Notice that these expressions are consistent with the expected $z=3$ scaling even though the time and space dependence is not a power law. The quasiparticle residue is then seen to vanish at the QCP:

$$Z = \lim_{x \rightarrow \infty} Z(x, 0) = 0 \quad (2.61)$$

However, the single particle density of states, $N(\omega) = -\frac{1}{\pi} \text{Im}G(\omega, 0)$, turns out to have a milder behavior:

$$N(\omega) = N(0) \left(1 - \text{const}' \cdot |\omega|^{2/3} \ln \omega \right) \quad (2.62)$$

Let us now turn to the behavior near the QCP. For $T=0$ and $\delta \ll 1$ (on the Fermi Liquid side) the quasiparticle residue is now finite (see Fig. 2.22)

$$Z \propto e^{-\text{const.}/\sqrt{\delta}} \quad (2.63)$$

but its dependence on the distance to the nematic QCP is an essential singularity. On the other hand, right at the QCP ($\delta = 0$), and for a temperature range $T_F \gg T \gg T_k$, the equal-time fermion propagator is found to vanish exactly

$$Z(x, 0) \propto e^{-\text{const.} T x^2 \ln(L/x)} \rightarrow 0 \quad \text{as } L \rightarrow \infty \quad (2.64)$$

but, the equal-position propagator $Z(0, t)$ remains *finite* in the thermodynamic limit, $L \rightarrow \infty$! This behavior has been dubbed “Local quantum criticality”.²⁴ On the other hand, irrelevant quartic interactions of strength u lead to a renormalization of δ that smears the QCP at $T > 0$ [194]

$$\delta \rightarrow \delta(T) = -uT \ln \left(uT^{1/3} \right) \quad (2.65)$$

leading to a milder behavior at equal-times

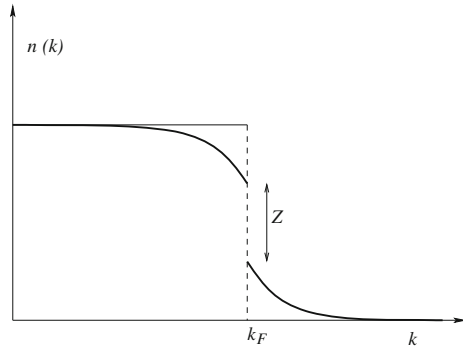
$$Z(x, 0) \propto e^{-\text{const.} T x^2 \ln(\xi/x)} \quad \text{where } \xi = \delta(T)^{-1/2} \quad (2.66)$$

These results are far from being universally accepted. Indeed Chubukov and coworkers [208–210] have argued that the perturbative non-Fermi liquid behavior, $\Sigma''(\omega) \sim \omega^{2/3}$, which is also found at a ferromagnetic metallic QCP, persists to all orders in perturbation theory and can recover the results of higher dimensional bosonization only by taking into account the most infrared divergent diagrams. The same non-Fermi liquid one-loop perturbative scaling has been found in other QCPs such as in the problem of fermions (relativistic or not) at finite density coupled to dynamical gauge fields. This problem has been discussed in various settings ranging from hot and dense QED and QCD [211–213], to the gauge-spinon system in RVB approaches to high T_c superconductors [214–219] to the compressible states of the 2DEG in large magnetic fields [198]. In all cases these authors have also argued that the one-loop scaling persists to all orders. In a recent paper Metlitski and Sachdev [179] found a different scaling behavior.

We end with a brief discussion on the results in lattice models of the nematic quantum phase transition. This is important since, with the possible exception of the 2DEG in large magnetic fields and in ultra-cold atomic systems, all strongly

²⁴ A similar behavior was found in the quantum Lifshitz model at its QCP [207].

Fig. 2.22 The discontinuity of the quasiparticle momentum distribution function in a Fermi liquid. Z is the quasiparticle residue at the Fermi surface



correlated systems of interest have very strong lattice effects. The main difference between the results in lattice models and in the continuum is that in the former the quantum phase transition (at the mean field, Hartree–Fock, level) has a strong tendency to be first order. Although fluctuations can soften the quantum transition and turn the system quantum critical (as emphasized in Ref. [220]), nevertheless there are good reasons for the transition to be first order more or less generically. One is that if the stabilizing quartic terms are negative (e.g. say due to the band structure), this also results, in the case of a lattice system, in a Lifshitz transition at which the topology of the FS changes from closed to open. This cannot happen in a continuous way.

2.7 Generalizations: Unconventional Magnetism and Time Reversal Symmetry Breaking

We will now consider briefly the extension of these ideas to the spin-triplet channel [16, 17]. In addition to particle-hole condensates in the singlet (charge) channel we will be interested in particle-hole condensates in the spin (triplet) channel. In 2D the order parameters for particle-hole condensates in the spin triplet channel are (here $\alpha, \beta = \uparrow, \downarrow$)

$$\mathcal{Q}_\ell^a(r) = \langle \Psi_\alpha^\dagger(r) \sigma_{\alpha\beta}^a (\partial_x + i\partial_y)^\ell \Psi_\beta(r) \rangle \equiv n_1^a + i n_2^a \quad (2.67)$$

These order parameters transform under both $SO(2)$ spatial rotations and under the internal $SU(2)$ symmetry of spin. If $\ell \neq 0$ the state has a broken rotational invariance in space and in spin space. These states are a particle-hole condensate analog of the unconventional superconductors and superfluids, such as He_3A and He_3B . Indeed one may call these states “unconventional magnetism” as the $\ell = 0$ (isotropic) state is just a ferromagnet. In 2D these states are then given in terms of two order parameters,

each in the vector (adjoint) representation of the $SU(2)$ spin symmetry.²⁵ We will discuss only the 2D case. The order parameters obey the following transformation laws:

1. Time reversal:

$$\mathcal{T} \mathcal{Q}_\ell^a \mathcal{T}^{-1} = (-1)^{\ell+1} \mathcal{Q}_\ell^a \quad (2.68)$$

2. Parity:

$$\mathcal{P} \mathcal{Q}_\ell^a \mathcal{P}^{-1} = (-1)^\ell \mathcal{Q}_\ell^a \quad (2.69)$$

3. \mathcal{Q}_ℓ^a rotates under an $SO_{\text{spin}}(3)$ transformation, and transforms as $\mathcal{Q}_\ell^a \rightarrow \mathcal{Q}_\ell^a e^{i\ell\theta}$ under a rotation in space by an angle θ .
4. \mathcal{Q}_ℓ^a is invariant under a rotation by π/ℓ followed by a spin flip.

Wu and collaborators [16, 17] have shown that these phases can also be accessed by a Pomeranchuk instability in the spin (triplet) channel.²⁶ They showed that the Landau-Ginzburg free energy takes the simple form

$$F[n] = r(|\mathbf{n}_1|^2 + |\mathbf{n}_2|^2) + v_1(|\mathbf{n}_1|^2 + |\mathbf{n}_2|^2)^2 + v_2 |\mathbf{n}_1 \times \mathbf{n}_2|^2 \quad (2.70)$$

The Pomeranchuk instability occurs at $r=0$, i.e., for $N_F F_\ell^A = -2$ (with $\ell \geq 1$), where F_ℓ^A are the Landau parameters in the spin- triplet channel. Notice that this free energy is invariant only by global $SO(3)$ rotations involving both vector order parameters, \mathbf{n}_1 and \mathbf{n}_2 . Although at this level the $SO(3)$ invariance is seemingly an internal symmetry, there are gradient terms that lock the internal $SO(3)$ spin rotations to the “orbital” spatial rotations (see Ref. [17]). A similar situation also occurs in classical liquid crystals [3].

At the level of the Landau–Ginzburg theory the system has two phases with broken $SO(3)$ invariance:

1. If $v_2 > 0$, then the two $SO(3)$ spin vector order parameters must be parallel to each other, $\mathbf{n}_1 \times \mathbf{n}_2 = 0$. They dubbed this the “ α ” phase. In the α phases the up and down Fermi surfaces are distorted (with a pattern determined by ℓ) but are rotated from each other by π/ℓ . One case of special interest is the α phase with $\ell = 2$. This is the “nematic-spin-nematic” discussed briefly in Ref. [4].²⁷ In this phase the spin up and spin down FS have an $\ell = 2$ quadrupolar (nematic) distortion but are rotated by $\pi/2$ (see Fig. 2.23).
2. Conversely, if $v_2 < 0$, then the two $SO(3)$ spin vector order parameters must be orthogonal to each other, $\mathbf{n}_1 \cdot \mathbf{n}_2 = 0$ and $|\mathbf{n}_1| = |\mathbf{n}_2|$. Wu et al. dubbed these

²⁵ In 3D the situation is more complex and the possible are more subtle. In particular, in 3D there are three vector order parameters involved [17].

²⁶ The $\ell = 0$ case is, of course, just the conventional Stoner ferromagnetic instability.

²⁷ The term “nematic-spin-nematic” is a poor terminology. A spin nematic is a state with a magnetic order parameter that is a traceless symmetric tensor, which this state does not.

Fig. 2.23 The α -phases in the $\ell = 1$ and $\ell = 2$ spin triplet channels. The Fermi surfaces exhibit the p and d -wave distortions, respectively

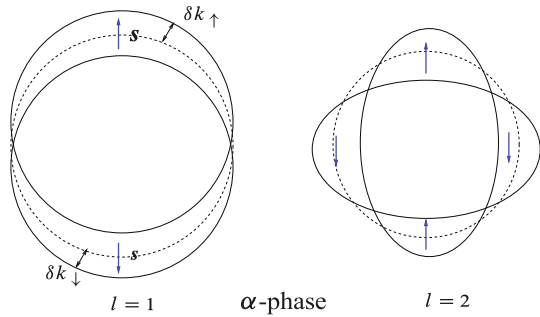
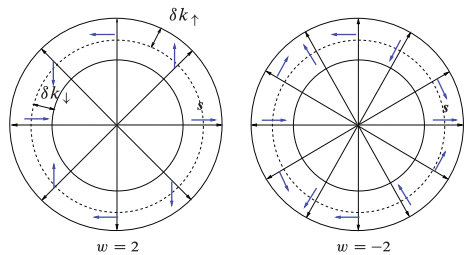


Fig. 2.24 The β -phases in the $\ell = 2$ triplet channel. Spin configurations exhibit the vortex structure with winding number $w = \pm 2$. These two configurations can be transformed to each other by performing a rotation around the x -axis with the angle of π



the “ β ” phases. In the β phases there are two isotropic FS but spin is not a good quantum number. In fact, the electron self energy in the β -phases acquires a spin-orbit type form with a strength given by the magnitude of the order parameter.

The mean-field electronic structure thus resembles that of a system with a strong and tunable spin-orbit coupling (i.e. not of $O((v_F/c)^2)$ as it is normally the case).

We can define now a \mathbf{d} vector:

$$\mathbf{d}(\mathbf{k}) = (\cos(\ell\theta_k), \sin(\ell\theta_k), 0) \quad (2.71)$$

In the β phases the \mathbf{d} vector winds about the undistorted FS. For the special case of $\ell = 1$, the windings are $w=1$ (corresponding to a “Rashba” type state) and $w = -1$ (corresponding to a “Dresselhaus” type state). For the d -wave case, the winding numbers are $w = \pm 2$ (see Fig. 2.24).

These phases have a rich phenomenology of collective modes and topological excitations which we will not elaborate on here. See Ref. [17] for a detailed discussion.²⁸

Fermionic systems with dipolar magnetic interactions may be a good candidate for phases similar to the ones we just described (See Refs. [186, 187], and it is quite possible that these systems may be realized in ultra-cold atomic gases. In that context the anisotropic form of the dipolar interaction provides for a mechanism to access some of this physics. Indeed, in the case of a fully polarized (3D) dipolar Fermi gas, the FS will have an uniaxial distortion. If the polarization is spontaneous (in the

²⁸ The p -wave ($\ell = 1$) β phase has the same physics as the ‘spin-split’ metal of Ref. [221]. A similar state was proposed in Ref. [222] as an explanation of the “hidden order” phase of URu₂Si₂.

absence of a polarizing external field) this phase is actually a ferro-nematic state, a state with coexisting ferromagnetism and nematic order. If the system is partially polarized then the phase is a mix of nematic order and ferromagnetism coexisting with a phase with a non-trivial “spin texture” in momentum space.

It turns out that generalizations of the Pomeranchuk picture of the nematic state to multi-band electronic systems can describe metallic states with a spontaneous breaking of time reversal invariance. This was done in Ref. [14] where it was shown that in a two-band system (i.e. a system with two Fermi surfaces) it is possible to have a metallic state which breaks time reversal invariance and exhibits a spontaneous anomalous Hall effect. While the treatment of this problem has a superficial formal similarity with the triplet (spin) case, i.e. regarding the band index as a “pseudo-spin” (or flavor), the physics differs considerably. At the free fermion level the fermion number on each band is separately conserved, leading to a formal $SU(2)$ symmetry. However, the interacting system has either a smaller $U(1) \times U(1)$ invariance or, more generally, $\mathbb{Z}_2 \times \mathbb{Z}_2$ invariance, as the more general interactions preserve only the *parity* of the band fermion number [14]. At any rate it turns out that analogs of the “ α ” and “ β ” phases of the triplet channel exist in multi-band systems. The “ α ” phases break time reversal and parity (but not the product). An example of such metallic (gapless) states is the “Varma loop state” [15, 223]. The “ β ” states break time reversal invariance (and chirality). In the “ β ” phases there is a spontaneous anomalous Hall effect, i.e. a zero field Hall effect with a Hall conductivity that is not quantized as this state is a metal,²⁹ whereas the “ α ” phases there is not.

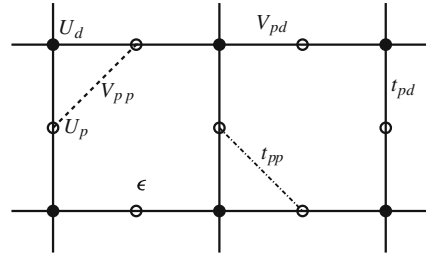
2.8 Nematic Order in the Strong Correlation Regime

We will now discuss how a nematic state arises as the exact ground state in the strong coupling limit of the Emery model [176]. The Emery model is a simplified microscopic model of the important electronic degrees of freedom of the copper oxides [123]. In this model, the CuO plane is described as a square lattice with the Cu atoms residing on the sites and the O atoms on the links (the medial lattice of the square lattice). On each site of the square lattice there is a single $d_{x^2-y^2}$ Cu orbital, and a p_x (p_y) O orbital on each site of the medial along the x (y) direction. We will denote by $d_\sigma^\dagger(\mathbf{r})$ the operator that creates a hole on the Cu site \mathbf{r} and by $p_{x,\sigma}^\dagger(\mathbf{r} + \frac{\mathbf{e}_x}{2})$ and $p_{y,\sigma}^\dagger(\mathbf{r} + \frac{\mathbf{e}_y}{2})$ the operators that create a hole on the O sites $\mathbf{r} + \frac{\mathbf{e}_x}{2}$ and $\mathbf{r} + \frac{\mathbf{e}_y}{2}$ respectively.

The Hamiltonian of the Emery model is the sum of kinetic energy and interaction terms. The kinetic energy terms consist of the hopping of a hole from a Cu site to its nearest O sites (with amplitude t_{pd}), an on-site energy $\varepsilon > 0$ on the O sites (accounting for the difference in “affinity” between Cu and O), and a (small) direct hopping between nearest-neighboring O sites, t_{pp} . The interaction terms are just the on-site Hubbard repulsion U_d (on the Cu sites) and U_p (on the O sites) as well as

²⁹ This is consistent with the general arguments of Ref. [224].

Fig. 2.25 The Emery model of the CuO lattice



nearest neighbor (“Coulomb”) repulsive interactions of strength V_{pd} (between Cu and O) and V_{pp} (between two nearest O) (see Fig. 2.25). It is commonly believed that this model is equivalent to its simpler cousin, the one band Hubbard model. However, while this equivalency is approximately correct in the weak coupling limit, it is known to fail already at moderate couplings. We will see that in the strong coupling limit, no such reduction (to a “Zhang-Rice singlet”) is possible.

Let us look at the energetics of the 2D Cu O model in the strong coupling limit. By strong coupling we will mean the regime in which the following inequalities hold:

$$\frac{t_{pd}}{U_p}, \frac{t_{pd}}{U_d}, \frac{t_{pd}}{V_{pd}}, \frac{t_{pd}}{V_{pp}} \rightarrow 0, \quad U_d > U_p \gg V_{pd} > V_{pp}, \quad \text{and} \quad \frac{t_{pp}}{t_{pd}} \rightarrow 0 \quad (2.72)$$

as a function of hole doping $x > 0$, where x is the number of doped holes per Cu. In this regime, neither Cu nor O sites can be doubly occupied. At half filling, $x=0$, the holes occupy all the Cu sites and all O sites are empty. At half-filling and in this strong coupling regime the Emery model (much as the Hubbard model) is equivalent to a quantum Heisenberg antiferromagnet with a small exchange coupling $J_H \approx \frac{8t_{pd}^4}{U_p V_{pd}^2}$. This is the double-exchange mechanism (It turns out that in this model the four-spin ring exchange interactions can be of the same order of magnitude as the Heisenberg exchange J_H [176]).

Let us consider now the very low doping regime, $x \rightarrow 0$. Any additional hole will have to be on an O site. The energy to add one hole (i.e. the chemical potential μ of a hole) is $\mu \equiv 2V_{pd} + \epsilon$. Similarly, the energy of two holes on nearby O sites is $2\mu + V_{pp}$. It turns out that in this strong coupling regime, with $t_{pp} = 0$, the dynamic of the doped holes is strongly constrained and effectively becomes one-dimensional. The simplest allowed move for a hole on an O site, which takes two steps, is shown in Fig. 2.26. The final and initial states are degenerate, and their energy is $E_0 + \mu$, where E_0 is the ground state energy of the undoped system. If this was the only allowed process, the system would behave as a collection of 1D fermionic systems.

To assess if this is correct let us examine other processes to the same (lowest) order in perturbation theory (in powers of the kinetic energy). One possibility is a process in which in the final state the hole “turned the corner” (went from being on an x oxygen to a near y oxygen). However for that to happen it will have to go through an intermediate state such as the one shown in Fig. 2.27a. This intermediate

Fig. 2.26 An allowed two-step move

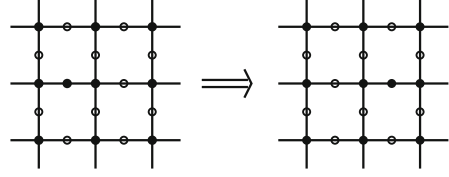
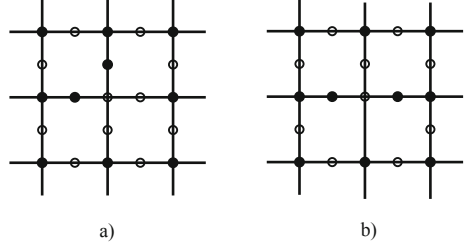


Fig. 2.27 Intermediate states for processes in which a hole **a** turns a corner and **b** continues on the same row



state has an energy $E_0 + \mu + V_{pp}$. Hence, the effective hopping matrix element to turn the corner is $t_{\text{eff}} = \frac{t_{pd}^2}{V_{pp}} \ll t_{pd}$, which is strongly suppressed by the Coulomb effects of V_{pp} . In contrast, the intermediate state for the hole to continue on the same row (see Fig. 2.27) is $E_0 + \mu + \epsilon$. Thus the effective hopping amplitude instead becomes $t_{\text{eff}} = \frac{t_{pd}^2}{\epsilon}$, which is not suppressed by Coulomb effects of V_{pp} . All sorts of other processes have large energy denominators and are similarly suppressed

(for a detailed analysis see Ref. [176].) The upshot of this analysis is that in the strong coupling limit the doped holes behave like a set of one-dimensional fermions (one per row and column). The argument for one-dimensional effective dynamics can in fact be made more rigorous. In Ref. [176] it is shown that to leading order in the strong coupling expansion the system is a generalized t - J type model (with J effectively set to zero). In this limit there are an infinite number of conserved charges, exactly one per row and one per column.

The next step is to inquire if, at fixed but very small doping $x \rightarrow 0$, the rows and columns are equally populated or not. Consider then two cases; a) all rows and columns have the same fermion density, and b) the columns (or the rows) are empty. Case a) is isotropic while case b) is nematic. It turns out that due to the effects of the repulsive Coulomb interaction V_{pp} , the nematic configuration has lower energy at low enough doping. The argument is as follows. For the nematic state (in which all rows are equally populated but all columns are empty), the ground state energy has an expansion in powers of the doping x of the form:

$$E_{\text{nematic}} = E(x=0) + \Delta_c x + W x^3 + O(x^5) \quad (2.73)$$

where $\Delta_c = 2V_{pd} + \epsilon + \dots$ and $W = \pi^2 \hbar^2 / 6m^*$. The energy of the isotropic state (at the same doping x) is

$$E_{\text{isotropic}} = E(x = 0) + \Delta_c x + (1/4)W x^3 + V_{\text{eff}} x^2 + \dots \quad (2.74)$$

where $V_{\text{eff}} \propto V_{pp}$ is an effective coupling for holes on intersecting rows and columns. Clearly, for x small enough $E_{\text{isotropic}} > E_{\text{nematic}}$. Therefore, at low enough doping the ground state of the Emery model in the strong coupling limit is a nematic, in the sense that it breaks spontaneously the point symmetry group of the square lattice, C_4 .³⁰ What happens for larger values of x is presently not known. Presumably a complex set of stripe phases exist. How this analysis is modified by the spin degrees of freedom is an open important problem which may illuminate our understanding of the physics of high temperature superconductors.

The nematic state we have found to be the exact ground state is actually maximally nematic: the nematic order parameter is 1. To obtain this result we relied on the fact that we have set $t_{pp} = 0$ as this is by far the smallest energy scale. The state that we have found is reminiscent of the nematic state found in 2D mean field theories of the Pomeranchuk transition [161] in which it is found that the nematic has an open Fermi surface, as we have also found. Presumably, for the more physical case of $t_{pp} \neq 0$, the strong 1D-like nematic state we found will show a crossover to a 2D (Ising) Nematic Fermi liquid state.

2.9 The Quantum Nematic-Smectic QCP and the Melting of the Stripe Phase

We will now turn to the problem of the quantum phase transition between electron stripe and nematic phases. For simplicity we will consider only the simpler case of the charge stripe and the charge nematic, and we will not discuss here the relation with antiferromagnetic stripes and superconductivity. Even this simpler problem is not well understood at present.

In classical liquid crystals there are two well established ways to describe this transition, known as the smectic A-nematic transition. One approach is the McMillan-de Gennes theory, and it is a generalization of the Landau–Ginzburg theory of phase transitions to this problem (see Ref. [2].) The other approach regards this phase transition as a melting of the smectic by proliferation of its topological excitations, the dislocations of the smectic order [3, 225, 226].

There are however important (and profound) differences between the problem of the quantum melting of a stripe phase into a quantum nematic and its classical smectic/nematic counterpart. The classical problem refers to three-dimensional liquid crystals whereas here we are interested in a two-dimensional quantum system. One may think that the time coordinate, i.e. the existence of a time evolution dictated by quantum mechanics, provides for the third dimension and that two

³⁰ It also turns out that in the (so far physically unrealizable) case of $x=1$, the ground state is a nematic insulator as each row is now full. However, for $x \rightarrow 1$ the ground state is again a nematic metal.

problems may indeed be closely related. Although to a large extent this is correct (this is apparent in the imaginary time form of the path integral representation) some important details are different. The problem we are interested in involves a metal and hence has dynamical fermionic degrees of freedom which do not have a counterpart in its classical cousin. One could develop a theory of quantum melting of the stripe phase by a defect proliferation mechanism by considering only the collective modes of the stripes. Theories of this type can be found in Refs. [227, 228] and in Ref. [156] (in the context of a system of cold atoms) which lead to several interesting predictions. Theories of this type would describe correctly an insulating stripe state in which the fermionic degrees of freedom are gapped and hence not part of the low energy physics. The problem of how to develop a non-perturbative theory of this transition with dynamical fermions is an open and unsolved problem.³¹

Another important difference is that in most cases of interest the quantum version of this transition takes place in a lattice system. thus, even if the stripe state may be incommensurate, and hence to a first approximation be allowed to “slide” over the lattice background, there is no continuous rotational invariance but only a point group symmetry leftover. Thus, at least at the lowest energies, the nematic Goldstone mode which plays a key role in the classical problem, is gapped and drops out of the critical behavior. However one should not be a purist about this issue as there may be significant crossovers that become observable at low frequencies and temperatures if the lattice effects are weak enough. Thus it is meaningful to consider a system in which the lattice symmetry breaking are ignored at the beginning and considered afterwards.

In Ref. [229] a theory of the quantum melting of a charge stripe phase is developed using an analogy with the McMillan-deGennes theory. The main (and important) difference is the role that the fermionic degrees of freedom play in the dynamics. Thus we will describe the stripe (which at this level is equivalent to a CDW) by its order parameter, the complex scalar field $\Phi(\mathbf{r}, t)$, representing the Fourier component of the charge density operator near the ordering wavevector \mathbf{Q} .³²

We will assume that the phase transition occurs in a regime in which the nematic order is well developed and has a large amplitude $|\mathcal{N}|$. In this regime the fluctuations of the amplitude of the nematic order parameter N are part of the high energy physics, and can be integrated out. In contrast we will assume that the phase mode of the nematic order, the Goldstone mode, is either gapless (as in a continuum system) or of low enough energy that it matters to the physics (as if the lattice symmetry breaking is sufficiently weak). In this case we will only need to consider the nematic Goldstone (or ‘pseudo-Goldstone’) field which we will denote by $\varphi(\mathbf{r}, t)$.

We should note that there is another way to think about this problem, in which one considers the competition between the CDW order parameters (two in this case), the nematic order and the normal Fermi liquid near a suitable multi-critical point. This problem was considered briefly in Ref. [229] and revisited in more detail in

³¹ Important work with a similar approach has been done on the problem of the quantum melting of the stripe state in quantum Hall systems [36, 37].

³² For a different perspective see Ref. [230].

Ref. [231]. The main conclusion is that for a (square) lattice system, the multicritical point is inaccessible as it is replaced by a direct (and weak) fluctuation-induced first-order transition from the FL to the CDW state. Thus, the theory that we discuss here applies far from this putative multicritical point in a regime in which, as we stated above, the nematic order is already well developed and large.

Following Ref. [229] we will think of this quantum phase transition in the spirit of a Hertz-Millis type approach and postulate the existence of an order parameter theory coupled to the fermionic degrees of freedom. The quantum mechanical action of the order parameter theory $S_{op}[\Phi, \varphi_N]$, has the McMillan-deGennes form

$$\begin{aligned}
 S_{op} = & |N|^2 \int d\mathbf{r} dt \left((\partial_t \varphi_N)^2 - K_1 (\partial_x \varphi_N)^2 - K_2 (\partial_y \varphi_N)^2 \right) \\
 & + \int d\mathbf{r} dt \left(|\partial_t \Phi|^2 - C_y |\partial_y \Phi|^2 - C_x \left| \left(\partial_x - i \frac{Q}{2} \varphi_N \right) \right|^2 \right. \\
 & \left. - \Delta_{CDW} |\Phi|^2 - u_{CDW} |\Phi|^4 \right)
 \end{aligned} \tag{2.75}$$

where $|N|$ is the amplitude of the nematic order parameter, K_1 and K_2 are the two Franck constants (which were discussed before), C_x and C_y are the stiffnesses of the CDW order parameter along the x and y directions, Q is the modulus of the CDW ordering wavevector, Δ_{CDW} and u_{CDW} are parameters of the Landau theory that control the location of the CDW transition ($\Delta_{CDW} = 0$) and stability. Here we have assumed a stripe state, a unidirectional CDW, with its ordering wavevector along the x direction. We have also assumed $z=1$ (“relativistic”) quantum dynamics which would be natural for an insulating system.

The fermionic contribution has two parts. One part of the fermionic action, $S_{FL}[\psi]$, where ψ is the quasiparticle Fermi field (we are omitting the spin indices), describes a conventional Fermi liquid, i.e. the quasiparticle spectrum with a Fermi surface of characteristic Fermi wavevector k_F , and the quasiparticle interactions given in terms of Landau parameters. What will matter to us is the coupling between the fermionic quasiparticles and the nematic order parameter (the complex director field N), and the CDW order parameter Φ ,

$$\begin{aligned}
 S_{\text{int}} = & g_N \int d\mathbf{r} dt \left(Q_2(\mathbf{r}, t) N^\dagger(\mathbf{r}, t) + \text{h.c.} \right) \\
 & + g_{CDW} \int d\mathbf{r} dt \left(n_{CDW}(\mathbf{r}, t) \Phi^\dagger(\mathbf{r}, t) + \text{h.c.} \right)
 \end{aligned} \tag{2.76}$$

where g_N and g_{CDW} are two coupling constants and, as before,

$$Q_2(\mathbf{r}, t) = \psi^\dagger(\mathbf{r}, t) (\partial_x + i \partial_y)^2 \psi(\mathbf{r}, t) \tag{2.77}$$

is the nematic order parameter (in terms of quasiparticle Fermi fields), and

$$n_{CDW}(\mathbf{q}, \omega) = \int d\mathbf{k} d\Omega \psi^\dagger(\mathbf{k} + \mathbf{q} + \mathbf{Q}, \omega + \Omega) \psi(\mathbf{k}, \Omega) \tag{2.78}$$

is the CDW order parameter (also in terms of the quasiparticle Fermi fields.)

This theory has two phases: a) a nematic phase, for $\Delta_{CDW} > 0$, where $\langle \Phi \rangle = 0$, and b) a CDW phase, for $\Delta_{CDW} < 0$, where $\langle \Phi \rangle \neq 0$, separated by a QCP at $\Delta_{CDW} = 0$. In the nematic (“normal”) phase the only low energy degrees of freedom are the (overdamped) fluctuations of the nematic Goldstone mode φ_N , and nematic susceptibility in the absence of lattice effects (which render it gapped otherwise)

$$\chi_{\perp}^N(\mathbf{q}, \omega) = \frac{1}{g_N^2 N(0)} \frac{1}{\left(i \frac{\omega}{q} \sin^2(2\phi_q) - K_1 q_x^2 - K_2 q_y^2\right)} \quad (2.79)$$

where $\sin(2\phi_q) = 2q_x q_y / q^2$ and $N(0)$ is the quasiparticle density of states at the FS.

We will consider here the simpler case in which the CDW ordering wavevector obeys $Q < 2k_F$ (see the general discussion in Ref. [229].) In this case one can see that the main effect of the coupling to the quasiparticles (aside from some finite renormalizations of parameters) is to change the dynamics of the CDW order parameter due to the effects of Landau damping. The total effective action in this case becomes

$$\begin{aligned} S = & \int \frac{d\mathbf{q} d\omega}{(2\pi)^3} C_0 i|\omega| |\Phi(\mathbf{q}, \omega)|^2 \\ & - \int d\mathbf{r} dt \left(C_y |\partial_y \Phi|^2 + C_x \left| \left(\partial_x - i \frac{Q}{2} \varphi_N \right) \Phi \right|^2 + \Delta_{CDW} |\Phi|^2 + u_{CDW} |\Phi|^4 \right) \\ & + \int \frac{d\mathbf{q} d\omega}{(2\pi)^3} \left(\tilde{K}_0 \frac{i|\omega|}{q} \sin^2(2\phi_q) - \tilde{K}_1 q_x^2 - \tilde{K}_2 q_y^2 \right) |\varphi_N(\mathbf{q}, \omega)|^2 \end{aligned} \quad (2.80)$$

where $C_0 \sim g_{CDW}^2$, $\tilde{K}_0 = g_N^2 |N|^2 N(0)$ and $K_{1,2} = g_N^2 |N|^2 N(0) K_{1,2}$.

By inspecting Eq. 2.80 one sees that at $\Delta_{CDW} = 0$, as before the nematic Goldstone fluctuations have $z=3$ (provided they remain gapless), and the CDW fluctuations have $z=2$. Thus the nematic Goldstone modes dominate the dynamics at the nematic-CDW QCP. Even if the nematic Goldstone modes were to become gapped (by the lattice anisotropy), the QCP now will have $z=2$ (due to Landau damping) instead of $z=1$ as in the “pure” order parameter theory. In both cases, the nematic Goldstone mode and the CDW order parameter fluctuations effectively decouple in the nematic phase. The result is that the nematic phase has relatively low energy CDW fluctuations with a dynamical susceptibility

$$\chi^{CDW}(\mathbf{q}, \omega) = -i \langle \Phi^\dagger(\mathbf{q}, \omega) \Phi(\mathbf{q}, \omega) \rangle_{\text{ret}} = \frac{1}{i C_0 |\omega| - C_x q_x^2 - C_y q_y^2 - \Delta_{CDW}} \quad (2.81)$$

In other terms, as the QCP is approached, the nematic phase exhibits low energy CDW fluctuations that would show up in low energy inelastic scattering experiments much in the same way as the observed *fluctuating stripes* do in inelastic neutron scattering experiments in the high temperature superconductors [4]. As we saw before, a regime with “fluctuating” CDW (stripe) order is a nematic.

A simple scaling analysis of the effective action of Eq. 2.80 shows that, since $z > 1$ at this QCP, the coupling between the nematic Goldstone mode φ_N and the CDW order parameter Φ is actually *irrelevant*. In contrast, in the (classical) case it is a marginally relevant perturbation leading to a fluctuation induced first order transition [3, 232]. Thus, this “generalized McMillan-de Gennes” theory has a continuous (quantum) phase transition which, possibly, may become weakly first order at finite temperature.

This is not to say, however, that the stripe-nematic quantum phase transition is necessarily continuous. In Ref. [229] it is shown that the nature of the quantum phase transition depends on the relation between the ordering wave vector \mathbf{Q} and the Fermi wave vector k_F . For $|\mathbf{Q}| < 2k_F$ the transition is continuous and has dynamical scaling $z=2$. Instead, for $|\mathbf{Q}| = 2k_F$ it depends on whether $|\mathbf{Q}|$ is commensurate or incommensurate with the underlying lattice: for the incommensurate case the transition is (fluctuation induced) first order (consistent with the results of Ref. [233]) but it is continuous for the commensurate case with $z=2$ and anisotropic scaling in space.

As in the case of the Pomeranchuk transition, the quasiparticles are effectively destroyed at the stripe-nematic QCP as well. Indeed, already to order one loop it is found [229] that the quasiparticle scattering rate scales with frequency as $\Sigma''(\omega) \propto \sqrt{|\omega|}$, signaling a breakdown of Fermi liquid theory. As in our discussion of the nematic-FL QCP, this behavior must be taken as an indication of a breakdown of perturbation theory and not as the putative ultimate quantum critical behavior, which remains to be understood.

In the quasiparticle picture we are using, the stripe state is similar to a CDW. Indeed, in the broken symmetry state the Fermi surface of the nematic is reconstructed leading to the formation of fermion pockets. As we noted above, we have not however assumed a rigid connection between the ordering wave vector and the Fermi surface and, in this sense, this is not a weak coupling state. Aside from that, in the presence of lattice pinning of the nematic Goldstone mode, the asymptotic low-energy properties of the stripe state are similar to those of a CDW (for details, see Ref. [229]).

2.10 Outlook

In these lectures we have covered a wide range of material on the theory of electronic liquid crystal phases and on the experimental evidence for them. As it is clear these lectures have a particular viewpoint, developed during the past decade in close collaboration with Steven Kivelson. I have tried, primarily at the level of citations as well as on numerous caveats, to make it clear that there are many important unsolved and still poorly understood questions that (at present) allow for more than one answer. It is a problem that requires the development of many points of view which eventually complement each other.

Several major problems remain open. One of them, in my view the most pressing one, is to establish the relation between the existence of these phases (stripes,

nematics, etc.) and the mechanism(s) of high temperature superconductivity. In my opinion there is mounting experimental evidence, some of which I discussed here, that strongly suggests the existence of a close and probably unavoidable connection. A question that deserves more consideration is the particular connection between nematic order and superconductivity. Superficially these two issues would seem quite orthogonal to each other. Indeed, it is hard to see any connection within the context of a weak coupling theory. However if the nematic order arises from melting a stripe state which has a spin gap (such as the pair density wave state we discussed in these lectures) it is quite likely that a close connection may actually exist and be related. The current experimental evidence suggests such a relation.

Another key theoretical question that is wide open is to develop a more microscopic theory of the pair density wave state. In spite with the formal analogy with the Larkin-Ovchinnikov state, it seems very unlikely that a “straight BCS approach” would be successful in this case. This state seems to have a strong coupling character.

As it must be apparent from the presentation of these lectures, the theory that has been done (and that is being done now) is for the most part quite phenomenological in character. There are very few “rigorous” results on the existence of these phases in strongly correlated systems. The notable exception are the arguments we presented for the existence of nematic order in the strong coupling limit of the Emery model. Clearly more work is needed.

Acknowledgments I am deeply indebted to Steve Kivelson with whom we developed many of the ideas that are presented here. Many of these results were obtained also in collaboration with my former students Michael Lawler and Kai Sun, as well as to John Tranquada, Vadim Oganesyan, Erez Berg, Daniel Barci, Congjun Wu, Benjamin Fregoso, Siddhartha Lal and Akbar Jaefari, and many other collaborators. I would like to thank Daniel Cabra, Andreas Honecker and Pierre Pujol for inviting me to this very stimulating Les Houches Summer School on “Modern theories of correlated electron systems” (Les Houches, May 2009). This work was supported in part by the National Science Foundation, under grant DMR 0758462 at the University of Illinois, and by the Office of Science, U.S. Department of Energy, under Contracts DE-FG02-91ER45439 and DE-FG02-07ER46453 through the Frederick Seitz Materials Research Laboratory of the University of Illinois.

References

1. Kivelson, S.A., Fradkin, E., Emery, V.J.: Electronic liquid-crystal phases of a doped Mott insulator. *Nature* **393**, 550 (1998)
2. de Gennes, P.G., Prost, J.: *The Physics of Liquid Crystals*. Oxford Science Publications/Clarendon Press, Oxford, UK (1993)
3. Chaikin, P.M., Lubensky, T.C.: *Principles of Condensed Matter Physics*. Cambridge University Press, Cambridge, UK (1995)
4. Kivelson, S.A., Fradkin, E., Oganesyan, V., Bindloss, I., Tranquada, J., Kapitulnik, A., Howald, C.: How to detect fluctuating stripes in high temperature superconductors. *Rev. Mod. Phys.* **75**, 1201 (2003)
5. Berg, E., Fradkin, E., Kim, E.-A., Kivelson, S., Oganesyan, V., Tranquada, J.M., Zhang, S.: Dynamical layer decoupling in a stripe-ordered high T_c superconductor. *Phys. Rev. Lett.* **99**, 127003 (2007)

6. Berg, E., Chen, C.-C., Kivelson, S.A.: Stability of nodal quasiparticles in superconductors with coexisting orders. *Phys. Rev. Lett.* **100**, 027003 (2008)
7. Fulde, P., Ferrell, R.A.: Superconductivity in a strong spin-exchange field. *Phys. Rev.* **135**, A550 (1964)
8. Larkin, A.I., Ovchinnikov, Y.N.: Nonuniform state of superconductors. *Zh. Eksp. Teor. Fiz.* **47**, 1136 (1964). (*Sov. Phys. JETP*, **20**, 762 (1965))
9. Fradkin, E., Kivelson, S.A., Manousakis, E., Nho, K.: Nematic phase of the two-dimensional electron gas in a magnetic field. *Phys. Rev. Lett.* **84**, 1982 (2000)
10. Cooper, K.B., Lilly, M.P., Eisenstein, J.P., Pfeiffer, L.N., West, K.W.: Onset of anisotropic transport of two-dimensional electrons in high Landau levels: possible isotropic-to-nematic liquid-crystal phase transition. *Phys. Rev. B* **65**, 241313 (2002)
11. Ando, Y., Segawa, K., Komiya, S., Lavrov, A.N.: Electrical resistivity anisotropy from self-organized one-dimensionality in high-temperature superconductors. *Phys. Rev. Lett.* **88**, 137005 (2002)
12. Borzi, R.A., Grigera, S.A., Farrell, J., Perry, R.S., Lister, S.J.S., Lee, S.L., Tennant, D.A., Maeno, Y., Mackenzie, A.P.: Formation of a nematic fluid at high fields in $\text{Sr}_3\text{Ru}_2\text{O}_7$. *Science* **315**, 214 (2007)
13. Hinkov, V., Haug, D., Fauqué, B., Bourges, P., Sidis, Y., Ivanov, A., Bernhard, C., Lin, C.T., Keimer, B.: Electronic liquid crystal state in superconducting $\text{YBa}_2\text{Cu}_3\text{O}_{6.45}$. *Science* **319**, 597 (2008)
14. Sun, K., Fradkin, E.: Time-reversal symmetry breaking and spontaneous anomalous Hall effect in Fermi fluids. *Phys. Rev. B* **78**, 245122 (2008)
15. Varma, C.M.: A theory of the pseudogap state of the cuprates. *Philos. Mag.* **85**, 1657 (2005)
16. Wu, C., Zhang, S.-C.: Dynamic generation of spin-orbit coupling. *Phys. Rev. Lett.* **93**, 036403 (2004)
17. Wu, C.J., Sun, K., Fradkin, E., Zhang, S.-C.: Fermi liquid instabilities in the spin channel. *Phys. Rev. B* **75**, 115103 (2007)
18. Anderson, P.W.: The resonating valence bond state of La_2CuO_4 and superconductivity. *Science* **235**, 1196 (1987)
19. Emery, V.J., Kivelson, S.A., Lin, H.Q.: Phase separation in the t-J model. *Phys. Rev. Lett.* **64**, 475 (1990)
20. Dagotto, E.: Correlated electrons in high-temperature superconductors. *Rev. Mod. Phys.* **66**, 763 (1994)
21. Emery, V.J., Kivelson, S.A.: Frustrated electronic phase separation and high-temperature superconductors. *Physica C* **209**, 597 (1993)
22. Seul, M., Andelman, D.: Domain shapes and patterns: the phenomenology of modulated phases. *Science* **267**, 476 (1995)
23. Lorenz, C.P., Ravenhall, D.G., Pethick, C.J.: Neutron star crusts. *Phys. Rev. Lett.* **70**, 379 (1993)
24. Fradkin, E., Kivelson, S.A., Lawler, M.J., Eisenstein, J.P., Mackenzie, A.P.: Nematic Fermi fluids in condensed matter physics. *Annu. Rev. Condens. Matter Phys.* **1**, 71 (2010)
25. Lilly, M.P., Cooper, K.B., Eisenstein, J.P., Pfeiffer, L.N., West, K.W.: Evidence for an anisotropic state of two-dimensional electrons in high Landau levels. *Phys. Rev. Lett.* **82**, 394 (1999)
26. Lilly, M.P., Cooper, K.B., Eisenstein, J.P., Pfeiffer, L.N., West, K.W.: Anisotropic states of two-dimensional electron systems in high Landau levels: effect of an in-plane magnetic field. *Phys. Rev. Lett.* **83**, 824 (1999)
27. Du, R.R., Tsui, D.C., Störmer, H.L., Pfeiffer, L.N., Baldwin, K.W., West, K.W.: Strongly anisotropic transport in higher two-dimensional Landau levels. *Solid State Comm.* **109**, 389 (1999)
28. Pan, W., Du, R.R., Störmer, H.L., Tsui, D.C., Pfeiffer, L.N., Baldwin, K.W., West, K.W.: Strongly anisotropic electronic transport at Landau level filling factor $\nu = 9/2$ and $\nu = 5/2$ under tilted magnetic field. *Phys. Rev. Lett.* **83**, 820 (1999)

29. Koulakov, A.A., Fogler, M.M., Shklovskii, B.I.: Charge density wave in two-dimensional electron liquid in weak magnetic field. *Phys. Rev. Lett.* **76**, 499 (1996)
30. Moessner, R., Chalker, J.T.: Exact results for interacting electrons in high Landau levels. *Phys. Rev. B* **54**, 5006 (1996)
31. Fradkin, E., Kivelson, S.A.: Liquid crystal phases of quantum Hall systems. *Phys. Rev. B* **59**, 8065 (1999)
32. MacDonald, A.H., Fisher, M.P.A.: Quantum theory of quantum Hall smectics. *Phys. Rev. B* **61**, 5724 (2000)
33. Barci, D.G., Fradkin, E., Kivelson, S.A., Oganessian, V.: Theory of the quantum Hall smectic phase. I. Low-energy properties of the quantum Hall smectic fixed point. *Phys. Rev. B* **65**, 245319 (2002)
34. Cooper, K.B., Lilly, M.P., Eisenstein, J.P., Jungwirth, T., Pfeiffer, L.N., West, K.W.: An investigation of orientational symmetry-breaking mechanisms in high Landau levels. *Sol. State Commun.* **119**, 89 (2001)
35. Cooper, K.B., Eisenstein, J.P., Pfeiffer, L.N., West, K.W.: Observation of narrow-band noise accompanying the breakdown of insulating states in high Landau levels. *Phys. Rev. Lett.* **90**, 226803 (2003)
36. Wexler, C., Dorsey, A.T.: Disclination unbinding transition in quantum Hall liquid crystals. *Phys. Rev. B* **64**, 115312 (2001)
37. Radzihovsky, L., Dorsey, A.T.: Theory of quantum Hall nematics. *Phys. Rev. Lett.* **88**, 216802 (2002)
38. Doan, Q.M., Manousakis, E.: Quantum nematic as ground state of a two-dimensional electron gas in a magnetic field. *Phys. Rev. B* **75**, 195433 (2007)
39. Oganessian, V., Kivelson, S.A., Fradkin, E.: Quantum theory of a nematic Fermi fluid. *Phys. Rev. B* **64**, 195109 (2001)
40. Grigera, S.A., Gegenwart, P., Borzi, R.A., Weickert, F., Schofield, A.J., Perry, R.S., Tayama, T., Sakakibara, T., Maeno, Y., Green, A.G. et al.: Disorder-sensitive phase formation linked to metamagnetic quantum criticality. *Science* **306**, 1154 (2004)
41. Fradkin, E., Kivelson, S.A., Oganessian, V.: Discovery of a nematic electron fluid in a transition metal oxide. *Science* **315**, 196 (2007)
42. Grigera, S.A., Perry, R.S., Schofield, A.J., Chiao, M., Julian, S.R., Lonzarich, G.G., Ikeda, S.I., Maeno, Y., Millis, A.J., Mackenzie, A.P.: Magnetic field-tuned quantum criticality in the metallic ruthenate $\text{Sr}_3\text{Ru}_2\text{O}_7$. *Science* **294**, 329 (2001)
43. Millis, A.J., Schofield, A.J., Lonzarich, G.G., Grigera, S.A.: Metamagnetic quantum criticality. *Phys. Rev. Lett.* **88**, 217204 (2002)
44. Perry, R.S., Kitagawa, K., Grigera, S.A., Borzi, R.A., Mackenzie, A.P., Ishida, K., Maeno, Y.: Multiple first-order metamagnetic transitions and quantum oscillations in ultrapure $\text{Sr}_3\text{Ru}_2\text{O}_7$. *Phys. Rev. Lett.* **92**, 166602 (2004)
45. Green, A.G., Grigera, S.A., Borzi, R.A., Mackenzie, A.P., Perry, R.S., Simons, B.D.: Phase bifurcation and quantum fluctuations in $\text{Sr}_3\text{Ru}_2\text{O}_7$. *Phys. Rev. Lett.* **95**, 086402 (2005)
46. Jamei, R., Kivelson, S., Spivak, B.: Universal aspects of Coulomb-frustrated phase separation. *Phys. Rev. Lett.* **94**, 056805 (2005)
47. Lorenzana, J., Castellani, C., Di Castro, C.: Mesoscopic frustrated phase separation in electronic systems. *Euro. Phys. Lett.* **57**, 704 (2002)
48. Kivelson, S.A., Fradkin, E.: In: Schrieffer, J.R., Brooks, J. (eds.) *Handbook of High Temperature Superconductivity*, pp. 569–595. Springer-Verlag, New York (2007)
49. Chakravarty, S., Laughlin, R.B., Morr, D.K., Nayak, C.: Hidden order in the cuprates. *Phys. Rev. B* **63**, 094503 (2001)
50. Fujita, M., Goka, H., Yamada, K., Tranquada, J.M., Regnault, L.P.: Stripe order depinning and fluctuations in $\text{La}_{1.875}\text{Ba}_{0.125}\text{CuO}_4$ and $\text{La}_{1.875}\text{Ba}_{0.075}\text{Sr}_{0.050}\text{CuO}_4$. *Phys. Rev. B* **70**, 104517 (2004)
51. Abbamonte, P., Rusydi, A., Smadici, S., Gu, G.D., Sawatzky, G.A., Feng, D.L.: Spatially modulated ‘Mottness’ in $\text{La}_{2-x}\text{Ba}_x\text{CuO}_4$. *Nature Phys.* **1**, 155 (2005)

52. Tranquada, J.M.: In: Schrieffer, J.R., Brooks, J. (ed.) *Treatise of High Temperature Superconductivity*, pp. 257–298. Springer-Verlag, New York (2007)
53. Tranquada, J.M., Sternlieb, B.J., Axe, J.D., Nakamura, Y., Uchida, S.: Evidence for stripe correlations of spins and holes in copper oxide superconductors. *Nature* **375**, 561 (1995)
54. Tranquada, J.M., Woo, H., Perring, T.G., Goka, H., Gu, G.D., Xu, G., Fujita, M., Yamada, K.: Quantum magnetic excitations from stripes in copper-oxide superconductors. *Nature* **429**, 534 (2004)
55. Haug, D., Hinkov, V., Suchaneck, A., Inosov, D.S., Christensen, N.B., Niedermayer, C., Bourges, P., Sidis, Y., Park, J.T., Ivanov, A. et al.: Magnetic-field-enhanced incommensurate magnetic order in the underdoped high-temperature superconductor $\text{YBa}_2\text{Cu}_3\text{O}_{6.45}$. *Phys. Rev. Lett.* **103**, 017001 (2009)
56. Hinkov, V., Bourges, P., Pailh  s, S., Sidis, Y., Ivanov, A., Frost, C.D., Perring, T.G., Lin, C.T., Chen, D.P., Keimer, B.: Spin dynamics in the pseudogap state of a high-temperature superconductor. *Nature Phys.* **3**, 780 (2007)
57. Hinkov, V., Bourges, P., Pailh  s, S., Sidis, Y., Ivanov, A., Lin, C., Chen, D., Keimer, B.: In-plane anisotropy of spin excitations in the normal and superconducting states of underdoped $\text{YBa}_2\text{Cu}_3\text{O}_{6+x}$. *Nature Phys.* **3**, 780 (2007)
58. Mook, H.A., Dai, P., Do  an, F., Hunt, R.D.: One-dimensional nature of the magnetic fluctuations in $\text{YBa}_2\text{Cu}_3\text{O}_{6.6}$. *Nature* **404**, 729 (2000)
59. Stock, C., Buyers, W.J.L., Liang, R., Peets, D., Tun, Z., Bonn, D., Hardy, W.N., Birgeneau, R.J.: Dynamic stripes and resonance in the superconducting and normal phases of $\text{YBa}_2\text{Cu}_3\text{O}_{6.5}$ ortho-II superconductor. *Phys. Rev. B* **69**, 014502 (2004)
60. Daou, R., Chang, J., LeBoeuf, D., Cyr-Choini  re, O., Lalibert  , F., Doiron-Leyraud, N., Ramshaw, B.J., Liang, R., Bonn, D.A., Hardy, W.N. et al.: Broken rotational symmetry in the pseudogap phase of a high- T_c superconductor. *Nature* **463**, 519 (2010)
61. Li, L., Wang, Y., Naughton, M.J., Komiya, S., Ono, S., Ando, Y., Ong, N.P.: Magnetization, nernst effect and vorticity in the cuprates. *J. Magn. Magn. Mater.* **310**, 460 (2007)
62. Cyr-Choini  re, O., Daou, R., Lalibert  , F., LeBoeuf, D., Doiron-Leyraud, N., Chang, J., Yan, J.-Q., Cheng, J.-G., Zhou, J.-S., Goodenough, J.B. et al.: Enhancement of the nernst effect by stripe order in a high- T_c superconductor. *Nature* **458**, 743 (2009)
63. Matsuda, M., Fujita, M., Wakimoto, S., Fernandez-Baca, J.A., Tranquada, J.M., Yamada, K.: Magnetic excitations of the diagonal incommensurate phase in lightly-doped $\text{La}_{2-x}\text{Sr}_x\text{CuO}_4$. *Phys. Rev. Lett.* **101**, 197001 (2008)
64. Lake, B., R  nnow, H.M., Christensen, N.B., Aeppli, G., Lefmann, K., McMorro, D.F., Vorderwisch, P., Smeibidl, P., Mangkorntong, N., Sasagawa, T., Nohara, M., Takagi, H., Mason, T.E.: Antiferromagnetic order induced by an applied magnetic field in a high temperature superconductor. *Nature* **415**, 299 (2002)
65. Li, Q., H  cker, M., Gu, G.D., Tsvelik, A.M., Tranquada, J.M.: Two-dimensional superconducting fluctuations in stripe-ordered $\text{La}_{1.875}\text{Ba}_{0.125}\text{CuO}_4$. *Phys. Rev. Lett.* **99**, 067001 (2007)
66. Valla, T., Fedorov, A.V., Lee, J., Davis, J.C., Gu, G.D.: The ground state of the pseudogap in cuprate superconductors. *Science* **314**, 1914 (2006)
67. He, R.-H., Tanaka, K., Mo, S.-K., Sasagawa, T., Fujita, M., Adachi, T., Mannella, N., Yamada, K., Koike, Y., Hussain, Z. et al.: Energy gaps in the failed high- T_c superconductor $\text{La}_{1.875}\text{Ba}_{0.125}\text{CuO}_4$. *Nat. Phys.* **5**, 119 (2008)
68. Berg, E., Fradkin, E., Kivelson, S.A.: Charge 4e superconductivity from pair density wave order in certain high temperature superconductors. *Nature Phys.* **5**, 830 (2009)
69. Schafgans, A.A., LaForge, A.D., Dordevic, S.V., Qazilbash, M.M., Komiya, S., Ando, Y., Basov, D.N.: Towards two-dimensional superconductivity in $\text{La}_{2-x}\text{Sr}_x\text{CuO}_4$ in a moderate magnetic field. *Phys. Rev. Lett.* **104**, 157002 (2010)
70. Kohsaka, Y., Taylor, C., Fujita, K., Schmidt, A., Lupien, C., Hanaguri, T., Azuma, M., Takano, M., Eisaki, H., Takagi, H. et al.: An intrinsic bond-centered electronic glass with unidirectional domains in underdoped cuprates. *Science* **315**, 1380 (2007)

71. Howald, C., Eisaki, H., Kaneko, N., Kapitulnik, A.: Coexistence of charged stripes and superconductivity in $\text{Bi}_2\text{Sr}_2\text{CaCu}_2\text{O}_{8+\delta}$. *Proc. Natl. Acad. Sci. U.S.A.* **100**, 9705 (2003)
72. Hanaguri, T., Lupien, C., Kohsaka, Y., Lee, D.H., Azuma, M., Takano, M., Takagi, H., Davis, J.C.: A 'checkerboard' electronic crystal state in lightly hole-doped $\text{Ca}_{2-x}\text{Na}_x\text{CuO}_2\text{Cl}_2$. *Nature* **430**, 1001 (2004)
73. Vershinin, M., Misra, S., Ono, S., Abe, Y., Ando, Y., Yazdani, A.: Local ordering in the pseudogap state of the high- T_c superconductor $\text{Bi}_2\text{Sr}_2\text{CaCu}_2\text{O}_{8+\delta}$. *Science* **303**, 1005 (2004)
74. Lawler, M.J., Fujita, K., Lee, J.W., Schmidt, A.R., Kohsaka, Y., Kim, C.K., Eisaki, H., Uchida, S., Davis, J.C., Sethna, J.P. et al.: Electronic nematic ordering of the intra-unit-cell pseudogap states in underdoped $\text{Bi}_2\text{Sr}_2\text{CaCu}_2\text{O}_{8+\delta}$. *Nature* **466**, 347 (2009)
75. Kamihara, Y., Watanabe, T., Hirano, M., Hosono, H.: Iron-based layered superconductor $\text{La}[\text{O}_{1-x}\text{F}_x]\text{FeAs}$ ($x=0.05\text{--}0.12$) with $T_c = 26$ K. *J. Am. Chem. Soc.* **130**, 3296 (2008)
76. Mu, G., Zhu, X., Fang, L., Shan, L., Ren, C., Wen, H.H.: Nodal gap in Fe-based layered superconductor $\text{LaO}_{0.9}\text{F}_{0.1-\delta}\text{FeAs}$ probed by specific heat measurements. *Chin. Phys. Lett.* **25**, 2221 (2008)
77. Fang, C., Yao, H., Tsai, W.-F., Hu, J.P., Kivelson, S.A.: Theory of electron nematic order in LaOFeAs . *Phys. Rev. B* **77**, 224509 (2008)
78. Xu, C., Müller, M., Sachdev, S.: Ising and spin orders in Iron-based superconductors. *Phys. Rev. B* **78**, 020501 (R) (2008)
79. Chuang, T.-M., Allan, M., Lee, J., Xie, Y., Ni, N., Bud'ko, S., Boebinger, G.S., Canfield, P.C., Davis, J.C.: Nematic electronic structure in the 'parent' state of the iron-based superconductor $\text{Ca}(\text{Fe}_{1-x}\text{Co}_x)_2\text{As}_2$. *Science* **327**, 181 (2010)
80. Dagotto, E., Hotta, T., Moreo, A.: Colossal magnetoresistant materials: the key role of phase separation. *Phys. Rep.* **344**, 1 (2001)
81. Rübhausen, M., Yoon, S., Cooper, S.L., Kim, K.H., Cheong, S.W.: Anisotropic optical signatures of orbital and charge ordering in $\text{Bi}_{1-x}\text{Ca}_x\text{MnO}_3$. *Phys. Rev. B* **62**, R4782 (2000)
82. Grüner, G.: The dynamics of charge-density waves. *Rev. Mod. Phys.* **60**, 1129 (1988)
83. Grüner, G.: The dynamics of spin-density-waves. *Rev. Mod. Phys.* **66**, 1 (1994)
84. McMillan, W.L.: Landau theory of charge density waves in transition-metal dichalcogenides. *Phys. Rev. B* **12**, 1187 (1975)
85. McMillan, W.L.: Theory of discommensurations and the commensurate-incommensurate charge-density-wave phase transition. *Phys. Rev. B* **14**, 1496 (1976)
86. Emery, V.J., Fradkin, E., Kivelson, S.A., Lubensky, T.C.: Quantum theory of the smectic metal state in stripe phases. *Phys. Rev. Lett.* **85**, 2160 (2000)
87. Carlson, E.W., Emery, V.J., Kivelson, S.A., Orgad, D.: In: Bennemann, K.H., Ketterson, J.B. (ed.) *The Physics of Conventional and Unconventional Superconductors*, vol. II, Springer-Verlag, Berlin (2004)
88. Snow, C.S., Karpus, J.F., Cooper, S.L., Kidd, T.E., Chiang, T.-C.: Quantum melting of the charge-density-wave state in 1T-TiSe_2 . *Phys. Rev. Lett.* **91**, 136402 (2003)
89. Morosan, E., Zandbergen, H.W., Dennis, B.S., Bos, J.W., Onose, Y., Klimczuk, T., Ramirez, A.P., Ong, N.P., Cava, R.J.: Superconductivity in Cu_xTiSe_2 . *Nature Phys.* **2**, 44 (2006)
90. Barath, H., Kim, M., Karpus, J.F., Cooper, S.L., Abbamonte, P., Fradkin, E., Morosan, E., Cava, R.J.: Quantum and classical mode softening near the charge-density-wave/superconductor transition of Cu_xTiSe_2 : Raman spectroscopic studies. *Phys. Rev. Lett.* **100**, 106402 (2008)
91. Dai, H., Chen, H., Lieber, C.M.: Weak pinning and hexatic order in a doped two-dimensional charge-density-wave system. *Phys. Rev. Lett.* **66**, 3183 (1991)
92. Kusmartseva, A.F., Sipos, B., Berker, H., Forró, L., Tutiš, E.: Pressure induced superconductivity in pristine 1T-TiSe_2 . *Phys. Rev. Lett.* **103**, 236401 (2009)
93. Brouet, V., Yang, W.L., Zhou, X.J., Hussain, Z., Ru, N., Shin, K.Y., Fisher, I.R., Shen, Z.X.: Fermi surface reconstruction in the CDW state of CeTe_3 observed by photoemission. *Phys. Rev. Lett.* **93**, 126405 (2004)

94. Laverock, J., Dugdale, S.B., Major, Z., Alam, M.A., Ru, N., Fisher, I.R., Santi, G., Bruno, E.: Fermi surface nesting and charge-density wave formation in rare-earth tritellurides. *Phys. Rev. B* **71**, 085114 (2005)
95. Sacchetti, A., Degiorgi, L., Giamarchi, T., Ru, N., Fisher, I.R.: Chemical pressure and hidden one-dimensional behavior in rare-earth tri-telluride charge-density-wave compounds. *Phys. Rev. B* **74**, 125115 (2006)
96. Fang, A., Ru, N., Fisher, I.R., Kapitulnik, A.: STM studies of Tb Te_3 : evidence for a fully incommensurate charge density wave. *Phys. Rev. Lett.* **99**, 046401 (2007)
97. Yao, H., Robertson, J.A., Kim, E.-A., Kivelson, S.A.: Theory of stripes in quasi-two-dimensional rare-earth tritellurides. *Phys. Rev. B* **74**, 245126 (2006)
98. Vojta, M.: Lattice symmetry breaking in cuprate superconductors: stripes, nematics, and superconductivity. *Adv. Phys.* **58**, 564 (2009)
99. Brazovskii, S., Kirova, N.: Electron self-localization and superstructures in quasi one-dimensional dielectrics. *Sov. Sci. Rev. A* **5**, 99 (1984)
100. Kivelson, S.A., Emery, V.J.: In: Bedell, K., Wang, Z., Meltzer, D.E., Balatsky, A.V., Abrahams, E. (ed.) *Strongly Correlated Electron Materials: The Los Alamos Symposium 1993*, pp. 619–650. Addison-Wesley, Redwood City (1994)
101. Zaanen, J., Gunnarsson, O.: Charged magnetic domain lines and the magnetism of high T_c oxides. *Phys. Rev. B* **40**, 7391 (1989)
102. Schulz, H.J.: Incommensurate antiferromagnetism in the 2-dimensional Hubbard model. *Phys. Rev. Lett.* **64**, 1445 (1990)
103. Poilblanc, D., Rice, T.M.: Charged solitons in the hartree–fock approximation to the large-U Hubbard model. *Phys. Rev. B* **39**, 9749 (1989)
104. Machida, K.: Magnetism in La_2CuO_4 based compounds. *Physica C* **158**, 192 (1989)
105. Kato, M., Machida, K., Nakanishi, H., Fujita, M.: Soliton lattice modulation of incommensurate spin density wave in two dimensional Hubbard model—a mean field study. *J. Phys. Soc. Jpn.* **59**, 1047 (1990)
106. Kivelson, S.A., Emery, V.J.: Topological doping. *Synth. Met.* **80**, 151 (1996)
107. Emery, V.J., Kivelson, S.A., Tranquada, J.M.: Stripe phases in high-temperature superconductors. *Proc. Natl. Acad. Sci. USA* **96**, 8814 (1999)
108. Pryadko, L.P., Kivelson, S.A., Emery, V.J., Bazaliy, Y.B., Demler, E.A.: Topological doping and the stability of stripe phases. *Phys. Rev. B* **60**, 7541 (1999)
109. Berg, E., Fradkin, E., Kivelson, S.A., Tranquada, J.M.: Striped superconductors: how the cuprates intertwine spin, charge and superconducting orders. *New J. Phys.* **11**, 115004 (2009)
110. Read, N., Sachdev, S.: Valence-bond and Spin-Peierls ground states in low-dimensional quantum antiferromagnets. *Phys. Rev. Lett.* **62**, 1694 (1989)
111. Vojta, M., Sachdev, S.: Charge order, superconductivity, and a global phase diagram of doped antiferromagnets. *Phys. Rev. Lett.* **83**, 3916 (1999)
112. Vojta, M., Zhang, Y., Sachdev, S.: Competing orders and quantum criticality in doped antiferromagnets. *Phys. Rev. B* **62**, 6721 (2000)
113. Kivelson, S.A., Rokhsar, D., Sethna, J.P.: Topology of the resonating valence-bond state: solitons and high T_c superconductivity. *Phys. Rev. B* **35**, 865 (1987)
114. Capello, M., Raczkowski, M., Poilblanc, D.: Stability of RVB hole stripes in high temperature superconductors. *Phys. Rev. B* **77**, 224502 (2008)
115. Himeda, A., Kato, T., Ogata, M.: Stripe states with spatially oscillating d-wave superconductivity in the two-dimensional $t - t' - J$ model. *Phys. Rev. Lett.* **88**, 117001 (2002)
116. Yamase, H., Metzner, W.: Competition of Fermi surface symmetry breaking and superconductivity. *Phys. Rev. B* **75**, 155117 (2007)
117. White, S.R., Scalapino, D.J.: Ground states of the doped four-leg t-J ladder. *Phys. Rev. B* **55**, 14701 (R) (1997)
118. White, S.R., Scalapino, D.J.: Density matrix renormalization group study of the striped phase in the 2D t-J model. *Phys. Rev. Lett.* **80**, 1272 (1998)

119. White, S.R., Scalapino, D.J.: Ground-state properties of the doped three-leg t-J ladder. *Phys. Rev. B* **57**, 3031 (1998)
120. White, S.R., Scalapino, D.J.: Phase separation and stripe formation in the two-dimensional t-J model: a comparison of numerical results. *Phys. Rev. B* **61**, 6320 (2000)
121. Hager, G., Wellein, G., Jackelmann, E., Fehske, H.: Stripe formation in doped Hubbard ladders. *Phys. Rev. B* **71**, 075108 (2005)
122. Kivelson, S.A., Emery, V.J., Lin, H.Q.: Doped antiferromagnets in the small t limit. *Phys. Rev. B* **42**, 6523 (1990)
123. Emery, V.J.: Theory of high T_c superconductivity in oxides. *Phys. Rev. Lett.* **58**, 2794 (1987)
124. Lorenzana, J., Seibold, G.: Metallic mean-field stripes, incommensurability, and chemical potential in cuprates. *Phys. Rev. Lett.* **89**, 136401 (2002)
125. Granath, M., Oganessian, V., Kivelson, S.A., Fradkin, E., Emery, V.J.: Nodal quasi-particles and coexisting orders in striped superconductors. *Phys. Rev. Lett.* **87**, 167011 (2001)
126. Arrigoni, E., Fradkin, E., Kivelson, S.A.: Mechanism of high temperature superconductivity in a striped Hubbard model. *Phys. Rev. B* **69**, 214519 (2004)
127. Emery, V.J.: In: Devreese, J.T., Evrard, R.P., van Doren, V.E. (ed.) *Highly Conducting One-Dimensional Solids*, p. 327. Plenum Press, New York (1979)
128. Luther, A., Emery, V.J.: Backward scattering in the one-dimensional electron gas. *Phys. Rev. Lett.* **33**, 589 (1974)
129. Noack, R.M., Bulut, N., Scalapino, D.J., Zacher, M.G.: Enhanced $d_{x^2-y^2}$ pairing correlations in the two-leg Hubbard ladder. *Phys. Rev. B* **56**, 7162 (1997)
130. Balents, L., Fisher, M.P.A.: Weak-coupling phase diagram of the two-chain Hubbard model. *Phys. Rev. B* **53**, 12133 (1996)
131. Lin, H.H., Balents, L., Fisher, M.P.A.: N-chain Hubbard model in weak coupling. *Phys. Rev. B* **56**, 6569 (1997)
132. Lin, H.H., Balents, L., Fisher, M.P.A.: Exact $SO(8)$ symmetry in the weakly-interacting two-leg ladder. *Phys. Rev. B* **58**, 1794 (1998)
133. Emery, V.J., Kivelson, S.A., Zachar, O.: Classification and stability of phases of the multi-component one-dimensional electron gas. *Phys. Rev. B* **59**, 15641 (1999)
134. Emery, V.J., Kivelson, S.A., Zachar, O.: Spin-gap proximity effect mechanism of high temperature superconductivity. *Phys. Rev. B* **56**, 6120 (1997)
135. Tsunetsugu, H., Troyer, M., Rice, T.M.: Pairing and excitation spectrum in doped t-J ladders. *Phys. Rev. B* **51**, 16456 (1995)
136. Vishwanath, A., Carpentier, D.: Two-dimensional anisotropic non-Fermi-liquid phase of coupled luttinger liquids. *Phys. Rev. Lett.* **86**, 676 (2001)
137. Fertig, H.A.: Unlocking transition for modulated surfaces and quantum Hall stripes. *Phys. Rev. Lett.* **82**, 3693 (1999)
138. Lawler, M.J., Fradkin, E.: Quantum Hall smectics, sliding symmetry and the renormalization group. *Phys. Rev. B* **70**, 165310 (2004)
139. O'Hern, C.S., Lubensky, T.C., Toner, J.: Sliding phases in XY-models, crystals, and cationic lipid-DNA complexes. *Phys. Rev. Lett.* **83**, 2746 (1999)
140. Carlson, E.W., Orgad, D., Kivelson, S.A., Emery, V.J.: Dimensional crossover in quasi one-dimensional and high T_c superconductors. *Phys. Rev. B* **62**, 3422 (2000)
141. Affleck, I., Halperin, B.I.: On a renormalization group approach to dimensional crossover. *J. Phys. A: Math. Gen.* **29**, 2627 (1996)
142. Lee, P.A., Nagaosa, N., Wen, X.-G.: Doping a mott insulator: physics of high temperature superconductivity. *Rev. Mod. Phys.* **78**, 17 (2006)
143. Berg, E., Fradkin, E., Kivelson, S.A.: Theory of the striped superconductor. *Phys. Rev. B* **79**, 064515 (2009)
144. Tranquada, J.M., Gu, G.D., Hücker, M., Kang, H.J., Klingerer, R., Li, Q., Wen, J.S., Xu, G.Y., Zimmermann, M.v.: Evidence for unusual superconducting correlations coexisting with stripe order in $\text{La}_{1.875}\text{Ba}_{0.125}\text{CuO}_4$. *Phys. Rev. B* **78**, 174529 (2008)

145. Hücker, M., Zimmermann, M.V., Debessai, M., Schilling, J.S., Tranquada, J.M., Gu, G.D.: Spontaneous symmetry breaking by charge stripes in the high-pressure phase of superconducting $\text{La}_{1.875}\text{Ba}_{0.125}\text{CuO}_4$. *Phys. Rev. Lett.* **104**, 057004 (2010)
146. Raczkowski, M., Capello, M., Poilblanc, D., Frésard, R., Oleś, A.M.: Unidirectional d-wave superconducting domains in the two-dimensional t-J model. *Phys. Rev. B* **76**, 140505 (R) (2007)
147. Yang, K.-Y., Chen, W.-Q., Rice, T.M., Sigrist, M., Zhang, F.-C.: Nature of stripes in the generalized t-J model applied to the cuprate superconductors. *New J. Phys.* **11**, 055053 (2009)
148. Loder, F., Kampf, A.P., Kopp, T.: Superconductivity with finite-momentum pairing in zero magnetic field. *Phys. Rev. B* **81**, 020511 (2010)
149. Chen, H.D., Vafek, O., Yazdani, A., Zhang, S.-C.: Pair density wave in the pseudogap state of high temperature superconductors. *Phys. Rev. Lett.* **93**, 187002 (2004)
150. Melikyan, A., Tešanović, Z.: A model of phase fluctuations in a lattice d-wave superconductor: application to the Cooper pair charge-density-wave in underdoped cuprates. *Phys. Rev. B* **71**, 214511 (2005)
151. Kosterlitz, J.M., Thouless, D.J.: Order metastability and phase transitions in two-dimensional systems. *J. Phys. C: Solid State Phys.* **6**, 1181 (1973)
152. José, J.V., Kadanoff, L.P., Kirkpatrick, S., Nelson, D.R.: Renormalization, vortices, and symmetry-breaking perturbations in the two-dimensional planar model. *Phys. Rev. B* **16**, 1217 (1977)
153. Cardy, J.: *Scaling and Renormalization in Statistical Physics*. Cambridge University Press, Cambridge, UK (1996) Chapter 8
154. Krüger, F., Scheidl, S.: Non-universal ordering of spin and charge in stripe phases. *Phys. Rev. Lett.* **89**, 095701 (2002)
155. Podolsky, D., Chandrasekharan, S., Vishwanath, A.: Phase transitions of $S = 1$ spinor condensates in an optical lattice. *Phys. Rev. B* **80**, 214513 (2009)
156. Radzihovsky, L., Vishwanath, A.: Quantum liquid crystals in imbalanced Fermi gas: fluctuations and fractional vortices in Larkin-Ovchinnikov states. *Phys. Rev. Lett.* **103**, 010404 (2009)
157. Baym, G., Pethick, C.: *Landau Fermi Liquid Theory*. Wiley, New York, NY (1991)
158. Polchinski, J.: In: Harvey, J., Polchinski, J. (ed.) *Recent directions in particle theory: from superstrings and black holes to the Standard Model (TASI - 92)*. Theoretical Advanced Study Institute in High Elementary Particle Physics (TASI 92), Boulder, Colorado, USA, 1–26 Jun, 1992. (World Scientific, Singapore, 1993).
159. Shankar, R.: Renormalization-group approach to interacting fermions. *Rev. Mod. Phys.* **66**, 129 (1994)
160. Pomeranchuk, I.I.: On the stability of a Fermi liquid. *Sov. Phys. JETP* **8**, 361 (1958)
161. Kee, H.-Y., Kim, E.H., Chung, C.-H.: Signatures of an electronic nematic phase at the isotropic-nematic phase transition. *Phys. Rev. B* **68**, 245109 (2003)
162. Khavkine, I., Chung, C.-H., Oganesyan, V., Kee, H.-Y.: Formation of an electronic nematic phase in interacting fermion systems. *Phys. Rev. B* **70**, 155110 (2004)
163. Yamase, H., Oganesyan, V., Metzner, W.: Mean-field theory for symmetry-breaking Fermi surface deformations on a square lattice. *Phys. Rev. B* **72**, 035114 (2005)
164. Halboth, C.J., Metzner, W.: D-wave superconductivity and pomeranchuk instability in the two-dimensional Hubbard model. *Phys. Rev. Lett.* **85**, 5162 (2000)
165. Metzner, W., Rohe, D., Andergassen, S.: Soft Fermi surfaces and breakdown of Fermi-liquid behavior. *Phys. Rev. Lett.* **91**, 066402 (2003)
166. Neumayr, A., Metzner, W.: Renormalized perturbation theory for Fermi systems: Fermi surface deformation and superconductivity in the two-dimensional Hubbard model. *Phys. Rev. B* **67**, 035112 (2003)
167. Dell'Anna, L., Metzner, W.: Fermi surface fluctuations and single electron excitations near pomeranchuk instability in two dimensions. *Phys. Rev. B* **73**, 45127 (2006)

168. Honerkamp, C., Salmhofer, M., Furukawa, N., Rice, T.M.: Breakdown of the Landau-Fermi liquid in two dimensions due to umklapp scattering. *Phys. Rev. B* **63**, 035109 (2001)
169. Honerkamp, C., Salmhofer, M., Rice, T.M.: Flow to strong coupling in the two-dimensional Hubbard model. *Euro. Phys. J. B* **27**, 127 (2002)
170. Hankevych, V., Grote, I., Wegner, F.: Pomeranchuk and other instabilities in the t-t' Hubbard model at the van hove filling. *Phys. Rev. B* **66**, 094516 (2002)
171. Lamas, C.A., Cabra, D.C., Grandi, N.: Fermi liquid instabilities in two-dimensional lattice models. *Phys. Rev. B* **78**, 115104 (2008)
172. Quintanilla, J., Haque, M., Schofield, A.J.: Symmetry-breaking Fermi surface deformations from central interactions in two dimensions. *Phys. Rev. B* **78**, 035131 (2008)
173. Sun, K., Yao, H., Fradkin, E., Kivelson, S.A.: Topological insulators and nematic phases from spontaneous symmetry breaking in 2D Fermi systems with a quadratic band crossing. *Phys. Rev. Lett.* **103**, 046811 (2009)
174. Yamase, H., Kohno, H.: Possible quasi-one-dimensional Fermi surface in $\text{La}_{2-x}\text{Sr}_x\text{CuO}_4$. *J. Phys. Soc. Jpn.* **69**, 2151 (2000)
175. Miyana, A., Yamase, H.: Orientational symmetry-breaking correlations in square lattice t-J model. *Phys. Rev. B* **73**, 174513 (2006)
176. Kivelson, S.A., Fradkin, E., Geballe, T.H.: Quasi-1D dynamics and the Nematic phase of the 2D emery model. *Phys. Rev. B* **69**, 144505 (2004)
177. Lawler, M.J., Barci, D.G., Fernández, V., Fradkin, E., Oxman, L.: Nonperturbative behavior of the quantum phase transition to a nematic Fermi fluid. *Phys. Rev. B* **73**, 085101 (2006)
178. Lawler, M.J., Fradkin, E.: Local quantum criticality in the nematic quantum phase transition of a Fermi fluid. *Phys. Rev. B* **75**, 033304 (2007)
179. Metlitski, M.A., Sachdev, S.: Quantum phase transitions of metals in two spatial dimensions: I. Ising-nematic order. *Phys. Rev. B* **82**, 075127 (2010)
180. Kee, H.Y., Kim, Y.B.: Itinerant metamagnetism induced by electronic nematic order. *Phys. Rev. B* **71**, 184402 (2005)
181. Yamase, H., Katani, A.A.: Van Hove singularity and spontaneous Fermi surface symmetry breaking in $\text{Sr}_3\text{Ru}_2\text{O}_7$. *J. Phys. Soc. Jpn.* **76**, 073706 (2007)
182. Puetter, C.M., Doh, H., Kee, H.-Y.: Meta-nematic transitions in a bilayer system: application to the bilayer ruthenate. *Phys. Rev. B* **76**, 235112 (2007)
183. Puetter, C.M., Rau, J.G., Kee, H.-Y.: Microscopic route to nematicity in $\text{Sr}_3\text{Ru}_2\text{O}_7$. *Phys. Rev. B* **81**, 081105 (2010)
184. Raghu, S., Paramakanti, A., Kim, E.-A., Borzi, R.A., Grigera, S., Mackenzie, A.P., Kivelson, S.A.: Microscopic theory of the nematic phase in $\text{Sr}_3\text{Ru}_2\text{O}_7$. *Phys. Rev. B* **79**, 214402 (2009)
185. Lee, W.C., Wu, C.: Nematic electron states enhanced by orbital band hybridization. *Phys. Rev. B* **80**, 104438 (2009)
186. Fregoso, B.M., Sun, K., Fradkin, E., Lev, B.L.: Biaxial nematic phases in ultracold dipolar Fermi gases. *New J. Phys.* **11**, 103003 (2009)
187. Fregoso, B.M., Fradkin, E.: Ferro-Nematic ground state of the dilute dipolar Fermi gas. *Phys. Rev. Lett.* **103**, 205301 (2009)
188. Kim, E.A., Lawler, M.J., Oret, P., Sachdev, S., Fradkin, E., Kivelson, S.A.: Theory of the nodal nematic quantum phase transition in superconductors. *Phys. Rev. B* **77**, 184514 (2008)
189. Huh, Y., Sachdev, S.: Renormalization group theory of nematic ordering in d-wave superconductors. *Phys. Rev. B* **78**, 064512 (2008)
190. Varma, C.M.: Non-Fermi-liquid states and pairing instability of a general model of copper oxide metals. *Phys. Rev. B* **55**, 4554 (1997)
191. Barci, D.G., Oxman, L.E.: Strongly correlated fermions with nonlinear energy dispersion and spontaneous generation of anisotropic phases. *Phys. Rev. B* **67**, 205108 (2003)
192. Zacharias, M., Wölfe, P., Garst, M.: Multiscale quantum criticality: Pomeranchuk instability in isotropic metals. *Phys. Rev. B* **80**, 165116 (2009)
193. Hertz, J.A.: Quantum critical phenomena. *Phys. Rev. B* **14**, 1165 (1976)

194. Millis, A.J.: Effect of a nonzero temperature on quantum critical points in itinerant Fermion systems. *Phys. Rev. B* **48**, 7183 (1993)
195. Sachdev, S.: *Quantum Phase Transitions*. Cambridge University Press, Cambridge, UK (1999)
196. Jain, J.K.: Composite-fermion approach for the fractional quantum Hall effect. *Phys. Rev. Lett.* **63**, 199 (1989)
197. Lopez, A., Fradkin, E.: Fractional quantum Hall effect and Chern-Simons gauge theories. *Phys. Rev. B* **44**, 5246 (1991)
198. Halperin, B.I., Lee, P.A., Read, N.: Theory of the half-filled Landau level. *Phys. Rev. B* **47**, 7312 (1993)
199. Rezayi, E., Read, N.: Fermi-liquid-like state in a half-filled Landau level. *Phys. Rev. Lett.* **72**, 900 (1994)
200. Doan, Q.M., Manousakis, E.: Variational Monte Carlo calculation of the nematic state of the two-dimensional electron gas in a magnetic field. *Phys. Rev. B* **78**, 075314 (2008)
201. Dell'Anna, L., Metzner, W.: Electrical resistivity near pomeranchuk instability in two dimensions. *Phys. Rev. Lett.* **98**, 136402 (2007). Erratum: *Phys. Rev. Lett.* **103**, 220602 (2009)
202. Haldane, F.D.M.: In: Schrieffer, J.R., Broglia, R. (ed.) *Proceedings of the International School of Physics Enrico Fermi, course 121, Varenna, 1992*. North-Holland, New York (1994)
203. Castro Neto, A.H., Fradkin, E.: Bosonization of the low energy excitations of Fermi liquids. *Phys. Rev. Lett.* **72**, 1393 (1994)
204. Castro Neto, A.H., Fradkin, E.H.: Exact solution of the Landau fixed point via bosonization. *Phys. Rev. B* **51**, 4084 (1995)
205. Houghton, A., Marston, J.B.: Bosonization and fermion liquids in dimensions greater than one. *Phys. Rev. B* **48**, 7790 (1993)
206. Houghton, A., Kwon, H.J., Marston, J.B.: Multidimensional bosonization. *Adv. Phys.* **49**, 141 (2000)
207. Ghaemi, P., Vishwanath, A., Senthil, T.: Finite temperature properties of quantum Lifshitz transitions between valence-bond solid phases: an example of local quantum criticality. *Phys. Rev. B* **72**, 024420 (2005)
208. Chubukov, A.V., Pépin, C., Rech, J.: Instability of the quantum critical point of itinerant ferromagnets. *Phys. Rev. Lett.* **92**, 147003 (2004)
209. Chubukov, A.V.: Self-generated locality near a ferromagnetic quantum critical point. *Phys. Rev. B* **71**, 245123 (2005)
210. Rech, J., Pépin, C., Chubukov, A.V.: Quantum critical behavior in itinerant electron systems—Eliashberg theory and instability of a ferromagnetic quantum critical point. *Phys. Rev. B* **74**, 195126 (2006)
211. Holstein, T., Norton, R.E., Pincus, P.: de Haas-van Alphen effect and the specific heat of an electron gas. *Phys. Rev. B* **8**, 2649 (1973)
212. Baym, G., Monien, H., Pethick, C.J., Ravenhall, D.G.: Transverse interactions and transport in relativistic quark-gluon and electromagnetic plasmas. *Phys. Rev. Lett.* **64**, 1867 (1990)
213. Boyanovsky, D., de Vega, H.J.: Non-Fermi-liquid aspects of cold and dense QED and QCD: equilibrium and non-equilibrium. *Phys. Rev. D* **63**, 034016 (2001)
214. Reizer, M.Y.: Relativistic effects in the electron density of states, specific heat, and the electron spectrum of normal metals. *Phys. Rev. B* **40**, 11571 (1989)
215. Ioffe, L.B., Wiegmann, P.B.: Linear temperature dependence of resistivity as evidence of gauge interaction. *Phys. Rev. Lett.* **65**, 653 (1990)
216. Nagaosa, N., Lee, P.A.: Experimental consequences of the uniform resonating-valence-bond state. *Phys. Rev. B* **43**, 1233 (1991)
217. Polchinski, J.: Low-energy dynamics of the spinon-gauge system. *Nucl. Phys. B* **422**, 617 (1994)
218. Chakravarty, S., Norton, R.E., Syljuasen, O.F.: Transverse gauge interactions and the vanquished Fermi liquid. *Phys. Rev. Lett.* **74**, 1423 (1995)
219. Lee, S.S.: Low-energy effective theory of Fermi surface coupled with U(1) gauge field in 2 + 1 dimensions. *Phys. Rev. B* **80**, 165102 (2009)

220. Jakubczyk, P., Metzner, W., Yamase, H.: Turning a first order quantum phase transition continuous by fluctuations. *Phys. Rev. Lett.* **103**, 220602 (2009)
221. Hirsch, J.E.: Spin-split states in metals. *Phys. Rev. B* **41**, 6820 (1990)
222. Varma, C.M., Zhu, L.: Helicity order: hidden order parameter in URu₂Si₂. *Phys. Rev. Lett.* **96**, 036405 (2006)
223. Simon, M.E., Varma, C.M.: Detection and implications of a time-reversal breaking state in underdoped cuprates. *Phys. Rev. Lett.* **89**, 247003 (2002)
224. Haldane, F.D.M.: Berry Curvature on the Fermi surface: anomalous Hall effect as a topological Fermi-liquid property. *Phys. Rev. Lett.* **93**, 206602 (2004)
225. Nelson, D.R., Toner, J.: Bond-orientational order, dislocation loops, and melting of solids and smectic-A liquid crystals. *Phys. Rev. B* **24**, 363 (1981)
226. Toner, J., Nelson, D.R.: Smectic, cholesteric, and Rayleigh-Benard order in two dimensions. *Phys. Rev. B* **23**, 316 (1981)
227. Zaanen, J., Nussinov, Z., Mukhin, S.I.: Duality in 2 + 1 D quantum elasticity: superconductivity and quantum nematic order. *Ann. Phys.* **310**, 181 (2004)
228. Cvetkovic, V., Nussinov, Z., Zaanen, J.: Topological kinematical constraints: quantum dislocations and glide principle. *Phil. Mag.* **86**, 2995 (2006)
229. Sun, K., Fregoso B.M., Lawler M.J., Fradkin E.: Fluctuating stripes in strongly correlated electron systems and the nematic-smectic quantum phase transition. *Phys. Rev. B* **78**, 085124 (2008). Erratum: *Phys. Rev. B* **80**, 039901(E) (2008).
230. Kirkpatrick, T.R., Belitz, D.: Soft modes in electronic stripe phases and their consequences for thermodynamics and transport *Phys. Rev. B* **80**, 075121 (2009)
231. Millis, A.J.: Fluctuation-driven first order behavior near the T=0 two dimensional stripe to Fermi liquid transition. *Phys. Rev. B* **81**, 035117 (2010)
232. Halperin, B.I., Lubensky, T.C., Ma, S.-K.: First-order phase transitions in superconductors and smectic—a liquid crystals. *Phys. Rev. Lett.* **32**, 292 (1974)
233. Altshuler, B.L., Ioffe, L.B., Millis, A.J.: Critical behavior of the T=0, $2k_F$, density-wave phase transition in a two-dimensional Fermi liquid. *Phys. Rev. B* **52**, 5563 (1995)

Modern Theories of Many-Particle Systems in
Condensed Matter Physics

Cabra, D.C.; Honecker, A.; Pujol, P. (Eds.)

2012, XIII, 368 p. 130 illus., Softcover

ISBN: 978-3-642-10448-0